Conducting Polymers for Electrochemically Mediated Separations

by

Yinying Ren

BS Chemical Engineering, Northwestern University (2014)

Submitted to the Department of Chemical Engineering
in partial fulfillment of the requirements for the degree of

Doctor of Philosophy in Chemical Engineering

at the

MASSACHUSETTS INSTITUTE OF TECHNOLOGY

June 2019

Author ..... Signature redacted .....
Department of Chemical Engineering
May 13, 2019

Certified by ..... Signature redacted .....
T. Alan Hatton
Ralph Landau Professor of Chemical Engineering
Director of David H. Koch School of Chemical Engineering Practice
Thesis Supervisor

Accepted by ..... Signature redacted .....
Patrick S. Doyle
Robert T. Haslam (1911) Professor of Chemical Engineering
Singapore Research Professor
Chairman, Committee for Graduate Students

Conducting Polymers for Electrochemically Mediated Separations

by

Yinying Ren

Submitted to the Department of Chemical Engineering
on May 13, 2019, in partial fulfillment of the
requirements for the degree of
Doctor of Philosophy in Chemical Engineering

Abstract

Many conventional separation technologies are limited by high energy costs, generation of chemical wastes, and lack of molecular selectivity. This thesis is motivated to develop novel separation techniques that overcome the aforementioned drawbacks for the separation of neutral organic compounds from aqueous solutions.

Adsorption is one of the most widely adopted technologies for the intended task. Polymeric adsorbents have shown great potential for replacing activated carbon for removing a wide range of toxic organic pollutants from wastewater streams since they do not suffer from costly regeneration needs and high attrition rates. An electrochemically regenerable polymeric adsorbent based on an intrinsically conducting polymer, polypyrrole (PPy), doped with anionic surfactant dioctylsulfosuccinate (AOT), denoted PPy(AOT), is developed for mitigating organic pollutants in wastewater. Highly porous PPy(AOT) can be synthesized using a facile electropolymerization protocol, and has an adsorption capacity of greater than 570 mg pollutant/g polymer in its superhydrophobic oxidized state. The hydrophobicity of PPy(AOT) and hence its affinity for organics can be modulated electrochemically through the reorientation of AOT dopants, which can be exploited to regenerate the adsorbent and use it repeatedly for multiple adsorption/desorption cycles. A combined density functional theory and molecular dynamics approach was used to study the interactions between the adsorbed organic molecules and the surfactant-doped conducting polymer adsorbent, and to elucidate the mechanism of electrochemical modulations of hydrophobicity and affinity of the sorbent.

The AOT doped polypyrrole (PPy(AOT)) and a polyvinylferrocene/polypyrrole hybrid (PVF-PPy) have complementary hydrophobicity tunability in response to electrochemical modulations: both materials are hydrophobic in their respective neutral states, exhibiting high affinities towards organics; upon application of a mild potential to oxidize PVF-PPy and reduce PPy(AOT), they can be simultaneously rendered hydrophilic, thereby driving desorption of organics and regeneration of the materials. Therefore, the two materials form an attractive pair for an asymmetric electrode

system to work in tandem. The asymmetric system can be used in a cyclic fashion, through repeated application of a small potential (close to 0 V) to program the capture of organics from a large volume of feed solution, and a higher potential (above 0.9 V) to stimulate the release of the adsorbed organics into a small volume of desorption solution.

The redox-responsive electrode system can be applied for remediation of organic pollution in wastewater as well as recovery of organic products from reaction mixtures. The asymmetric configuration has multiple benefits, including suppression of water parasitic reactions, high energetic efficiency, and selectivity for target organic species. The ability to modulate the hydrophobicity of conducting polymers and physicochemical insights about the material are significant for developing broader applications in drug delivery, sensing, self-cleaning surfaces, microfluidics, and artificial muscles.

Thesis Supervisor: T. Alan Hatton
Title: Ralph Landau Professor of Chemical Engineering
Director of David H. Koch School of Chemical Engineering Practice

Acknowledgments

Nine years ago, I moved to the United States for college instead of attending the same medical school from which my mom graduated because I wanted to add more "uncertainties" to my life. The dedicated and caring faculty members and mentors in the Chemical and Biological Engineering Department at my alma mater cultivated my research interests in polymer science. I have been extremely lucky to receive tremendous support from my advisor, mentors, colleagues, friends and family during my PhD at MIT. This journey would not be possible without them.

I would like to begin with expressing my sincere gratitude for my PhD advisor, Professor T. Alan Hatton. I have no doubt Alan is the best advisor I could have ever asked for. He strikes a remarkable balance between giving me respect and freedom, and ensuring scientific rigor in my work. He has always been very understanding whenever I got stuck on a research problem. I remembered, towards the end of the Fall semester of my third year after almost all my experiments for studying the surfactant-polymer interactions had failed in a half-year period, he finally gently reminded me whether it was the time to move on. But he was patient enough to let me try out yet another approach through a collaboration with a physical chemist, which eventually led to meaningful discoveries. He showed his respect for my efforts and gave me a lot of freedom to make all the important decisions for my research. When I was upset, he always tried to encourage me by saying that "graduate school is the best years of (my) life." Although I still want to keep my hope that the next chapter of my life will be awesome, I certainly believe my graduate school years have been very meaningful and rewarding, thanks to Alan's invaluable mentoring and generous support throughout my PhD.

I also want to thank my committee members, Professor Fikile Brushett and Professor Bradley Olsen, for their unique perspectives and insightful advice for my research. I am grateful for David H. Koch for the fellowship during my first year and the Abdul Latif Jameel World Water and Food Security Lab (J-WAFS) for funding my research. My UROPs, Sarah Curtis, Emily Penn, and Xiaochen Yang helped me carry out many

experiments in the past few years, and also gave me an opportunity to learn together with them.

I have been extremely fortunate to have lots of great colleagues in the group and beyond. Dr. Xianwen Mao was my mentor when I first joined group. He showed me how to be a creative thinker and an independent researcher. His intellectual curiosity and passion for research were truly impressive. Dr. Tonghan Gu, although we worked in different fields, was always willing to listen to my problems and offer his perspectives. Dr. Wenda Tian was a great officemate and has given me a lot of great advice about career development and personal life. Other members of the Hatton group, Miao Wang, Dr. Katherine Phillips, Sahag Voskian, Kai-Jher Tan, Krzysztof Rajczykowski, Fan He, and Dr. Ali Hemmatifar were all extremely helpful with experiments and discussions, and also very generous to share their instruments with me. My collaborator Dr. Zhou Lin, salvaged my surfactant-doped conducting polymer project, which meant so much to me as my first PhD project. The stewards at the Institute for Soldier Nanotechnologies (ISN), William F. DiNatale and Dr. Steven Kooi, were always extremely patient and ready to help me whenever I walked up to them.

My four months at practice school were an integral part of my graduate school experience. Not only because I got to travel to exotic once-in-a-lifetime places like Perth and Karratha in Western Australia, I also had a lot of inspirations for my future career and got to know my practice school cohort Stephanie Doong, Max Liu, Lisa Volpatti, Sarah Shapiro and others very well.

I met many awesome women at MIT and developed new perspectives on gender equity through Graduate Women at MIT (GWAMIT). I especially want to thank Molly Bird for always covering my back as my co-chair of GWAMIT.

The Chinese student community within the Chemical Engineering department has given me a lot of accompany throughout my time at MIT. My first semester in the PhD program was so tough and I wouldn't have survived without them. These long problem sets deepened my friendships with my study cohorts, Yiming Mo, Albert Tianxiang Liu, Steven Nian Liu, Jim Chu, and Joey Gu, which would certainly extend

beyond our time at MIT. Weitong (Victoria) Sun gave me a lot of advice before I came to MIT and during my first year. She was a great workout buddy and invited me to many great road and ski trips.

My ex-roomate Dr. Shan Huang helped me learn to better appreciate myself. My friends from childhood and college have always been on my side through good times and hardships even though we now live in different cities, countries and continents.

Last but not least, I want to say thank you to my parents and grandparents for their unconditional love, who raised me to be a strong independent person. I know it was so hard for them to send me away. I am glad I am almost ready to move back to China and be with my family.

THIS PAGE INTENTIONALLY LEFT BLANK

Contents

THIS PAGE INTENTIONALLY LEFT BLANK

List of Figures

List of Tables

THIS PAGE INTENTIONALLY LEFT BLANK

Chapter 1

Introduction

Water is the most vital resource on the planet. It sustains life, the ecosystem and climates, as well as provides inputs to agriculture, manufacturing and other human activities. Unfortunately, water scarcity and lack of clean water are pervasive and rising problems afflicting people throughout the world.[26,90] WHO and UNICEF estimated that 2.1 billion people or 29% of the global population lack access to safe drinking water.[1,90,108] Four out of every 10 people are affected by water scarcity.[1] Therefore, the United Nations Sustainable Development Goal 6 is focused on ensuring availability and sustainable management of water and sanitation for all.[108] Water pollution is a global issue with 80% of wastewater returned into the ecosystem without being properly treated.[1] Even among the high- and high-middle-income countries, only 59% of all domestic wastewater is safely treated.[108] The situation is even worse for developing countries in Africa and Asia where the water stress level is above 70%.[108] The use of freshwater for agricultural, industrial and domestic purposes has led to water contamination with significant chemical pollution of natural waters.[88] Unfortunately, current wastewater or drinking water treatment plants are not specifically equipped for eliminating neutral organic contaminants.[58,124]

This thesis aims to develop an energetically efficient and environmentally friendly solution for the separations of hydrophobic organic compounds from water. The proof-of-concept materials and systems are motivated by the need for decontamination of water affected by organic pollutants, and the need for capturing valuable organic

chemical products in industrial processes.

1.1 Motivations

Prevalent water pollution calls for efficacious technologies for purifying water at lower cost with less energy to prevent further stressing the environment and endangering human health.[90] Many pollutants that originate from municipal, industrial and agricultural wasterwaters such as hormones, pharmaceuticals, pesticides, personal care products and industrial chemicals are hydrophobic organic compounds and can have detrimental effects even at low concentrations.[88] Moreover, these organic pollutants are persistent and prone to long-range environment transport.[53] As a result, the presence of these toxic chemicals has affected the aquatic environment,[41] vegetation,[25] and ultimately human beings due to bioaccumulation to high concentrations through the food chain.[53]

Table 1.1 summarizes major categories of organic pollutants and their respective sources.[6,20,58,88] The variety of organic molecules complicates the tasks of separations. Nevertheless, most of the pollutants are in fact chemicals of commercial value if can be captured properly. Technologies for separation of these organic compounds will not only alleviate water pollution, but also seize the residual value of those chemicals.

1.1.1 Remediation of organic contaminants

Organics with simple structures and good hydrophilicity can be cleaned up by biodegradation, a process that uses microorganisms, fungi, and plants to digest pollutants and is a sustainable and economical mechanism.[126] However, many organic substances, such as phenols, nitrobenzene, and persistent organic pollutants (POPs) including pharmaceutical substances and pesticides, are non-biodegradable yet highly toxic and hazardous.[33,126] Therefore, chemical methods need to be developed to remove these organic compounds from water.

Table 1.1: Major organic pollutants and sources in the aquatic environment

Category	Selected examples	Related problems	Sources	
			Distinct	Nonexclusive
Pharmaceuticals	Propranolol hydrochloride, Acetaminophen, Chlorophene	Bacterial resistance, nontarget effects	Excretion, disposal of unwanted products	Sources that are not exclusive to individual category: indsutrial wastewater and landfill leachate
Personal care products	Nonylphenol ethoxylates, 3-(4-Methylbenzyliden) camphor, Musks	Endocrine effects	Domestic wastewater	
Steroid hormones	Ethinyl estradiol	Feminization of fish	Excretion, aquaculture, run-off from CAFOs[a]	
Biocides	DDT, Atrazine, Metolachlor	Toxic effects and persistent metabolites, effects on primary producers	Run-off from gardens, lawns, roadways and agriculture	
Industrial chemicals	Phthalates,Bisphenol A, azo dyes	Drinking-water contamination	Domestic wastewater	

[a]CAFOs: concentrated animal feeding operations

1.1.2 Recovery of organic products

In addition to mining clean water for pollution control, the recovery of valuable organic compounds from the aqueous phase is economically attractive and hence motivates further research.[26,118] In wastewater treatment, the process economics of separation processes can be dramatically enhanced if the inlet aqueous stream contains more than 1-2% organics.[118]. In pharmaceutical manufacturing, by-products and residual precursors, solvents and other impurities must be removed to ensure the purity of the desired pharmaceutical products.[75] But the variable composition and fluctuations in the inlet organics-water mixture, and the wide variety of products produced in the pharmaceutical industry have made recovery of valuable products exceptionally challenging.[126]

Despite ubiquitous applications, chemical separation processes are energy-intensive, constituting 10-15% of the world's total energy consumption and $\frac{1}{3}$ to $\frac{1}{2}$ of the energy used by the transportation sector in the US.[57] Technologies with high efficiency and efficacy for organics are highly desirable to encourage wider adoption and decrease energy consumption due to process inefficiencies. One revolutionary invention in the water industry is reverse osmosis: the current state-of-the-art systems are within a factor of two from the thermodynamic limit of the energy demands, much lower than thermal desalination,[117] and thus have essentially replaced the conventional thermal technologies and been widely implemented in most of the countries in the Middle East and North Africa.[57]

Therefore, development of molecularly selective and energetically efficient technologies for organics-water separation is critical for addressing the energy-water nexus faced by countries throughout the world, especially those economically disadvantaged.

1.2 Technologies for the mitigation of organics in water

The most common and essential form of pollution control is wastewater treatment plants (WWTPs): sewers collect wastewater from homes, businesses, and industries, and deliver it to WWTP for purifications; the processed water is then either discharged into streams or distributed for reuse.[109] There are two basic stages in the treatment of wastewater: the primary stage where solids are allowed to settle and removed from wastewater; and the secondary stage which uses biological processes to further purify wastewater. The effluent from the primary stage should be free of small stones, soils, sand, cinders, and minute solids after flowing through filters, grit chambers, and sedimentation tank. To further enhance the quality of water, organic matter is broken down to harmless by-products in the secondary stage by bacteria using trickling filters, activated sludge processes and increasingly membrane bioreactors.[46,109] WWTP completes the two-stage process with a disinfection step to kill pathogenic bacteria and to reduce odor using chlorine, ultraviolet light or ozone.

The increasing complexity of contaminants in wastewater and rising demands on water supply call for water reuse but have overburdened existing WWTPs. To allow proper pre-treatment of industrial waste and expand the treatment capabilities of WWTPs, many advanced wastewater treatment technologies have been developed. We have established in Section 1.1 that the need for removal of organic compounds from aqueous solutions is ubiquitous, and a wide array of technologies have been developed to carry out the task. Existing technologies can be divided into two broad categories based on the outcome, namely separations and degradation, which can work together depending on the treatment goal.

1.2.1 Separation of organics from aqueous solutions

Separations are at the heart of chemical engineering. Many technologies have been developed to provide options for separation of molecules of distinct properties present

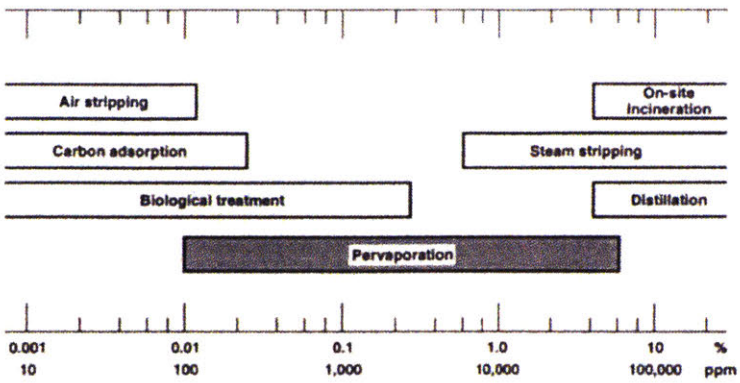

Figure 1-1: Competitive concentration range of organics in aqueous solutions for different separation processes. Reprint by permission from REF.[118], Springer Nature.

in various environments. Depending on the concentration of the organics to be separated, different technologies may become more suitable (Figure 1-1).[118]

1.2.1.1 Distillation and stripping

Distillation and stripping are commonly used in chemical manufacturing. Despite their widespread use, the efficiencies of distillation and stripping are only 11% and 50%, respectively.[19] Therefore, they are commonly applied to separating high concentrations of organics in water, or organic mixtures. However, many organic micropollutants are more than 4 orders of magnitude lower in concentration, making distillation or stripping unfavorable in energetic terms.

1.2.1.2 Pervaporation

The pervaporation process creates a vapor pressure gradient across a membrane by bringing a liquid feed in contact on one side and a vacuum drawn on the other side, allowing organic vapors to permeate through the membrane and collected in the gas phase which is subsequently condensed.[118] A typical membrane for pervaporation is hydrophobic and hence has higher selectivities for organics of intermediate hydrophobic character (e.g., ethyl acetate, methyl ethyl ketone, and acetone) than relatively hydrophilic ones (e.g. ethanol, methanol and acetic acid).[118] Pervaporation is more

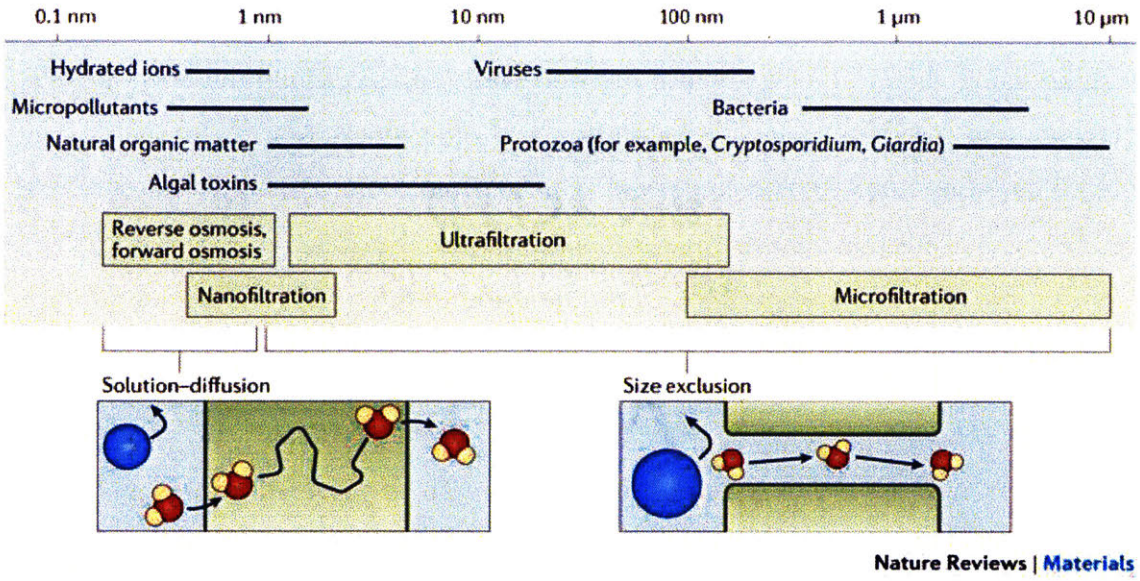

Figure 1-2: Membrane processes for water purification and desalination. Reprint by permission from REF.[117], Springer Nature.

suitable for the separation of organic at intermediate concentrations (Figure 1-1).

1.2.1.3 Membrane-based technologies

Membrane processes are a class of emerging technologies for the removal of organic compounds from water due to the improved efficiency and robustness of treating pollutants of different size. Microfiltration (MF), ultrafiltration (UF), nanofiltration (NF) and reverse osmosis (RO) are driven by hydraulic pressure and can be classified on the basis of the size of the solutes that are retained as shown in Figure 1-2.[117]

The membrane-based filtration is based on size-exclusion mechanisms, with MF membranes to remove suspended particles and microbial pathogens, UF membranes to retain macromolecules, and NF membranes to remove species down to 100 and 300 Da.[117] Current membranes still lack molecular-level design to achieve molecular selectivity. On the other hand, RO is mainly intended for desalination. Therefore, nanofiltration is the only technology that is suitable for dissolved organic compounds whose diameters fall in the 0.1 nm to 1 nm range.

Membranes are known to be susceptible to organic fouling by adsorption of dissolved organic matter.[117] Excessive fouling compromises the throughput of the pu-

rification process and lowers the selectivity of the membrane, as well as necessitates cleaning using chemical agents which are unfriendly to the membrane and the environment, and increases energy consumption and operating costs.[117] At the current stage, membrane-based technologies are still far from being the most effective and low-cost option for remediating organic contaminants in water.

1.2.1.4 Adsorption

Adsorption is a binding process in which a gas or liquid solute (adsorbate) accumulates on the surface of a solid or a liquid (adsorbent) with the formation of a molecular or atomic film. Adsorption is generally classified into two categories: chemisorption where covalent bonds form between adsorbates and adsorbents, and physisorption where only non-covalent interactions are involved.[39]

The main physical driving forces for adsorption are van der Waals forces, hydrogen bonds, polarity, dipole-dipole, $\pi - \pi$ stacking interactions, and hydrophobic interactions.[22,121] Besides adsorbate-adsorbent interaction, adsorption efficiency is also affected by adsorbent surface area, adsorbent-to-adsorbate ratio, adsorbent particle size, temperature, pH and contact time.[121] Activated carbons, agricultural residues after milling, industrial by-products, and zeolites have shown high adsorption capacity due to their porous structure and high surface area.[121]

- Activated carbon

  Activated carbon (AC) is one of the most widespread adsorbents due to its high specific surface area and strong interactions with target compounds.[44,68,85] To encourage widespread use of AC, extensive research has been done to find inexpensive precursors and optimize activation procedures for higher adsorption capacity.[22] Important characteristics of AC that impact the adsorption of organic compounds include pore size distribution (micropores are accessible to small organic molecules while natural organic matter can only access mesopores), surface chemistry (functionality, heteroatoms), and mineral matter content.[22]

Despite being a primary treatment for the remediation of organics in aqueous phase, AC suffers from major drawbacks with its regeneration methods: thermal desorption is energy-intensive, while solvent regeneration may lead to substantial loss of AC and result in secondary pollution.[6,45,50,126] The ability to regenerate the adsorbent efficiently is important to avoid merely transferring contaminants from the liquid phase to the solids, and to enable reuse of the sorbent.[77] Development of alternative adsorbent is therefore an active research field to overcome regeneration limitations.

- Redox-responsive polymer

  To overcome recyclability problems such as observed with AC, a redox-responsive polymer gel with tunable hydrophobicity that reversibly adsorbs and releases butanol in the presence of water has been developed via copolymerization of hydroxybutyl methacrylate (HBMA)and vinylferrocene (VF).[5] When the ferrocene moieties are in their reduced uncharged state, the gel is hydrophobic and selectively extracts butanol from water. When the gel is exposed to a chemical oxidant, the ferrocene units are oxidized to ferricenium ions, and the positive charges of the organometallic compound render the microenvironment within the gel more hydrophilic, releasing butanol to water. The hydrophobicity modulations are achieved through chemical oxidation and reduction of ferrocene using $FeCl_3$ oxidants and L-ascorbic acid reductants, respectively. However, the addition of chemical agents for redox switching increases the risk of contamination of the remediation process, and the efficacy of the chemical stimuli may be hampered by mass transfer limitations.[62] Nevertheless, the ability to modulate the hydrophobicity of redox-responsive adsorbents is a promising mechanism for achieving reversibility in the sorption of organics, and hence warrants further investigation on alternative stimuli for the redox switching.

Many stimuli have been explored to induce hydrophobic-hydrophilic transitions in polymeric materials, including temperature, pH, light illumination, adsorption of biopolymer or treatment of selective solvents.[5,120] Among these approaches, electrical

potential allows properties of materials to be varied locally in real-time with high resolution.[62]

Redox-active materials that respond to electrical potential stimuli have been developed to remove ionic species and charged biomacromolecules from aqueous solution in a reversible manner.[4,96–99,101] Functionalization of carbon-based anodes with polyvinyl ferrocene and carbon nanotube (PVF-CNT) hybrids supplement the capacitive charging of the electrode surface and achieve significantly higher selectivity for organic anions (carboxylates, sulfonates, and phosphonates) over inorganic anions in Faradaic capacitive deionization systems (FaCDI).[99,101] However, electrically neutral hydrophobic organic compounds lack electrostatic interactions with those charged surfaces and hence cannot be removed through FaCDI. New redox-active materials are needed for reversible separations of organic compounds from water.

1.2.2 Degradation of organic compounds

In contrast to separations where the chemcial identity of the target molecules is preserved, degradation processes transform the species to less harmful products. Degradation can be done biologically or chemically.

1.2.2.1 Biodegradation of organic compounds

Biodegradation is a process that uses microorganisms, fungi, plants and their enzymes to consume the sewage and other organic matter, turning them into new bacterial cells, carbon dioxide and other harmless substances.[126] It happens in nature and is a sustainable and economical way of cleaning up the environment. However, nature can no longer undertake all the burdens brought by the increasing population, human activities and industrial processes. Therefore, researchers have been studying the biodegradation mechanisms and trying to replicate them for the wastewater treatment. WWTPs generally use biodegradation in the second stage for treating wastewater.

The nature of the contaminant largely determines the efficacy of biodegradation

processes. Some organic pollutants such as organic matter, and organophosphorous pesticides are more prone to be consumed by bacteria and microorganisms than persistent organic pollutants (POPs), such as polychlorinated biphenyls (PCBs), polyaromatic hydrocarbons (PAHs), heterocyclic compounds and pharmaceutical substances.[126] As a result, these reluctant contaminants are accumulated along the food chain resulting in magnified toxicity effects on human beings. Alternative methods such as advanced oxidation processes (AOPs) are developed to chemically degrade those challenging chemical compounds.

1.2.2.2 Chemical oxidation technologies

The limitations of biological methods warrant development of chemical oxidation technologies to convert challenging or highly toxic chemical compounds to less harmful products that can either be discharged or treated biologically downstream. Chemical oxidants such as H_2O_2, ozone, and K_2MnO_4 are used to oxidize harmful chemical compounds to more manageable forms, but these oxidants suffer from a major drawback—low rates of degradation.[126]

Advanced oxidation processes (AOPs) are developed to overcome the slow degradation kinetics and use hydroxyl radicals and other reactive oxygen species to degrade recalcitrant organic pollutants.[21,69] Most organic compounds can react with hydroxyl radical by addition or hydrogen abstraction pathways and undergo serial chemical reactions to eventually form oxidation products (ketones, aldehydes, and alcohols) that are often less toxic and more susceptible to bioremediation.[69] The hydroxyl radical and reactive oxygen species can be generated using UV/O_3, UV/H_2O_2, Fenton, photo-Fenton, nonthermal plasmas, sonolysis, photocatalysis, radiolysis, and supercritical water oxidation processes.[69]

Because of their complexity, implementation of AOPs is limited due to economic reasons,[21] and sophisticated facilities for on-site production of H_2O_2 or for housing large-scale electron beams and other equipment are required.[69] Although centralized operations can improve the economical viability of AOPs, efficient and economical ways to separate and collect organic compounds in distributed locations need to be

developed.

Chemical separations followed by further degradation through either biodegradation or AOPs can together address water pollution caused by organic contaminants. Therefore, further development of energetically efficient, environmentally friendly, and molecularly selective technologies for organics-water separations will make significant contributions to water/wastewater treatment and other industrial separation needs.

1.3 Thesis objectives

The aim of the thesis is to develop a prototype for the electrochemically mediated separations of organics from water. This involves synthesizing functional materials and designing electrochemical cells to perform the reversible separation process efficiently.

1.3.1 Functional materials

Adsorption is chosen as the underlying principle for capturing organic molecules from the aqueous phase. Building on the expertise of the group, polymeric materials are engineered to function as electroactive adsorbent for hydrophobic molecules that are electrically neutral. For this purpose, the polymeric adsorbent needs to exhibit the following three features:

- Tunable hydrophobicity and affinity towards organic compounds

  Similar to the hydroxybutyl methacrylate (HBMA) and vinylferrocene (VF) copolymer gel,[5] the prototypical adsorbent should also contain redox-active moieties that modulate the hydrophobicity of the material. The material will have higher affinities towards organics in its hydrophobic state, and can be rendered hydrophilic to interact more favorably with water and thereby release the adsorbed hydrophobic compounds during regeneration. Therefore, a hydrophobic-hydrophilic transition is key to repeated use of the adsorbent.

- Electrical conductivity

The redox-active polymer when functionalized onto carbon-based electrodes for mechanical support and current collection, should be electrically conductive to receive and respond to the potential stimuli applied. This avoids the complication of introducing chemical agents to stimulate the redox moieties.[5] The immobilized redox moieties should undergo fast electron transfer and are compatible with common benign electrolytes such as sodium chloride and the narrow electrochemical stability window afforded by water.

- High surface area

  Porous structures within the functional materials allow adsorption sites to be readily exposed to target molecules and facilitate the transport of counterions during the redox processes.[104,120] The improved adsorption capacity and eletrochemical activities enable more effective utilization of the adsorbent. This is essential for enhancing key performance metrics such as adsorption capacity on gravimetric, volumetric or macroscopic area bases and for ensuring adsorption to be carried out in a compact adsorber.

1.3.2 Electrochemical cells

An eletrochemical cell will be assembled using dual-functionalized electrodes coated with adsorbents described above to perform the redox modulations using electrical potentials. For this proof-of-concept work, the electrochemically mediated separations of organics operates in a batch mode. The electorchemical cell can have higher energetic efficiency if the two electrodes exhibit complementary hydrophobicity tunability: electrode A is hydrophobic when oxidized while the counter electrode B is hydrophobic when reduced, and therefore both are in the states favoring adsorption of organic compounds. Once saturated, the two electrodes can be regenerated in the electrochemical cell by reducing electrode A and oxidizing B to render both of them hydrophilic and to desorb the organics previously adsorbed.

Development of two redox-active polymeric adsorbents that undergo hydrophobic-to-hydrophilic transitions in response to the same potential stimulus but with oppo-

site hydrophobicity gradient will allow the two electrodes to work in tandem in one electrochemical cell and deliver superior energetic efficiency.

Chapter 2

Surfactant-doped Conducting Polymers for Electrochemically Reversible Adsorption of Organics

2.1 Introduction

Adsorption is a common technology for removing organic pollutants from wastewater and activated carbon (AC) is one of the most widespread adsorbents due to its high surface area and strong interactions with target compounds.[6,14,86] Methods for AC regeneration have drawbacks, however: thermal desorption is energy-intensive, while solvent regeneration may lead to substantial loss of AC and result in secondary pollution.[6,45,50] To overcome recyclability problems such as observed with AC, our group has previously developed a redox-responsive polymer gel with tunable hydrophobicity that reversibly adsorbs and releases organics in the presence of water.[5] However, in this case, the redox switching relied on the addition of chemicals, which introduced additional chemical agents to the remediation process, and the efficacy of the chemical stimuli was hampered by mass transfer limitations.[5,61] Therefore, it is desirable to design new adsorbent materials whose redox-responsive hydrophobicity can be tuned using mild electrical stimuli, thereby eliminating the use of chemicals in the regen-

eration process, and ultimately reducing the material waste and operating cost of adsorption technology for wastewater remediation.

2.2 Results and discussion

The electrochemical reversibility of an adsorption process relies on adsorbent materials that are electrically conducting and exhibit tunable affinity for target contaminants in response to electrochemical stimuli. Polypyrrole (PPy) is a promising candidate for enabling electrochemical regeneration due to its intrinsic conductivity, fast electrochemical switching, low operating voltage, and relative ease of fabrication and potential modulation of its hydrophobicity through doping of the polymer with anionic surfactants.[40,65]

2.2.1 Electrochemical modulations of hydrophobicity of the adsorbent

A typical oxidative polymerization reaction of pyrrole yields conducting polymers (CP) in the oxidized state, and hence anions are incorporated into the polymer backbone during synthesis to neutralize the positive charges on the oxidized polymer. The size of the anionic dopants dictates whether the doping and dedoping are associated mainly with cations or anions during subsequent redox reactions of PPy.[79] Small anions can be easily inserted into PPy when it is oxidized and de-inserted when the polymer is reduced, as depicted in Figure 2-1a. However, bulky surfactant anions doped into PPy during synthesis are largely immobile. Therefore, subsequent reduction of the CP is accompanied by insertion of cations from the electrolyte to neutralize the charges of those immobilized surfactant anions (Figure 2-1b).[115]

The choice of anionic dopants also affects the hydrophobicity of the resulting PPy. For example, a PPy film doped with perfluorooctanesulfonate (PFOS) or dodecylbenzenesulfonate (DBS) exhibited hydrophobicity while perchlorate-doped PPy was hydrophilic.[40,120] Moreover, on electrochemical switching of the redox state of PPy

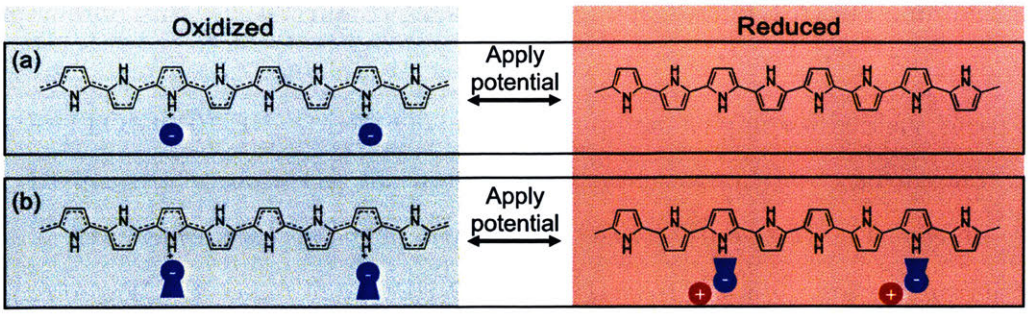

Figure 2-1: Schematic illustrations for two different ion exchange processes during the oxidation and reduction of PPy doped with (a) small anions and (b) bulky surfactant anions.

doped with perfluoro or alkyl sulfonate surfactants, the polymer exhibited changes in hydrophobicity: the oxidized PPy was more hydrophobic than the reduced polymer.[40,120] However, the loss of PFOS during electrochemical reduction of PPy required the use of fluorochemicals during subsequent reoxidation of PPy to replenish the dopants,[8,120] which could result in even worse contamination than caused by the original contaminants.[111] Unlike PFOS, surfactants with long alkyl chains such as DBS are believed to be retained during redox switching, and the re-orientation of the surfactant anions with respect to the PPy results in a hydrophobic/hydrophilic transition.[40,106] Therefore, in this work, we chose to dope PPy with alkyl sulfonates and relied on their bulky hydrophobic tails to modulate the hydrophobicity of PPy. We proposed to take advantage of the one additional alkyl chain in dioctylsulfosuccinate (AOT) to induce larger hydrophobicity swings than possible with DBS-doped PPy. The polypyrroles prepared in this work are identified according to the nomenclature PPy("dopant"). For example, PPy(AOT) refers to polypyrrole doped with AOT.

2.2.1.1 Synthesis of surfactant-doped polypyrrole

The surfactant-doped CP was synthesized by electropolymerizing pyrrole dissolved in an AOT aqueous electrolyte in the presence of a trace amount of bipyrrole (pyrrole dimer, 0.75 mol%). The resulting PPy(AOT) film was deposited on a flexible

commercial carbon fiber cloth substrate and had hierarchical porosity, as observed in the scanning electron microscopy (SEM) images (Figure 2-2a); this porous polymer is denoted as P-PPy(AOT). In contrast, electropolymerization in the absence of bipyrrole yielded a compact non-porous film, denoted as NP-PPy(AOT) (Figure 2-2b). The surface roughness factor derived from the 3D atomic force microscopy (AFM) images (Figure 2-2c-d), defined as the ratio of the actual surface area and the projected surface area,[10] was 1.92 and 1.07 for P-PPy(AOT) and NP-PPy(AOT), respectively. A nearly doubling in surface roughness in P-PPy(AOT) further supports the observation of porosity enhancement in the CP electropolymerized in the presence of bipyrrole. Despite the difference in morphology, the chemical compositions of P- and NP-PPy(AOT) were identical as evident by the Fourier-transform infrared spectroscopy and X-ray photoelectron spectroscopy (XPS) spectra (Figure 2-3). The characteristic peaks of the polymer and the dopant aligned in the FT-IR spectra: 1740 cm^{-1} for C=O groups of AOT, 1470 cm^{-1} for conjugated ring stretching, 1250 cm^{-1} for C-N bonds, and 1050 cm^{-1} for N-H bonds of pyrrole.[102] The sulfur (S) peaks in XPS spectra also confirmed the presence of AOT dopants within the CP in both cases.

2.2.1.2 Electrochemical tunability in the hydrophobicity of surfactant-doped PPy

To examine the electrochemical modulations of the hydrophobicity of the surfactant-doped polymer, the contact angle of a water droplet was measured on the surfaces of various PPy samples coated on stainless-steel substrates (Figure 2-4a). The greater the contact angle, the more hydrophobic is the surface. Larger water contact angles were measured on all three types of oxidized PPy films, namely P-PPy(AOT), NP-PPy(AOT) and P-PPy(DBS), compared with their respective reduced films (Figure 2-4c-e, Table 2.1).

Furthermore, it has been established in the literature that both composition effects and geometrical structure influence the hydrophobicity of a surface.[30] That is, both the type of dopant and the porosity of the film affected the hydrophobicity

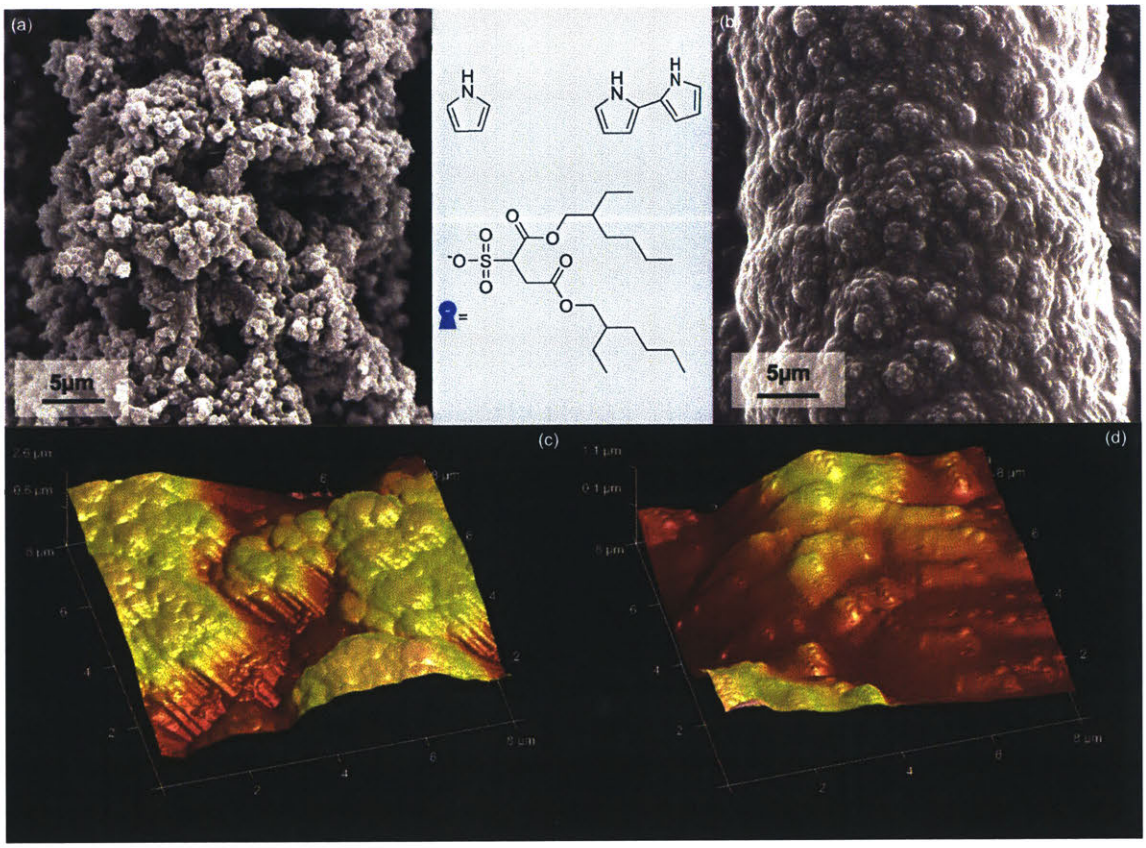

Figure 2-2: (a)An SEM image of porous AOT-doped PPy film electropolymerized and deposited on a carbon fiber cloths substrate in the presence a trace amount of bipyrrole (0.75 mol%), denoted as P-PPy(AOT), and structures of pyrrole monomer, bipyrrole, and an AOT surfactant. (b) An SEM image of compact AOT-doped PPy film electropolymerized without bipyrrole, denoted as NP-PPy(AOT). 3D AFM images showing height variations on the surface of (c) P-PPy(AOT) and (d) NP-PPy(AOT) films.

Table 2.1: Contact angle measurements of a water droplet on the surface of stainless-steel substrates coated with PPy films doped with AOT or DBS in oxidized or reduced states.

Polymer Film	Oxidized	Reduced	Difference
P-PPy(AOT)	$152.1° \pm 1.8°$	$43.8° \pm 3.1°$	108°
NP-PPy(AOT)	$55.6° \pm 4.2°$	$13.3° \pm 1.9$	42°
P-PPy(DBS)	$117.1° \pm 2.5°$	$22.5° \pm 2.2$	95°

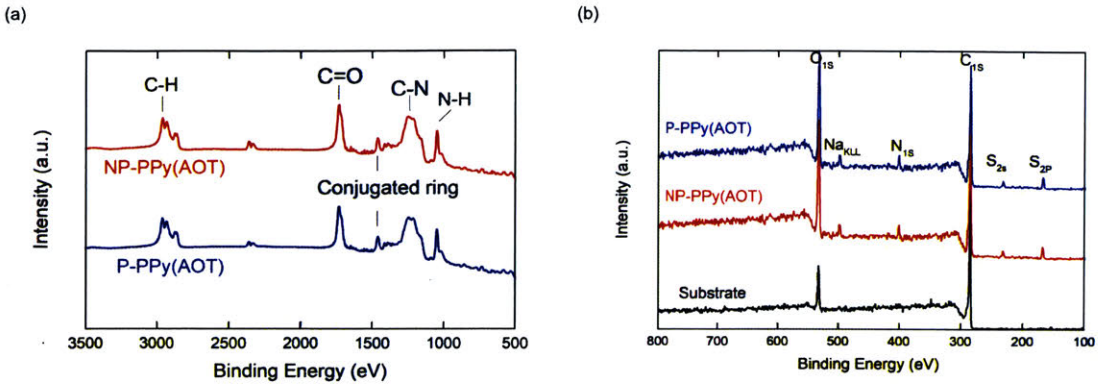

Figure 2-3: (a) FT-IR spectra of P-PPy(AOT) (blue) and NP-PPy(AOT) (red). (b) XPS survey scans of the pristine carbon fiber paper (black), P-PPy(AOT) (blue) and NP-PPy(AOT) (red) indicate the presence of oxygen, sodium, nitrogen, carbon and sulfur elements in the polymer.

of PPy. Although similar morphological behavior was observed in the NP- and P-PPy(DBS) (Figure 2-5), P-PPy(AOT) was more hydrophobic than P-PPy(DBS) in both the oxidized and reduced states (Table 2.1). This validates our hypothesis that AOT dopants can increase the hydrophobicity of the polymer over that of DBS owing to its additional alkyl chain. More importantly, a larger difference in contact angles between oxidized and reduced states was observed in P-PPy(AOT) than in P-PPy(DBS) (108° vs 95°), suggesting AOT is the better dopant as it increases the window for hydrophobicity switching.

On the other hand, surface roughness can induce the so-called "lotus effect" and its impact on water contact angles can be characterized by the Wenzel model[56]

$$cos\alpha = rcos\alpha_0 \tag{2.1}$$

where α_0 is the water contact angle on an ideal, smooth and homogeneous PPy(AOT) surface and r is the surface roughness factor measured using AFM. The rougher surface of P-PPy(AOT) renders its oxidized state superhydrophobic ($152.1° \pm 1.8°$), as well as amplifies the difference between its oxidized and reduced states in comparison with that of NP-PPy(AOT) (108° vs 42°).[17] Contact angle measurements suggest that P-PPy(AOT) is the most promising candidate for an electrochemically regener-

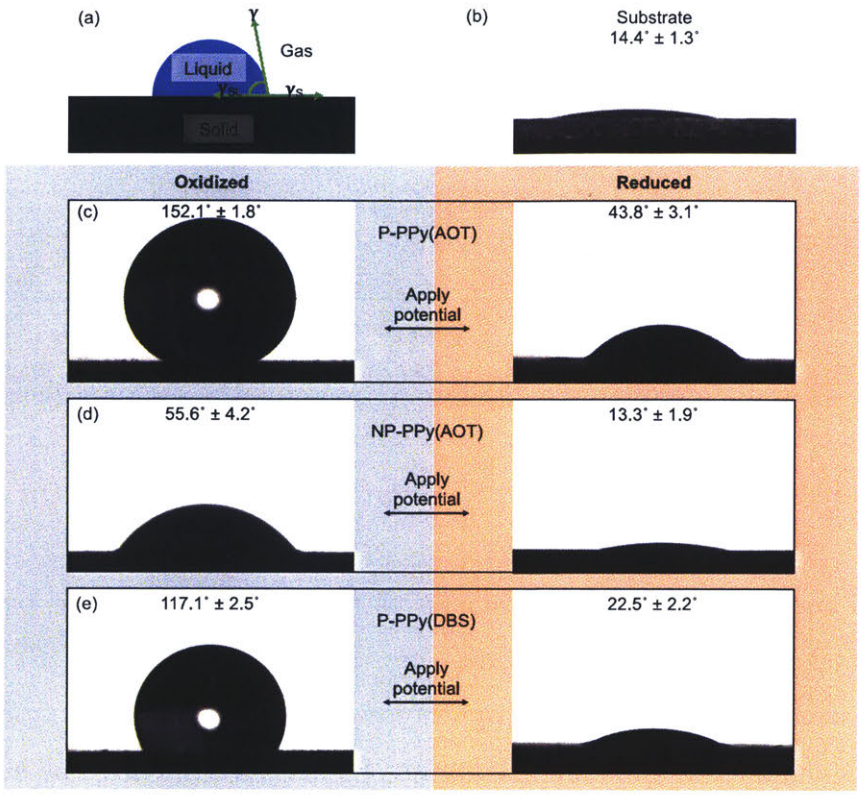

Figure 2-4: (a) Schematic of a water droplet on a solid surface and the related contact angles and surface tensions. (b) The surface of the stainless-steel substrate is hydrophilic with a contact angle of $14.4° \pm 1.3°$. Redox-responsive hydrophobicity for (c) P-PPy(AOT), (d) NP-PPy(AOT), and (e) P-PPy(DBS) coated on stainless-steel substrates. The surface is rendered more hydrophilic upon electrochemical reduction, as evident by decreases in water contact angles.

able adsorbent, with a superhydrophobic oxidized state for adsorption and a larger hydrophobicity disparity to lower the affinity for organics in the reduced state and thereby drive desorption.

2.2.1.3 Electrochemically modulated affinity for organics

It is important for the ability to electrochemically modulate the hydrophobicity of surfactant-doped PPy to be translated into affecting the affinity of the polymer towards organic pollutant molecules. Herein, three model compounds were selcted, namely Sudan Orange G (SOG), a neutral organic molecule representing an impor-

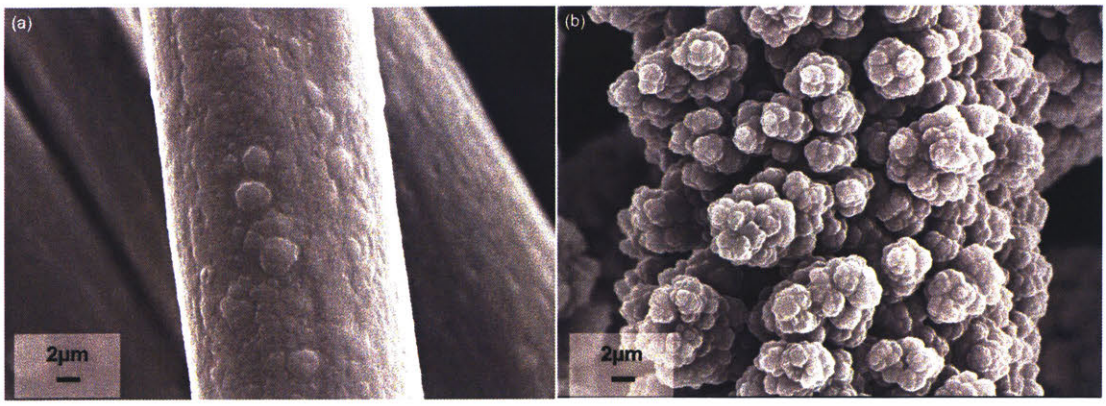

Figure 2-5: SEM images of (c) NP-PPy(DBS) and (d) P-PPy(DBS).

tant class of organic pollutant—azo dye molecules widely used in textile, paper, food, cosmetics, and pharmaceutical industries; propranolol hydrochloride (PP), a beta-blocking pharmaceutical agent; and Bisphenol A (BPA), a component of plastics and epoxy resins and also an endocrine disruptor. Figure 2-6 compares the equilibrium distribution coefficient (L g^{-1} polymer) defined as

$$K_d = Q_e/C_e \tag{2.2}$$

which is the ratio of the amount of pollutant adsorbed per gram of polymer (Q_e) to the concentration of pollutant in the solution phase (C_e), for SOG and PP at an initial concentration of 0.01 mM, and BPA at 0.02 mM, in contact with the oxidized and reduced NP-PPy(AOT) and P-PPy(AOT) coated on carbon fiber cloths. The oxidized NP- and P-PPy(AOT) both demonstrated a greater K_d than did the respective reduced polymers, indicating that oxidation of PPy(AOT) activated the polymer to exhibit higher affinity for the neutral organic molecules. In particular, the difference in K_d between the oxidized and reduced states was even more dramatic for P-PPy(AOT), in agreement with the earlier observation of a larger disparity in contact angle measurements in the more porous film. The highly porous morphology also increased the surface area of of PPy(AOT) for adsorbing organic molecules. For example, the equilibrium SOG distribution coefficient for the oxidized P-PPy(AOT)

($K_d = 44.1$) was 3.3 times higher than for oxidized NP-PPy(AOT) ($K_d = 13.3$).

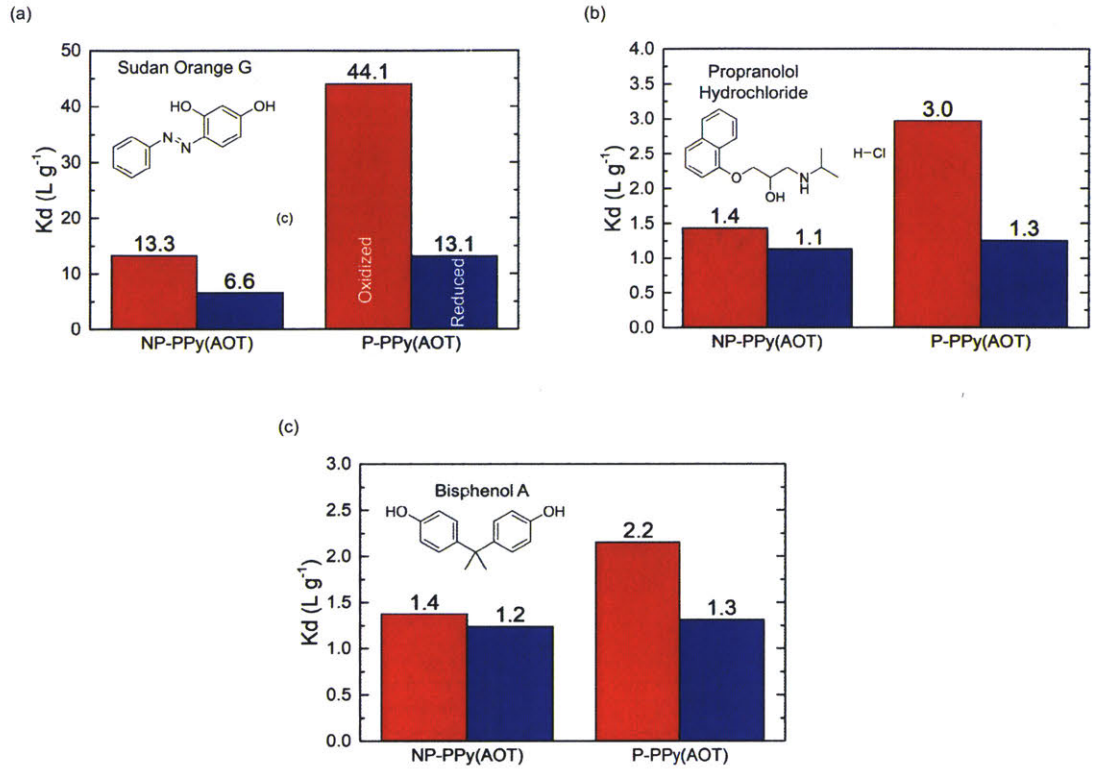

Figure 2-6: Equilibrium distribution coefficient K_d of (a) SOG, (b) PP, and (c) BPA.

The adsorption thermodynamics of the better-performing P-PPy(AOT) are presented in Figure 2-7. In the low concentration regime, the experimental data can be fitted with linear isotherms, indicating operation in the Henry's Law regime (Figure 2-7a, c-d). The larger slope of the curve for the oxidized P-PPy(AOT) (the Henry's Law constant) further confirmed its stronger affinity for the organic molecules. The capacity of the P-PPy(AOT) for adsorbing SOG from water was also tested over a wide range of concentrations (Figure 2-7b), which can be fitted well with the Freundlich adsorption isotherm

$$Q_e = kC_e^{1/n} \tag{2.3}$$

The Freundlich exponent $1/n$ is related to favorability of adsorption—the degree of favorability increases as $1/n$ approaches zero.[47] For oxidized and reduced P-PPy(AOT), the fitted $1/n$ values were 1.5 and 1.8, respectively, consistent with the fact that the

oxidized polymer has higher affinity for SOG. Moreover, the equilibrium solid phase concentration reached a maximum of 578 mg SOG per g polymer when the initial liquid phase concentration was at the solubility limit. The fitting parameters for both Freundlich and Henry's Law isotherms can be found in 2.2 for SOG, as well as in Table 2.3 for PP and Table 2.4 for BPA.

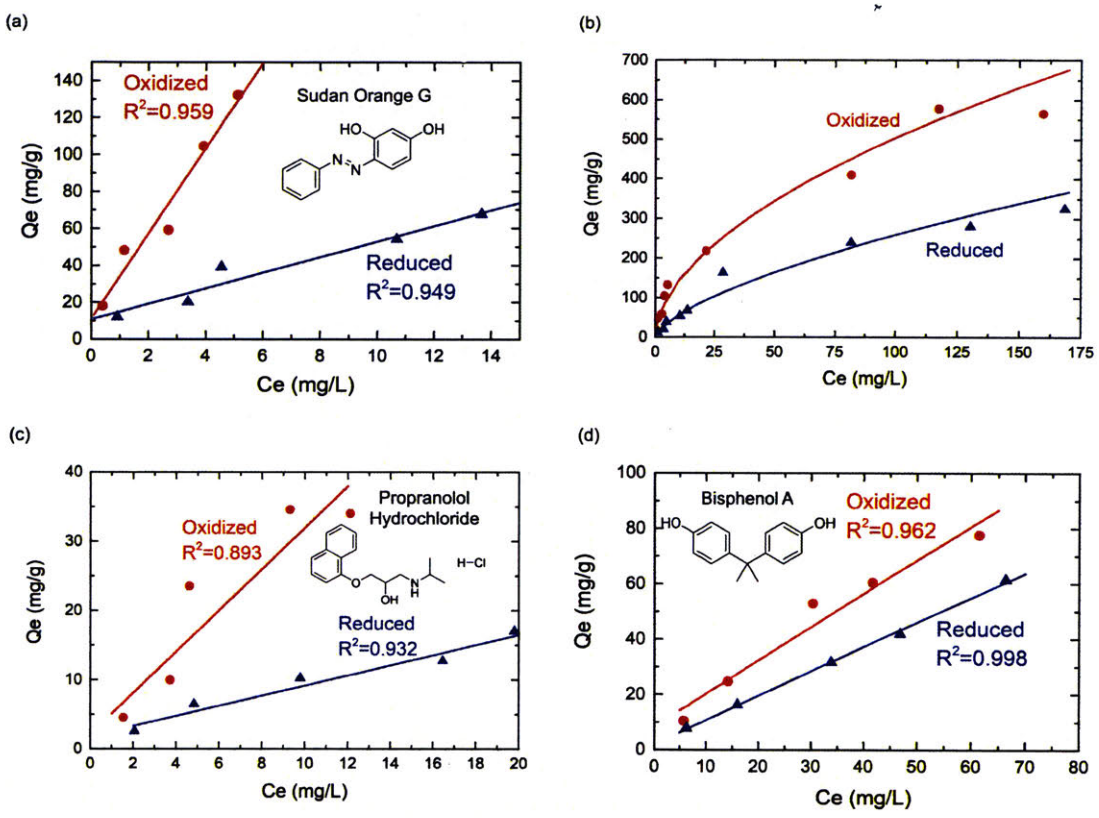

Figure 2-7: Adsorption isotherms of (a) SOG, (c) PP, and (d) BPA in oxidized and reduced states fitted with the linear model in the low concentration regime. (b) Equilibrium adsorption for a wide range of SOG concentrations fitted with the Freundlich isotherm. Line: fitted isotherms; Symbols: experimental data; Red: oxidized; Blue: reduced.

Table 2.2: Fitting parameters of Freundlich and linear isotherms of SOG on P-PPy(AOT).

State	Freundlich isotherm $ln(Q_e) = ln(k) + \frac{1}{n}ln(C_e)$			Linear isotherm $Q_e = aC_e + b$		
	$ln(k)$	$1/n$	R^2	a	b	R^2
Oxidized	-1.5	1.5	0.975	23.1	10.9	0.959
Reduced	-2.8	1.8	0.974	4.2	10.7	0.949

Table 2.3: Fitting parameters of linear isotherms of PP on P-PPy(AOT).

State	Linear isotherm $Q_e = aC_e + b$		
	a	b	R^2
Oxidized	3.0	2.1	0.893
Reduced	0.7	1.9	0.932

Table 2.4: Fitting parameters of linear isotherms of BPA on P-PPy(AOT).

State	Linear isotherm $Q_e = aC_e + b$		
	a	b	R^2
Oxidized	1.2	8.2	0.962
Reduced	0.9	1.9	0.998

2.2.2 Investigations of molecular interactions

The ability to modulate the hydrophobicity and the affinity for organics electrochemically in surfactant-doped CP, as reflected by changes in the water contact angles and adsorption affinity after application of redox stimuli, has been attributed to a reorientation of the surfactant molecules.[40,106] In the oxidized state of PPy, AOT or DBS anions with the negatively charged sulfonate group are bound to the positively charged PPy backbone via electrostatic attractions, leaving the alkyl chains pointing away from the polymer backbone. The hydrophobic alkyl chains constitute the surface layer of the polymer film, causing a relatively large water contact angle. In the reduced state, on the other hand, the PPy backbone becomes less positively charged, if not completely neutral. The absence of the electrostatic attractions between AOT

and PPy allows AOT molecules to rotate freely and rearrange themselves such that more sulfonate groups and fewer alkyl chains are exposed at the outermost surface, rendering the surface hydrophilic and decreasing the water contact angle. During the reduction process, sodium ions from the supporting electrolyte might also enter the PPy film to neutralize the charges of the immobilized anions.

2.2.2.1 Physico-chemical interactions in the PPy(AOT) complex

To validate the aforementioned hypothesis about surfactant reorientation upon oxidation/reduction of the PPy backbone, the surfactant-PPy interactions in the oxidized and reduced states were studied using a combination of density functional theory (DFT) and molecular dynamics (MD). A minimal model system was constructed with a PPy oligomer consisting of eight pyrrole repeating units and two AOT doping anions. These choices were made based on earlier literature reports that various physical properties of the PPy polymer have converged with as few as six to eight repeating units,[64,68,85,107] and that usually one electron is removed from every four pyrrole units when a PPy complex is oxidized resulting in a 4:1 stoichiometric ratio of pyrrole to dopant.[44] In addition, abundant water molecules and a few sodium (Na^+), chloride (Cl^-) and hydroxide (OH^-) ions were introduced to model the aqueous electrolyte environment in which the redox process takes place in the actual experiments, as well as to balance the charges of the system.

The geometries of the isolated PPy oligomers in oxidized (with two positive charges) and reduced (neutral) states and that of an isolated AOT anion were optimized independently using the B3LYP+D3 exchange-correlation functional at the 6-31G* level in Q-Chem 5.0.[12,32,54,91] The oxidized PPy oligomer backbone is more planar compared to its reduced counterpart due to its higher conjugation and conductivity (Figure 2-8a,b). An AOT anion with its geometry optimized in vacuum is shown in Figure 2-8c.

The PPy(AOT) complex was then constructed by placing two AOT dopants close to an oxidized or reduced PPy oligomer whose configurations were obtained from gas-phase optimizations. Using the same approach and package, the geometries of

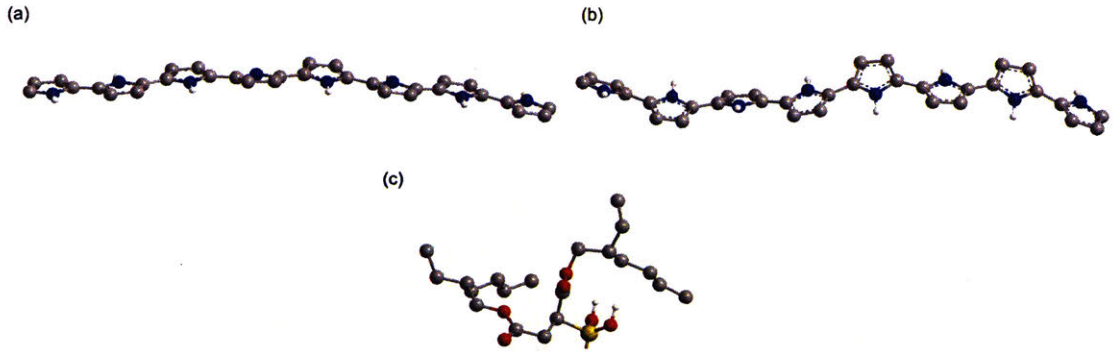

Figure 2-8: Optimized geometries of individual PPy oligomers consisting of 8 repeating units in (a) oxidized and (b) reduced states, and (c) an AOT anion. Only polar hydrogen atoms are shown.

the PPy(AOT) complex were optimized by allowing the two AOT to relax around the frozen PPy oligomers. To improve the accuracy of the subsequent MD simulations, the partial charge associated with each atom in PPy and AOT was evaluated based on the CHarges from ELectrostatic Potentials using a Grid-based (CHELPG) method53 at a more accurate B3LYP+D3/6-311G** level in Q-Chem 5.052 and later implemented as a modification to the latest OPLS/AA force field[12,54] that was used for MD simulations. The DFT-optimized geometries of the PPy(AOT) complexes in the gas phase (Figure 2-9) provided initial configurations for the MD simulations in an aqueous environment. The interactions of AOT and PPy in the aqueous environment were studied using MD simulations in GROMACS 5.1.[76] The initial configuration of the simulation system for the oxidized PPy(AOT) complex was generated in Packmol[63] by randomly placing 4 Na^+ cations, 2 Cl^- anions, 2 OH^- anions, and 2131 water molecules around the optimized oxidized PPy(AOT) geometry, while that associated with the reduce PPy(AOT) complex included 4 Na^+ cations, 2 Cl^- anions and 2133 water molecules. Each system was contained in a 4 nm $\times$ 4 nm $\times$ 4 nm cubic box with periodic boundary conditions (PBC) on all surfaces. An energy minimization was performed to optimize both initial configurations using the conjugate gradient (CG) method with a minimum energy step size of 0.01 kJ mol^{-1} and a maximum force of 10 kJ mol^{-1} nm^{-1}. The production NVT simulations (constant number (N), volume (V), and temperature (T)) were performed at 298 K using a Nose-Hoover

thermostat for 100 ps at a time step of 1 fs. Both systems were equilibrated within the first 1 ps as indicated by their stabilized temperatures. The complete MD trajectories are captured in Movies 1 and 2 in Appendix B.

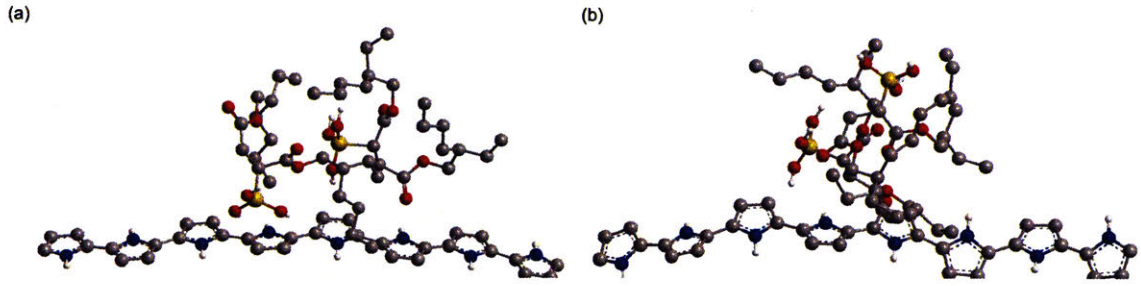

Figure 2-9: DFT-optimized geometries of PPy(AOT) complexes in the (a) oxidized and (b) reduced states showing the distinct orientations of AOT dopants relative to the PPy backbone. The atomic color schemes include: Gray (carbon), Blue (nitrogen), Yellow (sulfur), Red (oxygen). White (polar hydrogen atoms).

In agreement with the aforementioned assertion, the MD trajectory of the oxidized PPy(AOT) complex shows that the sulfonate groups constituting the hydrophilic heads of the AOT anions exhibit strong electrostatic attractions with the oxidized and positively charged PPy backbone and orient themselves towards PPy (Figure 2-10a, Movie 1 in Appendix B). In contrast, upon an artificial "reduction" of PPy, the hydrophilic heads of the AOT anions tend to reorient away from the neutral PPy backbone due to the decreased strength of attractions and eventually constitute the surface layer of the PPy film (Figure 2-10b, Movie 2 in Appendix B). Our DFT-MD calculations show that the minimum distance between a sulfur atom in the hydrophilic heads of AOT and a carbon atom in the polymer backbone increases from 6.01 ± 0.64 Å to 6.75 ± 0.43 Å upon reduction (Figure 2-11a). Moreover, the binding of AOT to PPy is stronger when the polymer is oxidized, regardless of the media considered (Figure 2-11b). The changes in distance and binding energy of AOT and PPy render a quantitative description of the reorientation.

The interaction between AOT and PPy was analyzed for oxidized and reduced states based on the results of the MD simulations. One hundred and one snapshots of the MD trajectories were extracted, with an interval of 1 ps starting from 0 ps. For each snapshot, we evaluated the binding energy (E_{bind}) between the PPy oligomer

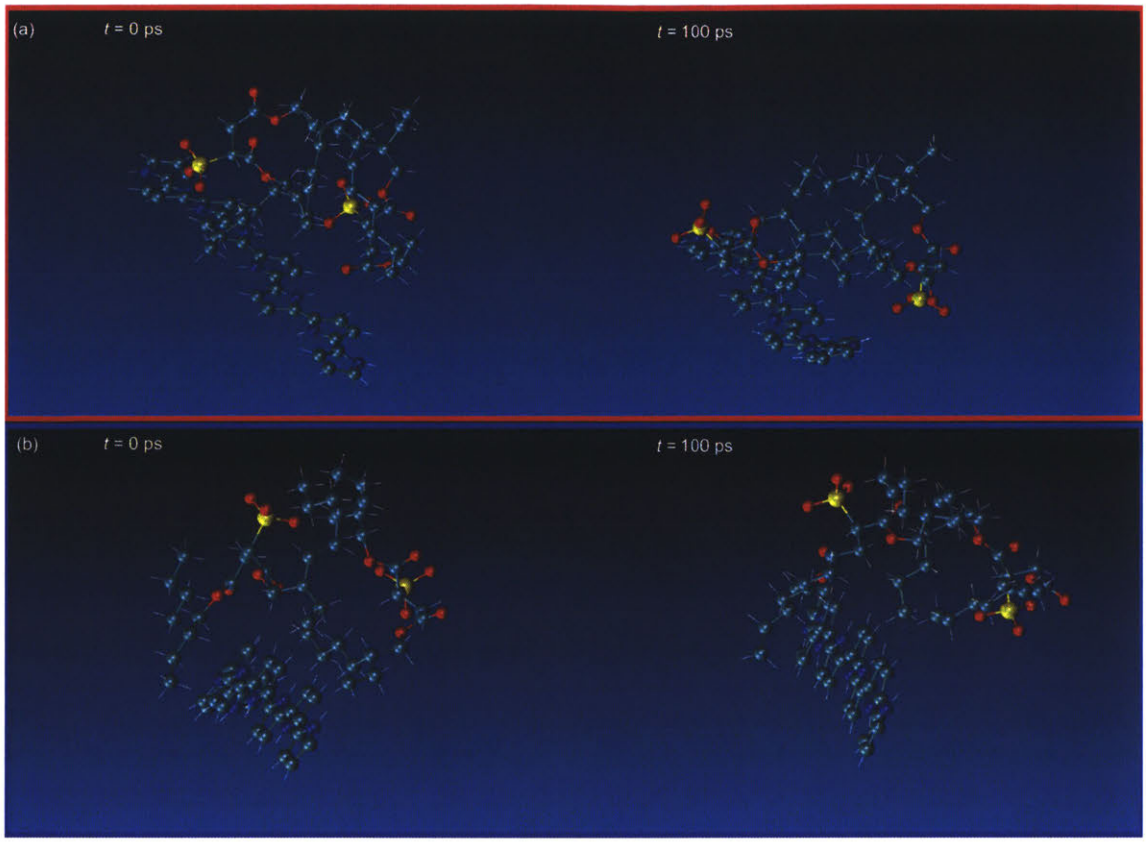

Figure 2-10: Snapshots of MD simulations of (a) oxidized and (b) reduced PPy(AOT) complexes in aqueous solutions at $t = 0$ ps and 100 ps. All hydrogen atoms are shown as white sticks.

and a single AOT anion in the gas phase and the aqueous solution,

$$E_{bind}[PPy(AOT)] = \frac{E(PPy) + E(AOT) - E[PPy(AOT)]}{2} \tag{2.4}$$

A similar equation was applied to evaluate the binding energy between PPy and the chloride anion (Cl^-). To quantify the physico-chemical nature of the interaction between PPy and AOT, a detailed energy decomposition analysis was conducted based on absolutely-localized molecular orbitals (ALMO-EDA)[9,37,38] in the gas phase and with the binding energy (E_{bind}) broken down into the attraction from electrostatic interaction (E_{elec}), dispersion (E_{disp}), polarization (E_{pol}) and charge transfer (E_{CT}), and the repulsion from Pauli principle (E_{Pauli})[73]:

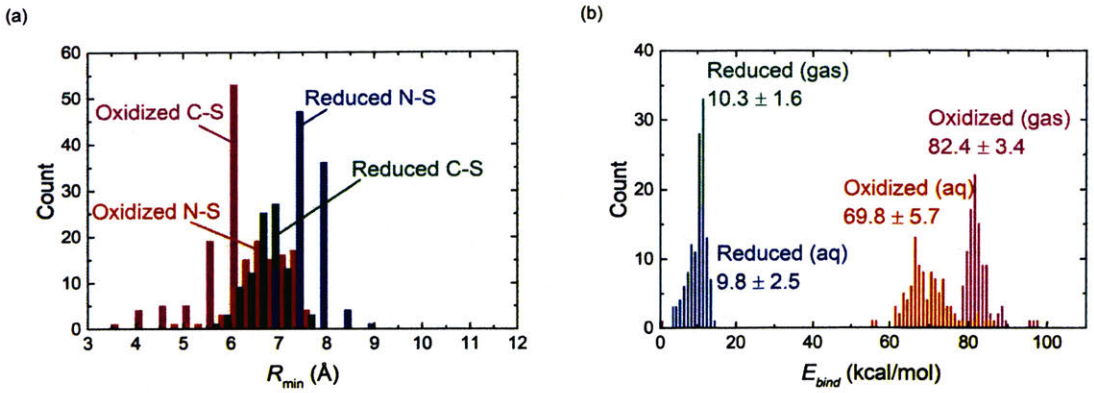

Figure 2-11: Statistical results of (a) minimum distance (Å) between one of the sulfur atoms in AOT and one of the carbon or nitrogen atoms in PPy. (b) Statistical results of total binding energy (kcal mol^{-1}) between AOT and PPy in the gas phase and the aqueous solution in oxidized and reduced states.

$$E_{bind} = E_{elec} + E_{disp} + E_{pol} + E_{CT} + E_{Pauli} \tag{2.5}$$

The gas-phase calculations were performed using DFT and the solution-phase simulations were accomplished using a hybrid quantum mechanical/molecular mechanical (QM/MM) approach in which PPy and AOT were treated quantum mechanically while other ions and solvents were treated molecular mechanically, at the B3LYP+D3/6-31G* level using Q-Chem 5.0.[91] The statistical results for E_{bind} from all snapshots are summarized in Figure 2-11. Our evaluations show that the difference in E_{bind} between PPy and AOT between oxidized and reduced states is dramatic, and that the stronger attraction between PPy and AOT when PPy is oxidized results in a smaller distance between the dopant and polymer.

The total binding energy E_{bind} of the oxidized PPy(AOT) complex (69.8 ± 5.7 kcal mol^{-1} in the aqueous environment and 82.4 ± 3.4 kcal mol^{-1} in the gas phase) is approximately seven to eight times that of the reduced PPy(AOT) complex (9.8 ± 2.5 kcal mol^{-1} in the aqueous environment and 10.3 ± 1.6 kcal mol^{-1} in the gas phase), corroborating the observed shorter distance between AOT and PPy when it is oxidized (Figure 2-11b). The total binding energies calculated in the gas phase agree well with those obtained from the aqueous environment, and the slight overestimation in the

gas phase can be ascribed to the partial screening of electrostatic and polarization interactions between AOT and PPy by water.[116]

The difference of these non-covalent interactions between AOT and PPy in oxidized and reduced states was quantified and deconvoluted the relevant contributions of the intermolecular interactions using energy decomposition analysis based on absolutely-localized molecular orbitals (ALMO-EDA).[9,37,38] The gas-phase ALMO-EDA shows that the electrostatic attraction E_{elec} contributes to the majority of the enhanced interactions between AOT and oxidized PPy—the value of E_{elec} of the oxidized PPy(AOT) is almost seven times higher than that of the reduced PPy(AOT) (Table 2.5, 66.7 ± 4.4 kcal mol^{-1} vs 9.9 ± 3.3 kcal mol^{-1}). The charge-transfer stabilization E_{CT} in oxidized PPy(AOT) is an order of magnitude higher than its reduced counterpart (9.8 ± 2.5 kcal mol^{-1} vs 0.8 ± 0.4 kcal mol^{-1}), although the charge-transfer contribution is smaller than can be attributed to electrostatics. Other non-bonding interactions include Pauli repulsion E_{Pauli}, dispersion stabilization E_{disp}, and polarization stabilization E_{pol}, which remain almost unaffected in the redox process. In addition, although the reduced PPy(AOT) complex exhibits a weaker interaction, its intermolecular binding in the aqueous environment (9.8 ± 2.5 kcal mol^{-1}) is still twice as strong as a typical hydrogen bond in water (4 to 5 kcal mol^{-1}),[95] and much higher than the binding of chloride anions to reduced PPy (2.1 ± 0.6 kcal mol^{-1}), enough to prevent AOT from straying away from PPy at room temperature.

Table 2.5: Statistical results of binding energies and their energy decomposition analysis (EDA) between PPy and an AOT anion (in kcal mol^{-1}) in the gas phase.

State	Binding E_{bind}	Electrostatic E_{elec}	Pauli Repulsion E_{Pauli}	Dispersion E_{disp}	Polarization E_{pol}	Charge Transfer E_{CT}
Oxidized	82.4 ± 3.4	66.7 ± 4.4	-10.2 ± 3.0	11.9 ± 1.7	4.3 ± 1.4	9.8 ± 2.5
Reduced	10.3 ± 1.6	9.9 ± 3.3	-13.5 ± 4.4	10.5 ± 1.6	2.6 ± 0.6	0.8 ± 0.4

Our DFT calculations and MD simulations provided theoretical and quantitative evidence for surfactant reorientation during redox reactions of PPy, which in turn leads to the changes in hydrophobicity of the polymer observed on the macroscopic scale.

2.2.2.2 Adsorbent-adsorbate interactions

The configurational study of oxidized and reduced PPy(AOT) complexes reveals the geometric rearrangement in the complex in response to electrochemical redox stimuli. This warrants further exploration of the molecular interactions between the PPy(AOT) complex in different oxidation states and the adsorbate molecule. DFT calculations in the gas phase are sufficient for providing representative molecular configurations and qualitative assessment of the adsorbate-adsorbent interaction energies.[99] The interaction between the PPy(AOT) adsorbent and the SOG adsorbate was explored using gas-phase DFT calculations and ALMO-EDA at the at the B3LYP+D3/6-31G* level using Q-Chem 5.0.[91] In the initial geometry, the SOG molecule was placed in parallel with the PPy backbone and was then allowed to relax around the frozen PPy(AOT) complex.

The optimized geometry of an isolated SOG molecule (Figure 2-12a) is planar owing to the delocalized π-conjugation across two aromatic rings connected via the aryl azo structure. The introduction of the reduced PPy(AOT) complex allows the SOG to orient itself in parallel with the conjugated PPy backbone due to a $\pi - \pi$ stacking interaction (Figure 2-12b, Movie 3 in Appendix B. In addition to the $\pi - \pi$ interaction, in the oxidized PPy(AOT) complex the distance between the hydrogen atom in one of the hydroxyl groups of SOG and one of the oxygen atoms the in the sulfonate group of AOT can be as short as 2.66 Å, forming a moderate to strong hydrogen bond and bending one of the aromatic rings in SOG by 27.0° (Figure 2-12c, Movie 4 in Appendix B).

An auxiliary ALMO-EDA study shows that the binding energies between SOG and PPy(AOT) in the reduced and oxidized states are 12.90 kcal mol^{-1} and 24.47 kcal mol^{-1}, respectively. The enhanced adsorbate-adsorbent interactions when PPy(AOT) is oxidized is due to a combination of strong electrostatic, polarization and charge-transfer interactions while the dispersion stabilization is dominant when PPy(AOT) is reduced. Intuitively, the small distance and the hydrogen bonds foster a higher affinity of SOG to the oxidized PPy(AOT) in which the sulfonate groups of AOT

orient towards the PPy backbone to allow stronger adsorbate-adsorbent interactions. The mechanistic understanding of the interaction of the PPy(AOT) complex with SOG suggests the electrochemical redox process of PPy(AOT) can mediate the separations of uncharged aromatic contaminant species containing hydrogen bond donors. Hydrogen bond donors are present in many neutral organic contaminants, including the two aforementioned species propranolol hydrochloride and Bisphenol A, as well as a wide array of micropollutants due to the use of industrial chemicals, biocides, and pharmaceuticals and personal care products.[6]

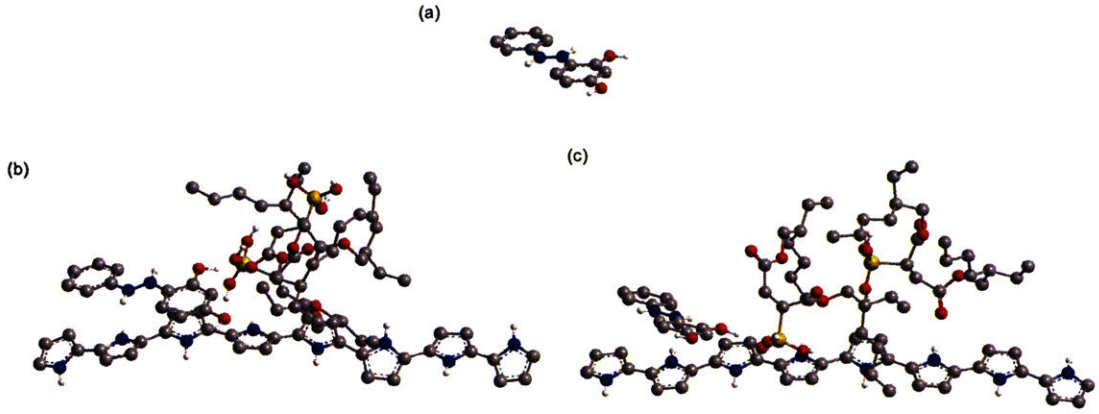

Figure 2-12: Optimized geometries of (a) a Sudan Orange G molecule interacting with (b) reduced, and (c) oxidized PPy(AOT) complexes.

2.2.3 Highly porous morphology of the adsorbent

Besides the ability to respond to the electrochemical redox stimuli and modulate affinity for contaminant molecules, the P-PPy(AOT)-based adsorbent also has a key feature—a highly porous morphology—which manifests three-fold benefits over the NP-PPy(AOT): surface roughness for leading to superhydrophobicity in oxidized P-PPy(AOT),[17,30,52,72,120] high surface area for adsorbing pollutant molecules as evidenced by higher K_d values described above, and porous structure for exposure to electrolyte solution during the electrochemical redox reaction,[104] as discussed below.

2.2.3.1 Enhanced electrochemical responses

The porosity of P-PPy(AOT) significantly enhances the electrochemical performance of the electrode by increasing the exposure of the polymer to the electrolyte solution during electrochemical redox reactions.[104] Both types of PPy(AOT) demonstrated a pair of redox peaks: the anodic and cathodic peaks observed in their cyclic voltammetry (CV) profiles are around - 0.8 V and - 0.4 V (vs Ag/AgCl), characteristic of expulsion and insertion of sodium (Na^+) ions, respectively (Figure 2-13a).[94] However, NP-PPy(AOT) exhibited a pair of less prominent redox peaks, a larger peak separation, and smaller current density, suggesting that the Na^+ reaction kinetics was slower, likely due to reduced surface accessibility.[35] Specific capacitance of the P- and NP-PPy(AOT) was calculated from the CV curves at various scan rates according to the equation:

$$C = \frac{\int I dV}{2vmV} \tag{2.6}$$

where C is the specific capacitance (F g^{-1}) based on the mass of polymer, I is the current (A), V is the potential window (V) and v is the potential scan rate (V s^{-1}). Figure 2-13b reveals that the specific capacitance of P-PPy(AOT) is more than double that of NP-PPy(AOT) at various scan rates ranging from 1 to 50 mV s^{-1}. The superior electrochemical performance of P-PPy(AOT), as evidenced by the shape of the CV curve and higher specific capacitance, can be attributed to the larger surface area afforded by the microstructures in P-PPy(AOT) for interaction with the electrolyte. The CV profiles also suggested that potentials of + 0.5 V and - 0.8 V (vs Ag/AgCl) be applied for driving complete oxidation and reduction of PPy(AOT) films, respectively.

The high-resolution N1s core-level XPS spectra of oxidized and reduced P-PPy(AOT) can be deconvoluted into 4 peaks with increasingly higher binding energies for increasingly more positively charged nitrogen, namely imine (=N-) at 398.7 eV, neutral amine (-NH-) at 399.8 eV, nitrogen atoms with delocalized positive charge (400.5 eV), and positivity charged amine nitrogen ($-NH^+-$) (402.4 eV) (Figure 2-13c and d).[49,66] The lower shoulder at higher binding energies and higher shoulder at lower binding energies of the reduced P-PPy(AOT) confirm it contains higher portions of neutral

nitrogen atoms than does the oxidized polymer. This confirms the redox actuations of the AOT doped PPy.

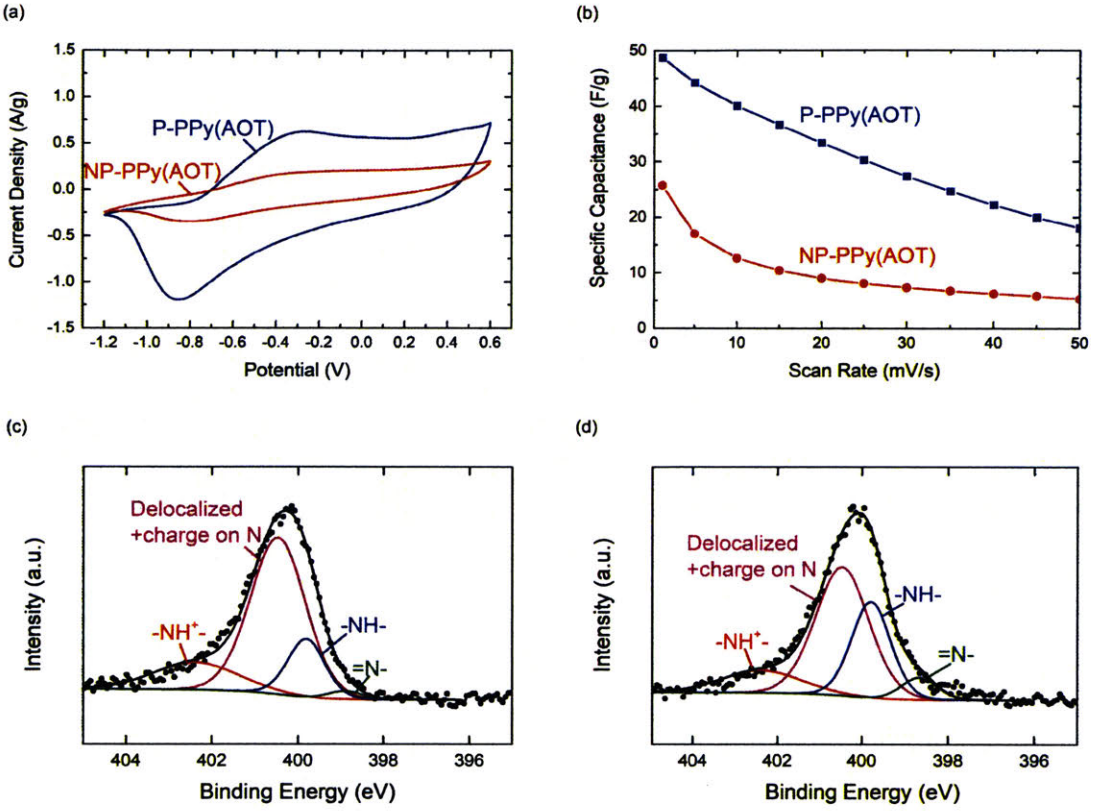

Figure 2-13: (a) CV profiles of P-PPy(AOT) (Blue) and NP-PPy(AOT) (Red) at various scan rates in 0.1 M NaCl. (b) The specific capacitance of P-PPy(AOT) (Blue) and NP-PPy(AOT) (Red) as a function of CV scan rates. High-resolution XPS scans of N1s of (c) oxidized and (d) reduced P-PPy(AOT).

2.2.3.2 Formation of the Porous Morphology

The highly porous structures offer many benefits to P-PPy(AOT) as an electrochemically regenerable adsorbent. It is therefore of interest to understand mechanistically the formation of the morphology. Previous studies have reported that the amphiphilic nature of AOT can influence the morphology of PPy by aligning the monomers during chemical oxidative polymerization.[13,42] In order to investigate the impact of bipyrrole alone on the morphology of the electropolymerized PPy and exclude any confounding

factors associated with AOT, sodium chloride (NaCl) solution was used as the electrolyte to provide chloride ions (Cl^-) for doping the polymer. A similar phenomenon was observed: the addition of bipyrrole induced hierarchical porous structures in the PPy(Cl) film (Figure 2-14b and c), suggesting that the formation of the unique morphology in the PPy film, independent of the doping anions, was due to the presence of bipyrrole in the electropolymerization bath.

Figure 2-14a illustrates schematically our hypothesis for the morphological evolution of electropolymerized PPy in the presence of bipyrrole which induced temporally segregated growth of the fibrillar and the granular structures. The two types of microstructures combined to form a highly porous interconnecting network of PPy aggregates. The electropolymerization of pyrrole begins with the oxidation of monomers to form radical cations which then react with other monomers present in the solution to form dimers, oligomers and eventually the polymer.[82] The extended conjugation in the PPy oligomers or polymers lowers the oxidation potential compared to that of the monomer.[82] As a result, the slow dimerization of pyrrole is the rate-limiting step.[105] This explains the shape of the potential-time curves of the galvanostatic electropolymerization process of NP-PPy(Cl) formed in the absence of bipyrrole — the potential decreased at early times and eventually leveled off (Figure 2-15a).

The introduction of pyrrole dimers to the electropolymerization bath accelerated the rate of polymerization by allowing chain extension to occur from the added bipyrrole nuclei before pyrrole monomers completed the slow dimerization step on the electrode surface. Sufficiently fast polymerization favors homogeneous nucleation and generates nanofibrillar structures,[105] which are observed to be embedded in granular PPy(Cl) networks in the high-resolution scanning electron microscopy (HRSEM) image (Figure 2-14b). As these oligomeric nanofiber chains surpassed the solubility limit, they precipitated onto the electrode surface. At later times, dimerization of pyrrole monomers occurred on the electrode surface or along the PPy nanofibers previously formed. Due to the retardation of dimerization and high concentration of pyrrole monomers, heterogeneous nucleation was dominant at later stages and resulted in the growth of granular PPy particles on the PPy nanofibrillar structures, as

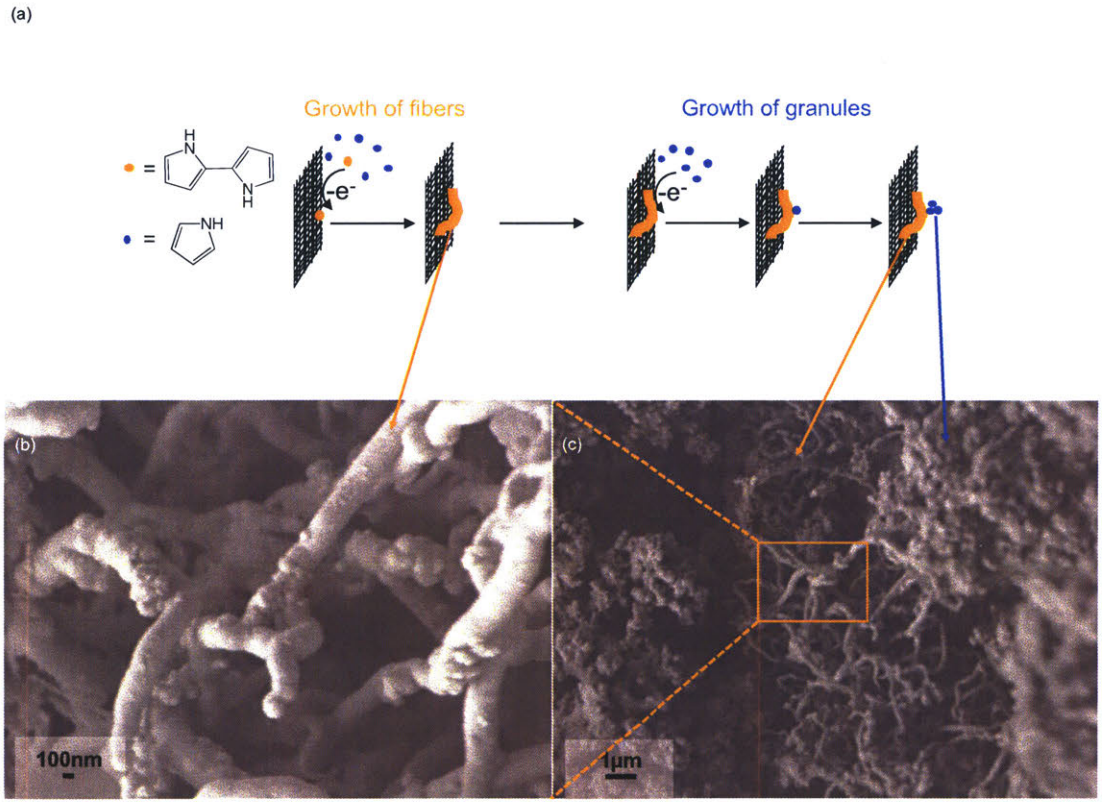

Figure 2-14: (a) A schematic illustration for the proposed mechanism of forming a highly porous morphology in the PPy film due to the temporally segregated growth of the fibrillar and the granular structures. HRSEM images of (b) PPy(Cl) fibers forming an underlying network on top of which (c) granular structures are deposited.

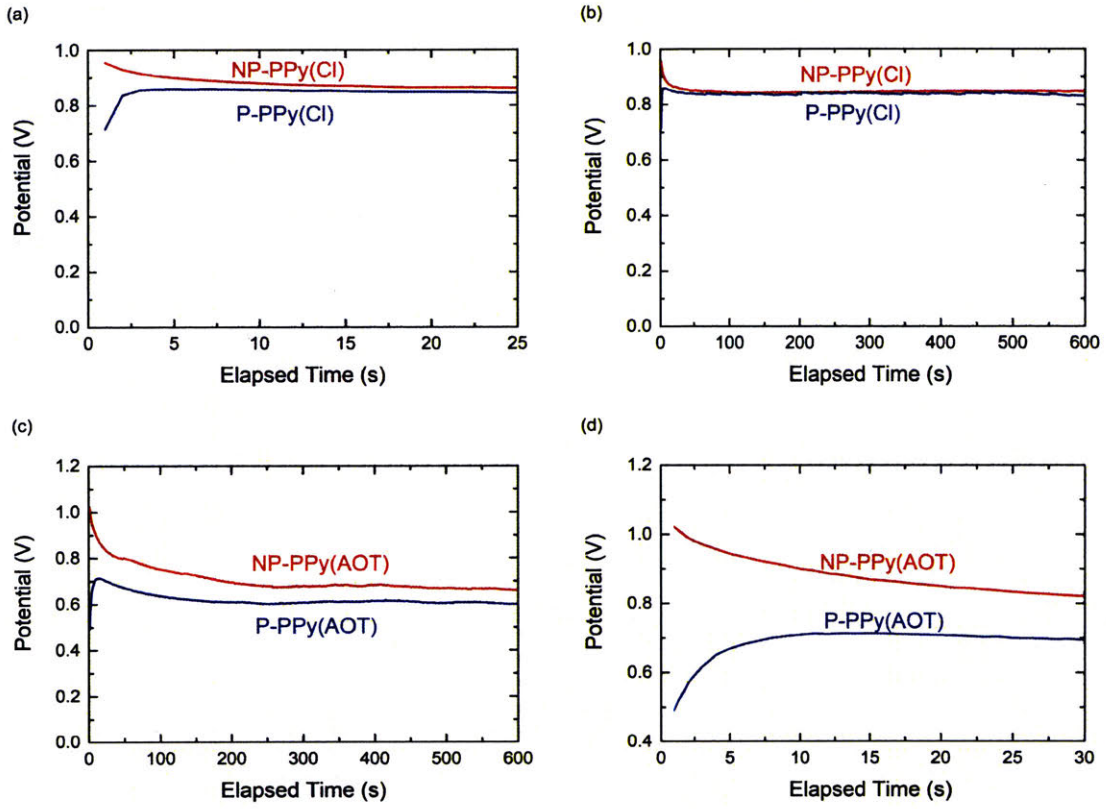

Figure 2-15: Chronopotentiometric potential-time curves of the electropolymerization process of (a)-(b) P- and NP-PPy(Cl), as well as (c)-(d) P- and NP-PPy(AOT) in the presence (Blue) or absence of bipyrrole (Red), respectively.

seen in Figure 2-14c.

Figure 2-15a and b shows that the shape of the potential-time curve for P-PPy(Cl) electropolymerization was different from that of NP-PPy(Cl), further corroborating our hypothesis. The initial increase in potential indicates that chain extension from bipyrrole readily takes place at the outset of electropolymerization while the dimerization of pyrrole monomer slowly catches up at a higher potential with 10 seconds' delay (Figure 2-15b). The accumulation of pyrrole oligomers gradually led to a decrease in the oxidation potential required for further chain extension and eventually reached a constant level, similar to the case of NP-PPy(Cl). The potential-time curves had similarly distinct shapes that depended on the presence of bipyrrole when the electrolyte used was NaAOT instead of NaCl in electropolymerization (Figure 2-15c and d). Therefore, the highly porous morphology of PPy(AOT) formed in the presence of bipyrrole was induced by a mechanism similar to that proposed above, irrespective of the doping anions used.

2.2.4 Electrochemically reversible adsorption

The high capacity for neutral organic molecules, as well as the electrochemically controlled affinity, suggest that P-PPy(AOT) is an effective adsorbent material for removing neutral organic pollutants from water with potential for repeated use in cyclic operations. Desorption of dye molecules from traditional adsorbents has remained a challenge, especially without the aid of heat, pH adjustment or organic solvent.[128] In our case, however, the distinct affinities of oxidized and reduced P-PPy(AOT) for organic contaminants can be exploited to regenerate the adsorbent. To demonstrate the recyclability of P-PPy(AOT) for removing neutral organic molecules from water in the micromolar range, five consecutive cycles of sorption experiments were conducted with 0.01 mM or 2.14 mg L^{-1} SOG aqueous solutions. As illustrated in 2-16a, each sorption cycle began with a P-PPy(AOT)-coated carbon cloth electrode in the oxidized state (+0.5 V vs Ag/AgCl). After adsorption of SOG reached equilibrium, the electrode potential was reduced to -0.8 V (vs Ag/AgCl) in an aqueous stripping solution containing NaCl as the supporting electrolyte. Subsequently, the electrode

was reoxidized in the same NaCl solution used in the reduction step to reactivate the P-PPy(AOT). This reoxidation step marked the completion of one sorption cycle and regenerated the electrode for another cycle of adsorption. During the five cycles, limited decay in adsorption capacity was observed (Figure 2-16b), which demonstrated the reusability of P-PPy(AOT).

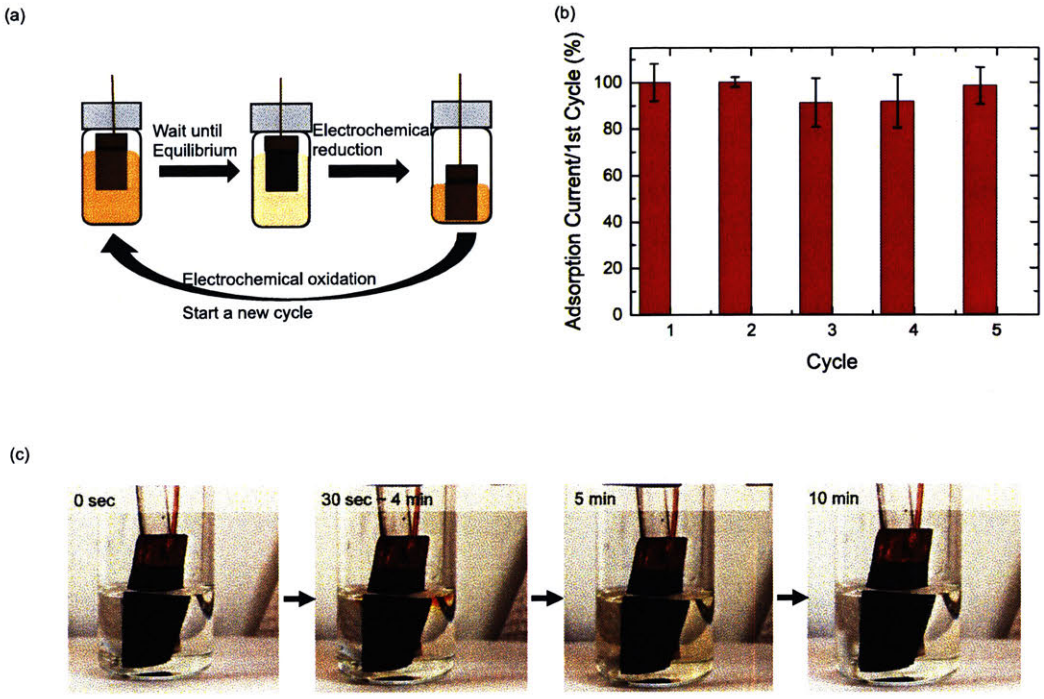

Figure 2-16: (a) Schematic of the electrochemically reversible adsorption process of the P-PPy(AOT) coated on a carbon fiber cloth electrode. (b) Over five cycles, the adsorption capacity of P-PPy(AOT) remained above 90% of the capacity of the first cycle. (c) Snapshots of the desorption video (Movie 5 in Appendix B).

The nearly complete restoration of adsorption capacity in P-PPy(AOT) exhausted by electrochemical reduction suggested that all of the SOG molecules adsorbed in the previous cycle should have been released to free up sites for SOG uptake in the subsequent cycle. Interestingly, during the electrochemical reduction of P-PPy(AOT), it was observed that shortly after the onset of electrochemical reduction, SOG adsorbed

on the electrode started to be released from the solid to the stripping solution, as indicated by the yellow color of the solution (Figure 2-16c and Movie 5 in Appendix B). However, after a contact period of several minutes the stripping solution began to clarify instead of becoming darker while the reduction potential was still being applied. This could be due to the electrochemical reduction of the azo compound SOG released during the regeneration.[34] To help visualize the color change in the stripping solution during the regeneration process, the results presented in Figure 2-16c and Movie 5 were collected from a P-PPy(AOT)-coated electrode equilibrated with an SOG solution at a higher concentration than the actual diluted concentration (0.01 mM SOG) used in the cyclic sorption. The exact desorption step of the cyclic sorption of 0.01 mM SOG solutions are captured in Figure 2-17 and Movie 6 in Appendix B (sped up by 10 times). Similar color changes were observed: no SOG was released when the electrode was immersed in the clear water containing NaCl; and thirty seconds after the onset of the electrochemical reduction (0:15 in Movie 6), yellow SOG dyes started to permeate from the electrode; finally, stirring began 5 minutes after the beginning of the reduction (0:42 in Movie 6), and the color of the entire stripping solution started to fade and eventually disappeared by the end of 10 minutes of desorption process.

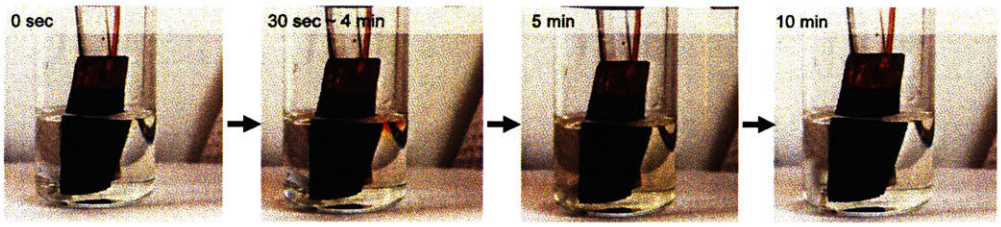

Figure 2-17: Snapshots of the desorption step during the cyclic sorption of 0.01 mM SOG solutions (Movie 6 in Appendix B).

Figure 2-18a shows the potential electrochemical reduction pathway of SOG in aqueous media: a two-electron reduction leads to hydrogenation of the azo group to hydrazo, and the N-N bond can be cleaved by a further two-electron reduction reaction. The hydrazo product of SOG reduction was detected in the aqueous stripping

solution after regeneration of P-PPy(AOT) by electrochemical reduction using liquid chromatography-mass spectrometry (LCMS). All three samples have a peak at about 5.65 min due to the use of mobile phase in LCMS (Figure 2-18b). The mass spectra of the 5.12 min peak of the SOG solution and 5.42 min peak of the stripping solution collected during desorption indicate the presence of SOG (m/z 215) and of hydrazo compound after hydrogenation of SOG (m/z 217), respectively (Figure 2-18c). Because the pH of the stripping solution was neutral, only the first reduction reaction took place and further reduction of the hydrazo compound leading to the N-N bond cleavage was not observed.

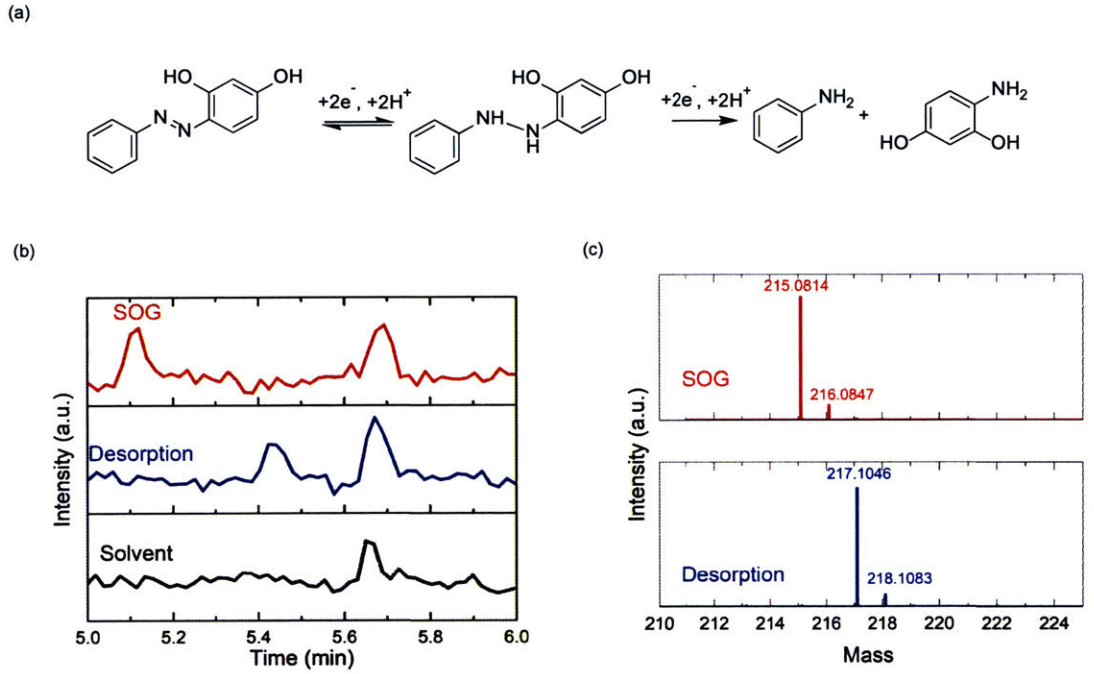

Figure 2-18: (a) A potential pathway for the electrochemical reduction of SOG.[34] (b) Liquid chromatography chromatograms of blank solvent (Black), stripping solution collected during desorption (Blue), and SOG solution (Red). (c) Mass spectra of the 5.12 min peak of the SOG solution (Red) and 5.42 min peak of the stripping solution collected during desorption (Blue).

Such electrochemical reduction of SOG to its hydrazo counterpart can be reversed as the azo-hydrazo redox reaction is reversible in protic media,[34] allowing SOG to be recycled if desired. The relative amounts of SOG and the hydrazo compound in the final stripping solution will depend on the rate of desorption relative to the kinetics

of the reduction reaction. If reaction kinetics are slower than release rates, then the released product can be removed intact by minimization of the contact time during desorption.

The electrochemical reduction of P-PPy(AOT) renders the polymer more hydrophilic, due to the rearrangement of AOT relative to the polymer backbone, to induce the desorption of the adsorbed SOG molecules. This desorption, in combination with an electrochemically catalyzed reduction of SOG, regenerates the functional material to regain full capacity for adsorption of SOG in subsequent cycles.

To test the stability of the P-PPy(AOT) adsorbent, 100 repeated reduction and oxidation cycles were carried out and the atomic composition of the film was tracked using XPS. The polymer and its dopants are intact up to 50 cycles with almost no change in composition while some degradation or dissolution of the polymer film is observed at the 75th and 100th cycles. The nearly complete restoration of the adsorption capacity of P-PPy(AOT) over 5 cycles and the ability to retain AOT in the polymer film after extended cycles demonstrate the robustness of P-PPy(AOT) for reversible sorption of neutral organic pollutants from water (Table 2.6).

Table 2.6: Elemental compositions of P-PPy(AOT) after oxidation/reduction cycles.

Cycle	Atomic Concentration %					
	C 1s	Cl 2p	N 1s	Na 1s	O 1s	S 2p
0	72.18	0	4.37	1.95	20.34	1.16
1	62.22	1.72	4.2	8.27	22.14	1.44
2	61.25	2.03	4.59	9.3	21.41	1.41
3	60.54	1.42	4.24	8.96	22.94	1.9
4	61.62	1.15	3.84	8.83	23.2	1.36
5	51.99	2.76	4.2	14.78	25.17	1.09
10	56.66	1.5	4.36	10.15	26.06	1.27
25	57.61	1.22	5.33	10.63	25.28	1.52
50	58.5	1.61	5.4	9.74	23.48	1.27
75	69.17	2.72	1.97	9.68	15.44	1.02
100	70.28	8.88	0.62	8.88	16.95	1.04

2.3 Materials and methods

2.3.1 Materials

Pyrrole, dioctylsulfosuccinate sodium (NaAOT) salt, sodium chloride (NaCl), Sudan Orange G (SOG), propranolol hydrochloride (PP), and Bisphenol A (BPA) (Sigma Aldrich), and 2,2'-bipyrrole (Toronto Research Chemicals) were used as received throughout the study. Carbon fiber cloth substrates were obtained from Fuelcell.com and used without pretreatment prior to electrochemical functionalization with conducting polymers or electrochemical testing.

2.3.2 Experimental methods

2.3.2.1 Electrode fabrication and electrochemical characterizations

All electropolymerization and electrochemical characterizations were performed on a VersaSTAT4 potentiostat (Princeton Applied Research) in a three-electrode configuration where the counter electrode was a platinum wire and the reference electrode was Ag/AgCl (BASi). Electropolymerization was carried out by applying a constant current density of 5 mA cm^{-2} for 10 min to a carbon fiber cloth substrate. In a typical preparation of the porous PPy film, the solution for electropolymerization consisted of 5 mL of aqueous solution containing 0.1 M of the corresponding electrolyte, 0.3 M pyrrole, and 0.3 mg mL^{-2} bipyrrole. For comparison, the solution for electropolymerization of nonporous PPy film did not contain bipyrrole while other composition remained the same.

2.3.2.2 Polymer Characterizations

Scanning electron microscopy (SEM) images were taken using JEOL-6010LA and JEOL-6700 SEMs for regular and high-resolution imaging, respectively. AFM was performed on Veeco Nanoscope V with Dimension 3100 in tapping mode and the images were analyzed using the Nanoscope Analysis software. The contact angles

formed by a 2 μL water droplet on a polymer-coated stainless-steel substrate were measured using a Rame-Hart goniometer at room temperature. Fourier-transform infrared spectroscopy (FT-IR) was measured on a Nicolet NEXUS 8700 with KBr pellets. X-ray photoelectron spectroscopy (XPS) was performed on a Surface Science Instruments SSX-100 with operating pressure around 2×10^{-9} Torr and Monochromatic Al Kα X-ray (1486.6 eV) of 1 mm diameter beam and collected photoelectrons at a 55o emission angle. XPS scans were analyzed using the CasaXPS software with spectra calibrated with the C1s peak (284.8 eV).

2.3.2.3 Separations of organic contaminants

Adsorption studies were performed at ambient temperature in 20 mL scintillation vials continuously shaken at 150 rpm min^{-1} to increase mixing. The concentrations of the model contaminant Sudan Orange G (SOG), propranolol hydrochloride (PP) and Bisphenol A (BPA) in the aqueous phase (C_e) were measured by a Cary 60 Ultraviolet-visible (UV-Vis) spectroscope. The amount of pollutant molecules adsorbed to PPy(AOT)- and PVF-PPy-coated electrodes was determined as $Q_e = \frac{(C_0 - C_e)Vol}{m}$, where Q_e (mg g^{-1} polymer) is the amount of pollutant adsorbed per gram of polymer, C_0 (mg L^{-1}) and C_e (mg L^{-1}) are the initial and final concentrations of pollutant in the solution phase, respectively, m (g) is the mass of the particular type of polymer on the carbon fiber cloth substrate, and Vol (L) is the volume of solution. The Freundlich isotherm or linear isotherm equations were fitted to the batch adsorption data.

The P-PPy(AOT)-coated electrode was regenerated by reducing at - 0.8 V vs Ag/AgCl for 10 minutes in 5 mL of 0.1 M NaCl solution with a platinum counter electrode. To reuse the P-PPy(AOT)-coated electrode in subsequent cycles of adsorption, the polymer was reactivated for adsorption by applying a constant potential + 0.5 V vs Ag/AgCl for 10 minutes in the same stripping solution using a platinum counter electrode.

2.3.2.4 Study of the electrochemical degradation of contaminants

Liquid chromatography-mass spectrometry (LCMS) was used to verify the presence of the transformation of SOG during the electrochemical regeneration. The LCMS analysis was performed on an Xterra MS C18 3.5 μm, 2.1 × 50 mm column. The mobile phases were 0.2% acetic acid in water and 0.2% acetic acid in acetonitrile, respectively.

2.4 Summary

In conclusion, a facile method has been developed to synthesize highly porous homogeneous conducting polymers on carbon fiber cloths by electrochemical polymerization of pyrrole with a trace amount of bipyrrole and simultaneous doping of the polymer with surfactant anions. The resulting P-PPy(AOT) is superhydrophobic in the oxidized state and exhibits electrochemically tunable hydrophobicity. The MD-DFT simulations corroborate the hypothesis that reorientation of AOT dopants with respect to the polymer backbone during redox processes modulates the hydrophobicity of the polymer. The electrochemically modulated reorientation of the surfactant relative to PPy also facilitates the hydrogen bond formation between the adsorbate and the AOT dopant when PPy is oxidized, increasing the affinity of the material towards organic molecules. The compositional and morphological advantages lead to the high adsorption capacity and reversibility of P-PPy(AOT) for removing organic micropollutants from water. The understanding of the interactions between dopants, polymers, and adsorbates on the molecular level is significant for developing broader applications of the materials with electrochemically tunable hydrophobicity in drug delivery, sensing, self-cleaning surfaces, microfluidics, and artificial muscles.[40,94,106,120]

Chapter 3

Asymmetric Redox-Responsive Electrode Systems with Complementary, Electrochemically Tunable Hydrophobicity

3.1 Introduction

Chemical separation processes are energy-intensive, and are responsible for 10 to 15% of the world's total energy consumption, with distillation, evaporation and other conventional technologies accounting for more than 80% of this energy expenditure.[57] Improved separation efficiencies can be achieved through more recent technologies such as reverse osmosis, nanofiltration, and capacitive deionization, which are particularly effective for removing charged ions from water.[57,61,101] The separation of neutral organic species in processes such as wastewater treatment and pharmaceutical product purification is also of importance, and there are still opportunities for the development of energetically efficient operations.[61] Water pollution by neutral organic contaminants, including industrial chemicals, pesticides, pharmaceuticals, and personal care products, is an emerging issue globally, and their presence at low concen-

trations complicates the separation processes.[6,16,58,70,74,88,124] Current wastewater or drinking water treatment plants are not specifically equipped for eliminating neutral organic contaminants[58,124] which can therefore pass through domestic and industrial wastewater discharges and end up in the aquatic environment. Many neutral organic contaminants have proven to have ecotoxicological effects on aquatic life, animals and even human beings, that include short-term and long-term toxicity, endocrine disrupting effects and antibiotic resistance of microorganisms.[6,58,70] Similar to wastewater treatment, purification of pharmaceutical compounds involves a wide array of organic compounds and is essential for ensuring the quality of medications. Removal of neutral organic species by adsorbents such as activated carbon (AC) is a common practice but sorbent regeneration through thermal processes, pH adjustments, or solvent extraction is often challenging or costly.[89] Therefore, AC regeneration is usually done in centralized treatment facilities, adding transportation cost to the operations.[7] Electrical energy is inexpensive, widely available, and can be more efficient compared to the aforementioned alternative ways to regenerate adsorbents.[43] Adsorbents that can be regenerated by electricity present a practical and scalable point-of-use solution for separating neutral organic compounds from aqueous solutions.

Jemaa et al. proposed a cyclical electrochemical stage process that uses complexing agents dissolved in a contacting phase to transfer organic species from a feed phase to a receiving phase.[43] The complexation between the organics and the agents is reversible and can be modulated by electrochemical redox reactions. In order to recycle the complexing agents and avoid contamination of the feed and stripping solutions, the contacting phase must be immiscible with these solutions, in which the agents should also be insoluble.

To work around the stringent solubility requirements of this electrochemical separation process, the mass separation agents were immobilized on conductive solid substrates to form adsorbents responsive to electrochemical modulations. The benefits are two-fold: first, electrons are transferred directly from the electrodes to the immobilized adsorbents, in contrast to the approach taken by Jemaa et al., in which the complexing agents needed to migrate to be within the vicinity of the electrode for

redox reactions to take place; second, the solid electrodes can be contacted with the feed or receiving phase in a swing process akin to that used in traditional adsorption operations, but with voltage swings rather than changes in temperature, pressure or solution conditions. Electrodes functionalized with redox-active materials have been developed to remove ionic species and charged biomacromolecules from aqueous solution in a reversible manner,[4,96–99,101] and our group have shown recently that electrically conductive materials with immobilized redox responsive moieties can be applied also to the separation of neutral organic species from solution,[61,81] including those presented in Chapter 2. Polypyrrole (PPy) was deposited on carbon substrates as the adsorbent and two different approaches were adopted to modulate its hydrophobicity and hence affinity towards organic solutes in water: incorporation of a polyvinylferrocene (PVF) redox-responsive polymer in the PPy electrode coating,[61] and doping of the PPy with the amphiphilic surfactant dioctyl sulfosuccinate (AOT).[81] The two types of material will be refered to as PVF-PPy and PPy(AOT), respectively. Building on the previous efforts on material design, the synergistic properties of PVF-PPy and PPy(AOT) were exploited in electrochemically mediated separations of organics by pairing them as opposing electrodes in an asymmetric electrochemical cell.

As in the electrosorption of ionic species by redox-active materials, the tradeoff between energy cost and separation extent warrants careful choice of electrochemical cell configurations, electrode material and process parameters to achieve the most efficient separation.[61,101] Since PVF-PPy is more hydrophobic when reduced, and hydrophilic when oxidized, while PPy(AOT) behaves in the opposite manner, i.e. is more hydrophilic when reduced, and more hydrophobic when oxidized, the PVF-PPy and PPy(AOT) electrodes form an attractive pair for an asymmetric system to work in tandem. With no voltage applied to the cell, both electrodes are relatively hydrophobic and able to adsorb neutral organic molecules, but when an appropriate electrical potential is applied to the cell to charge both electrodes, the organics will desorb from the loaded electrodes. Reactivation of the two electrodes to prepare them for the next adsorption cycle is spontaneous on simple shorting of the two electrodes. With only the desorption step costing energy, the asymmetric system has the potential

to achieve high energetic efficiency.

In this chapter, it is first demonstrated that the asymmetric system can be used reversibly to remove model organic species from water, with limited decay in capacity over a number of cycles and an ability to suppress parasitic reactions in water. The energetic efficiency and economic viability of electrochemically mediated separation of organics were compared to conventional adsorption by activated carbons regenerated by thermal desorption or solvent extraction. Lastly, the generality and selectivity of the PPy-based asymmetric system were presented in the context of a separation that is of direct relevance to pharmaceutical purification.

3.2 Results and discussion

The functional materials in an asymmetric system for electrochemically mediated separations need to exhibit three properties: (1) electrical conductivity to respond to applied potentials, (2) different affinities towards organic species depending on the applied electrochemical modulation, and (3) high surface area for interactions with organic species to foster a high adsorption capacity. Therefore, polypyrrole, a common intrinsically conducting polymer, coated on carbon fibers was chosen to serve as an underlying conductive network, with two approaches, involving ferrocene moieties and amphiphilic AOT surfactants, to modulate the affinities of the materials towards organic species.[61,81] The PVF-PPy hybrids and doped PPy(AOT) were synthesized using electropolymerization techniques. The resulting polymer films coated on commercial carbon cloth substrates possessed desired highly porous morphology (Figure 3-1a and c). An asymmetric system was assembled with a PVF-PPy positive electrode and a PPy(AOT) negative electrode (Figure 3-1b).

3.2.1 Asymmetric redox-responsive electrode systems

It is important to balance the charge of the positive and negative electrodes constituting the asymmetric system. One common approach is to adjust the mass of the functional materials on the two electrodes such that the capacitances are

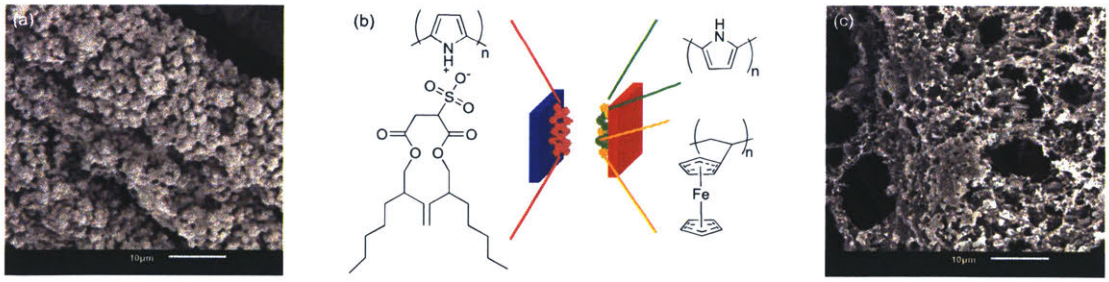

Figure 3-1: Scanning electron microscopy (SEM) images of (a) PPy(AOT) and (c) PVF-PPy. (b) A schematic of the asymmetric system.

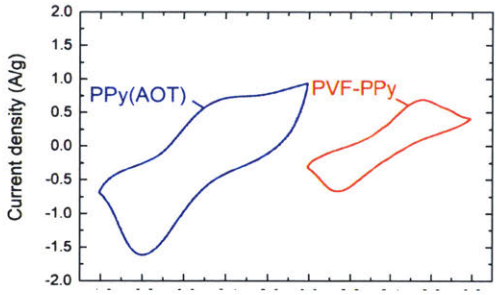

Figure 3-2: Cyclic voltammograms for the PVF-PPy and PPy(AOT) electrodes in a three-electrode configuration (scan rates 10 mV s^{-1}).

equalized.[113,114,122] Therefore, the specific capacitances (C) of the PVF-PPy and PPy(AOT) electrodes were first estimated using the three-electrode cyclic voltammetry (CV) profiles (Figure 3-2) of the individual electrodes in a three-electrode configuration using a platinum counter electrode and a Ag/AgCl reference electrode according to the equation:[18]

$$C = \frac{\int I dV}{2vm\Delta V} \tag{3.1}$$

where I is the current (A), v is the potential scan rate (V s^{-1}), m is the mass of the electrode, and ΔV is the applied potential window (V). The specific capacitance of PPy(AOT) is approximately twice that of PVF-PPy at low scan rates (49.5 F g^{-1} vs 22.8 F g^{-1}). Therefore, the electropolymerization reaction times were adjusted such that the mass loading ratio of the PVF-PPy to PPy(AOT) was approximately 2:1.

The electrochemical behavior of the asymmetric system with PVF-PPy and PPy(AOT) electrodes of balanced charges was investigated by cyclic voltammetry (CV) in a two-electrode configuration. The CV responses of the full cell were monitored by setting a potential window of 1.2 V and recorded the responses of the individual electrodes versus a Ag/AgCl reference electrode (Figure 3-3). The paired Faradaic reactions on the two electrodes are the oxidation and reduction of the ferrocene moieties in PVF-PPy hybrids,[104] and potassium insertion and repulsion accompanied by reorientation of the surfactant dopants in PPy(AOT).[71]

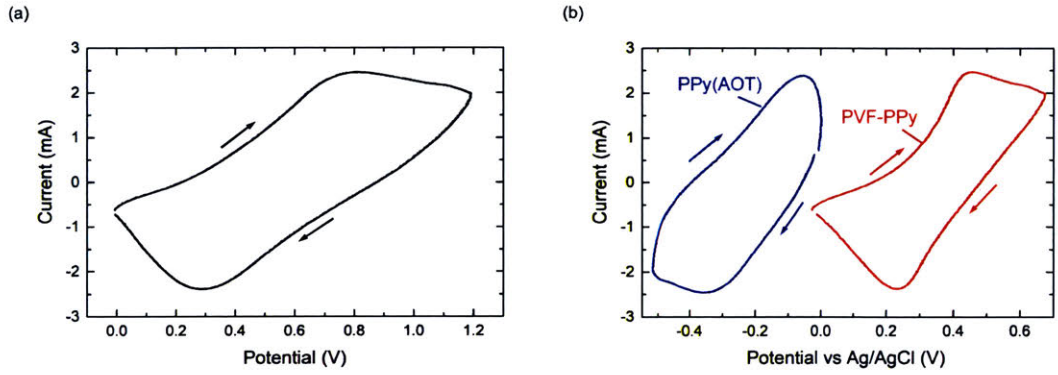

Figure 3-3: Cyclic voltammograms of (a) the full cell and (b) the individual electrodes in the PVF-PPy//PPy(AOT) asymmetric system in a two-electrode configuration (scan rates 10 mV s^{-1}). The arrows indicate the direction of voltage scans for the whole cell and the individual electrodes.

The two adsorbent materials exhibited differences in hydrophobicity depending on the electrochemical signals. For PVF-PPy, when the applied potential (E) is lower than the formal potential of ferrocene (E^0 = 0.34 V vs. Ag/AgCl), the PVF-PPy adsorbent is hydrophobic; most ferrocene moieties are reduced, and organics can be taken up by reduced PVF-PPy. For $E >> E^0$, the PVF-PPy adsorbent becomes relatively hydrophilic; most ferrocene moieties are oxidized and positively charged, and therefore water molecules interact more favorably with the adsorbent and displace neutral organic species previously adsorbed on the polymer.[61] In contrast, for PPy(AOT), when the applied potential (E) is higher than the formal potential of potassium insertion and repulsion ($E^0 = -0.21$ V vs. Ag/AgCl), the polymer is hydrophobic, since the positively charged PPy backbone attracts the negatively charged

sulfonate groups of AOT such that the hydrophobic tails of the surfactant rearrange to be on the surface of the material. When $E << E^0$, PPy(AOT) is more hydrophilic as the relatively neutral PPy backbone induces AOT anions to reorient themselves such that the hydrophobic tails move closer to the polymer chains; the sulfonate groups are exposed on the surface.[81]

The Nernst equation describes the impact of applied potential on the relative amounts (R) of the oxidized to reduced moieties on the polymers (i.e., a measure of the relative hydrophilicity of the ferrocene-containing electrodes and of the hydrophobicity of the AOT-doped PPy coating):

$$E = E^0 + \frac{k_B T}{e} ln(R) \tag{3.2}$$

where k_B is the Boltzmann constant, T the temperature, and e the elementary charge. Therefore, the affinities of the two PPy-based polymers for organics can be modulated by adjusting the potential.

The CV profile of the full PVF-PPy//PPy(AOT) system shows a pair of redox peaks around 0.55 V (Figure 3-3a). This suggests that a potential drop across the two electrodes of greater than 0.55 V should be applied to render both materials hydrophilic to release adsorbed compounds. Subsequently, applying a potential below 0.55 V or simply shorting the two dual-functionalized electrodes (0 V) will reoxidize PPy(AOT) and reduce PVF-PPy, thereby reactivating the materials for further adsorption in their hydrophobic states.

3.2.2 Electrochemically mediated separations of organics

The adsorption capability of the asymmetric system is demonstrated with a common azo dye compound widely used in in the textile industry, Sudan Orange G (SOG), as a model contaminant. The equilibrium adsorption of SOG by the PVF-PPy//PPy(AOT) asymmetric system can be fitted well by the Freundlich adsorption isotherm

$$Q_e = kC_e^{1/n} \tag{3.3}$$

where the Freundlich exponent $1/n$, an indication of the extent to which adsorption is favored, increases as $1/n$ approaches zero (Figure 3-4a).[47] When the asymmetric system is charged at a high potential of 1.2 V, $1/n$ takes on a value close to unity (0.95), i.e., the isotherm is almost linear, following Henry's Law. For the shorted asymmetric system in which PPy(AOT) is oxidized and PVF-PPy reduced, the fitted $1/n$ value was 0.52, consistent with the fact that the oxidized PPy(AOT) and reduced PVF-PPy have higher affinities for SOG in their hydrophobic states.[61,81]

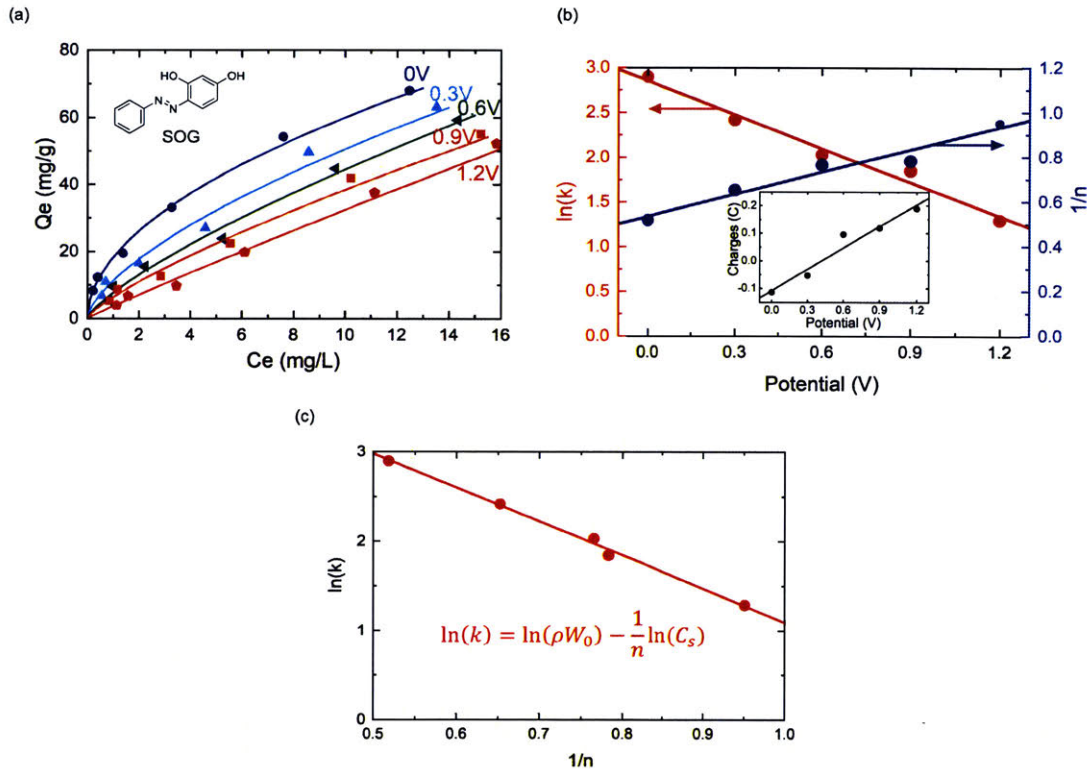

Figure 3-4: (a) Adsorption isotherms for Sudan Orange dye on the PVF-PPy//PPy(AOT) asymmetric system modulated by various applied potentials as fitted with the Freundlich equation. (b) Linear dependence of the fitting parameters of the Freundlich equation on applied potentials/charges. The R^2 value for $ln(k)$ and $1/n$ vs Applied potential, and Charges vs Applied potential were 0.981, 0.957, and 0.951, respectively. (c) Linear correlation between the two Freundlich parameters obtained at different potentials ($R^2 = 0.995$).

The Freundlich isotherm parameters $ln(k)$ and $1/n$ correlate linearly with the applied potential (Figure 3-4b), reflecting the changes in hydrophilicity of the adsorbent

with charging of the electrodes; the linearity arises because the electrochemical cell exhibited capacitance-like features such that for a fixed charging time of 10 minutes, the total number of charges exchanged (and hence hydrophilicity) increased linearly with the applied potential, as shown in the inset on Figure 3-4b. Moreover, the Figure 3-4c shows that the Freundlich equation parameters are themselves correlated linearly, as has been observed by others for the adsorption of a wide range of organic compounds from aqueous solution onto activated carbons.[2,3] This behavior can be interpreted in terms of the Polanyi adsorption theory on the adsorption of organic compounds from an aqueous solution to a heterogeneous surface.[2,24,110,123] Polanyi defined the adsorption potential (ϵ_s) as the energy required to remove the molecule from a saturated solution to a point outside the attractive force field of the adsorbent

$$\epsilon_s = RTln(\frac{C_S}{C_e}) \tag{3.4}$$

where C_s and C_e are, respectively, the solubility limit and bulk equilibrium concentrations of the solutes in the liquid phase. Dubinin related the volume of solutes adsorbed on one gram of adsorbent to the adsorption potential via the equation

$$W = W_0 exp(-\frac{a}{V_S}\epsilon_s) \tag{3.5}$$

where W_0 is the limiting volume per gram of the adsorbent available for adsorption, a is a parameter characteristic of the adsorbent and independent of adsorbates, and V_s is the molar volume of solutes.[2,24,59,123] With $Q_e = \rho W$, where ρ is the solute density, and with ϵ_s given by Equation (3.4), the mass of solute on the polymer can be written as

$$Q_e = \rho W_0 (\frac{C_e}{C_S})^{\frac{aRT}{V_S}} \tag{3.6}$$

which is of the form given in Equation (3.3), and from which the fitting parameters of the Freundlich equations can be identified as

$$k = \rho W_0 C_S^{-\frac{aRT}{V_S}} \tag{3.7}$$

and

$$\frac{1}{n} = \frac{aRT}{V_S} \tag{3.8}$$

Therefore,

$$ln(k) = ln(\rho W_0) - \frac{1}{n} C_S \tag{3.9}$$

The intercept in Equation (3.9) reflects the limiting capacity of the adsorbent, which should be independent of solute for solutes of similar density.[2,24,59,123] The value of ρW_0 estimated for our system is 130 mg g^{-1}, which is of similar magnitude as the value of 227 mg g^{-1} obtained by Abe et al. for a wide range of organic compounds on activated carbon.

The disparity in hydrophobicity and hence affinity for organics under different charging conditions allows for the simultaneous reversibility of sorption by both the adsorbents that is crucial for a swing separation process. The electroswing separation is more effective for the separations of solutes present at low concentrations where the availability of the sites for adsorption is modulated by electrochemical stimuli.

3.2.3 Cyclic separation processes

As was previously shown with individual PVF-PPy and PPy(AOT) polymers, the potential-dependent affinity permits the use of electrochemical means to program adsorption and desorption, thereby enabling the loading and regeneration of the sorbent materials.[61,81] Figure 3-5a depicts the application of a PVF-PPy//PPy(AOT) asymmetric electrochemical cell for removing organics from water. The electrode pair is immersed in the feed solution, and, after reaching equilibrium, the system can be charged for 10 minutes, for example at 1.2 V, to render both polymers hydrophilic and to drive the desorption of the organics. Subsequently, the system can be discharged at 0 V for 10 minutes to return the polymers to their hydrophobic states for adsorption in the next cycle. The electrochemical characterization of the electrode cell has suggested that the half-cell potential of the asymmetric system is 0.55 V (Figure 3-3a), and therefore it is permissible to charge and discharge at less extreme potentials, for example, at 0.9 V and 0.3 V, respectively.

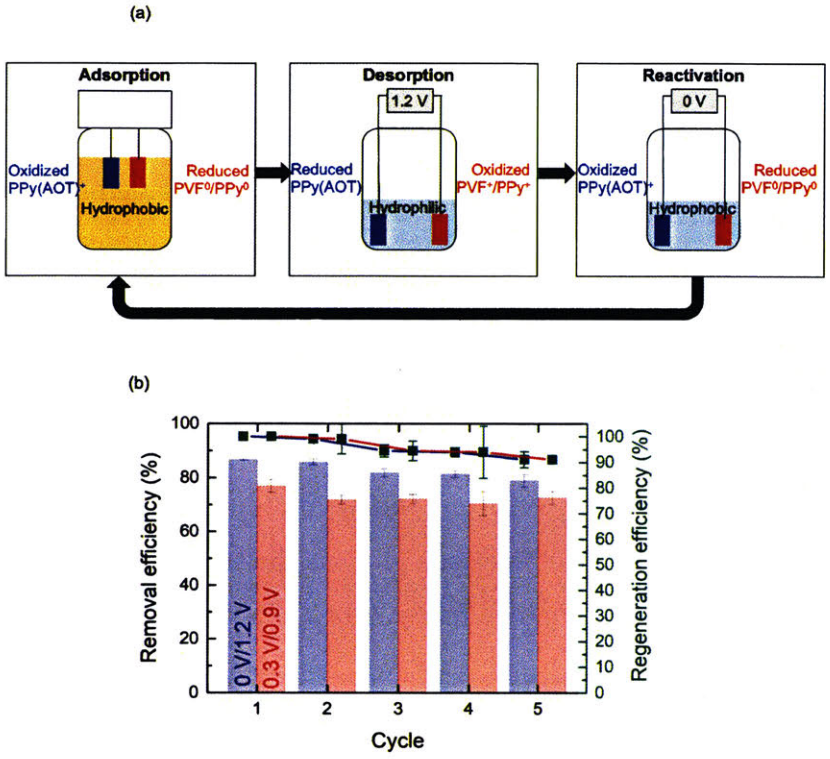

Figure 3-5: (a) A schematic illustration of the cyclic adsorption process. (b) Removal (left y axis and bars) and regeneration (right y axis and squares) efficiencies of the PVF-PPy//PPy(AOT) asymmetric system discharged/charged at 0 V / 1.2 V and 0.3 V / 0.9 V over five consecutive adsorption/desorption cycles.

The reusability of both materials is challenged by conducting adsorption and desorption of SOG using the asymmetric system for five consecutive cycles. Figure 3-5b shows the evolution over the course of five cycles of pollutant removal efficiency (left y axis), defined as the percentage of contaminants removed from the feed, and regeneration efficiency (RE, right y axis) defined as the fraction of contaminants removed in a later cycle relative to those removed in the first cycle. The charge/discharge cycle at more extreme potentials (1.2 V and 0 V vs 0.9 V and 0.3 V) allows roughly 10% more organics to be removed in each cycle. Moreover, most of the adsorption capacity of the asymmetric system can be recovered through electrochemical modulations, indicated by RE greater than 91% over the five cycles for either pair of applied potentials.

Since the electrochemically mediated separation process is not thermodynamically spontaneous, it requires electrochemical energy to charge the system to drive desorption, the amount of which is dependent on the potentials applied. Therefore, the optimum pair of applied potentials has to be determined by considering the tradeoff between energy expenditure (more extreme potentials) and separation extent (more contaminant removal), as discussed below.

3.2.4 Suppression of parasitic reactions

A major challenge for electrochemical devices operating in an aqueous environment is the narrow stable operating voltage window afforded by water. Water splitting can cause loss of energy to side reactions and pH fluctuations that may impact the adsorption capacity. The thermodynamic potential for water electrolysis is only 1.23 V, beyond which undesired parasitic reactions will occur:[11]

$$2H^+ + 2e^- \rightarrow H_2(g) \tag{3.10}$$

$$2H_2O(l) \rightarrow O_2(g) + 4H^+ + 4e^- \tag{3.11}$$

where 3.10 and 3.11 are the hydrogen evolution reaction (HER) and the oxygen evolution reaction (OER), respectively. In addition to the effects of the whole cell potential, a side reaction can occur if the potential window of an individual cathode or anode reaches its respective stability limit.[112] The equilibrium potential of 3.10 varies as a function of pH in water:

$$E = E^0 + \frac{k_B T}{2e} ln(\frac{a^2_{H^+} a^2_{e^-}}{a_{H_2}}) = -0.06pH \tag{3.12}$$

where $E^0 = 0$ V is the standard reduction potential of the HER (SHE), and a_{H^+}, a_{e^-}, and a_{H_2} are the activities of the reactants and reaction products. For example, with an initial pH of 6.94 in an aqueous solution, the HER can take place when the potential on the cathode reaches - 0.42 V vs. SHE or - 0.60 V vs. Ag/AgCl.

Cells in which the anode is functionalized with PVF-containing materials are prone

to the HER side reaction when the anode is paired with various types of materials on the cathode, including platinum (Pt), carbon nanotubes, or chemically identical PVF-based material in the neutral state.[101] In the desorption step of an electrochemically mediated separation, an electrode functionalized with PVF-PPy is oxidized to render the polymer hydrophilic. If the negative electrode is Pt, the HER and OH^- production can occur to a significant extent.

Table 3.1 shows the final solution phase pH after potentials are applied to electrochemical cells consisting of a PVF-PPy positive electrode and a PPy(AOT) counter electrode, or of the two PPy-based materials independently paired with Pt. When the potential difference across the full cell is 1.2 V, the potentials on the positive PVF-PPy electrode and the negative PPy(AOT) electrode are 0.68 V and - 0.52 V vs Ag/AgCl, respectively (Figure 3-3b). Therefore, for a fair comparison with the asymmetric system charged at 1.2 V, the individual PVF-PPy eletrode was charged at 0.7 V vs Ag/AgCl and the PPy(AOT) at - 0.5 V vs using a platinum counter electrode in a three electrode configuration with in-situ monitoring of the pH changes.

Even when a constant 1.2 V is applied to the asymmetric PVF-PPy//PPy(AOT) system for 10 minutes, the pH increase for the asymmetric system is quite limited, because the Faradaic reaction occurring during the reduction of the PPy(AOT) electrode accommodates electrons from the oxidation of the PVF-PPy in lieu of the HER that would otherwise occur. Without a dual-functionalized asymmetric system, the regeneration of the PVF-PPy electrode at 0.7 V vs. Ag/AgCl in a PVF-PPy//Pt system causes significant HER, indicated by the solution phase pH increasing from nearly neutral (6.94) up to 10.41. Similarly, without PVF-PPy as the counter electrode, to provide electrons for the reduction of PPy(AOT) at - 0.5 V vs. Ag/AgCl, the OER occurs on the Pt anode, with a resultant decrease in the pH to 5.48. The asymmetric electrochemical cell configuration is clearly successful in preventing pH fluctuations during the electroswing operation.

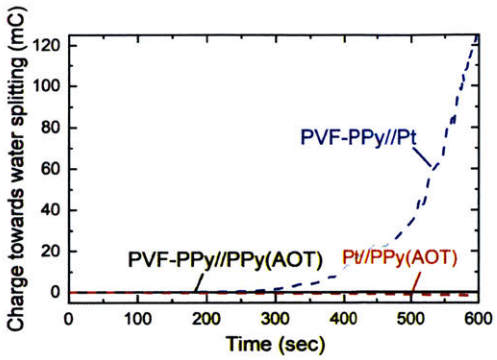

Figure 3-6: The amount of charge (mC) going toward water splitting in the course of modulating the PVF-PPy//PPy(AOT) asymmetric system and either PVF-PPy or PPy(AOT) paired with a Pt counter electrode.

Table 3.1: Final solution phase pH after different applied potentials are applied to electrochemical cells assembled with electrodes coated with different PPy-based polymers or platinum (Pt).

Positive electrode	Negative electrode	Potential (V)	Final pH	% charge towards water splitting[1]
PVF-PPy	PPy(AOT)	0.0	6.97	0.00
PVF-PPy	PPy(AOT)	0.3	7.13	0.04
PVF-PPy	PPy(AOT)	0.9	7.29	0.04
PVF-PPy	PPy(AOT)	1.2	7.30	0.03
PVF-PPy	Pt	0.7	10.41	42.0
Pt	PPy(AOT)	0.5	5.48	-0.81

The other benefit of suppressing parasitic reactions is that the Faradaic efficiency of the electrochemical modulations is enhanced. Figure 3-6 shows the loss of charges to water splitting or OH^- production due to HER in the PVF-PPy//Pt, PVF-PPy//PPy(AOT) and Pt//PPy(AOT) systems. The dual-functionalized asymmetric system PPy(AOT) counter electrode allows over 99% of the charges to be utilized in electrochemical modulations of the polymers whereas almost 42% of charges are lost to OH^- production when PVF-PPy is paired with Pt. The dramatic reduction in HER enhances current efficiencies by eliminating parasitic water splitting reactions.

[1]The position sign represents the production of OH^- while the negative sign indicates the generation of H^+.

3.2.5 Energetic efficiency

Adsorption has proven to be an effective unit operation for the removal of organics from wastewater. The ability to regenerate the adsorbent efficiently is important to avoid merely transferring contaminants from the liquid phase to the solids, and to enable reuse of the sorbent.[77] To assess the practicality of the PPy-based asymmetric system, the economic viability and environmental impact of electrochemically mediated separations using the PPy-based system under different applied potentials were compared to those of conventional activated carbons regenerated, which are used extensively for the mitigation of organic contaminants, by thermal desorption or solvent extraction.[83,84] As with the comparison between capacitive deionization and reverse osmosis in desalination,[78] the concept of specific energy consumption (SE) is adopted, defined as energy consumption per gram of organic contaminants removed, to evaluate the energetic efficiencies of alternative adsorbents and regeneration strategies:

$$SE = \frac{E}{Q_e RE} \tag{3.13}$$

where E is the energy consumed per gram of adsorbent during the regeneration step (J g^{-1} adsorbent), Q_e is the adsorption capacity (g contaminant g^{-1} adsorbent), and RE is the regeneration efficiency.

Thermal regeneration of activated carbons typically involves heating the saturated AC to remove the retained adsorbate. The intensive heating may cause changes in the carbonaceous structure of, or mass losses in, the adsorbent, or charred residues may be left behind on the AC, all of which contribute to the loss of activity in the regenerated AC.[84] To estimate the energy consumption during the thermal regeneration of activated carbons, the heat requirements can be calculated according to[48,87]

$$Q = nC_{pg}(T_R - T_0) \tag{3.14}$$

where n is the total purge gas used (mol of purge gas per gram of activated carbons), C_{pg} is the heat capacity of the purge gas, and T_R and T_0 are the regeneration and

reference temperatures, respectively.

Experimental results of AC prepared from cattail by H_3PO_4 activation were taken as an example.[92] This type of AC has an adsorption capacity of 192 mg g^{-1} for neutral red with an RE of 83% after being heated at 300°C for 30 min in a furnace.[92] There is a trade-off between regeneration temperature and purge gas quantity.[48] In the best-case scenario where an infinite temperature gradient can be assumed, the purge gas quantity asymptotically approaches a minimum value

$$n_{min} = \frac{C_{ps}}{C_{pg}} \tag{3.15}$$

where C_{ps} (J g^{-1} K^{-1})and $C_{pg}(Jmol^{-1}1\ K^{-1})$ are the heat capacities of AC and purge gas, respectively.[48] The resulting energy consumption of the thermal regeneration is 235 J g^{-1} adsorbent (Equation 3.14) and the SE is 1474 J g^{-1} contaminant. Since the energy consumption during thermal regeneration is highly sensitive to the purge gas quantity, it is necessary to determine how likely the thermal regeneration would become more efficient than electrochemical regeneration. Additional sensitivity analysis was conducted on the SE ratio of thermally regenerated activated carbons and the electrochemically modulated PVF-PPy//PPy(AOT) system desorbed at 0.9 V and reactivated at 0.3 V as a function of purge gas quantity (Figure 3-7). Unless the purge gas quantity for regenerating the AC can be reduced to 0.024 mol g^{-1} at 300°C (which is 15% less than the minimum value 0.028 mol g^{-1} calculated based on the reference[48]), the electrochemically regenerated PPy-based asymmetric system would be more energetically efficient.

Activated carbons can also be regenerated through extraction of adsorbates with organic solvents, followed by removal of any retained solvent. Although this method may prevent mass losses or damage to the porous structure of AC, the use of a solvent can incur high economic costs or raise toxicity concerns.[83] Moreover, solvent regeneration may take days for soaking AC and the subsequent solvent removal step requires additional unit operations and energy inputs.[103] For example, the adsorption capacity of the AC (CAL, 16-20 mesh) for orange II is 157 mg g^{-1} AC with an RE

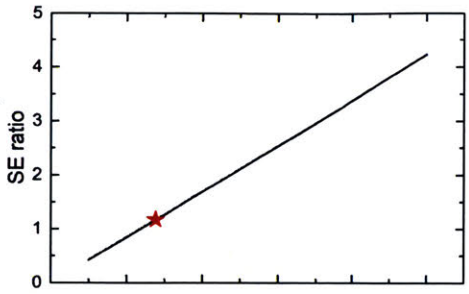

Figure 3-7: The ratio of specific energy consumption of thermally regenerated activated carbons and the PVF-PPy//PPy(AOT) system electrochemically modulated at 0.9 V / 0.3 V. The labeled point represents purging 0.028 mol of hot air for every gram of AC,[48] at which point the thermal regeneration costs 17% more energy than the PVF-PPy//PPy(AOT) system.

of 48% by ethanol.[103] The batch regeneration protocol includes soaking the spent AC in ethanol (1 L solvent for 1 g adsorbent) for 6 days followed by drying in nitrogen at 140°C; this extended period of soaking, cost of solvent, and downstream removal of solvent from regenerated AC may be prohibitive for the adoption of solvent regeneration on an industrial scale. The high cost of solvent and capital requirements of solvent regeneration may be prohibitive for industrial scale applications. Therefore, solvent extraction is excluded from the energetic efficiency analysis and the focus is on benchmarking thermal regeneration of AC for comparison with the electrochemical regeneration operations instead.

For the electrochemically regenerated PVF-PPy//PPy(AOT) asymmetric system, the energy consumption was determined experimentally from the electrical energy consumed in the discharging process only. The energy that may be recovered from the reactivation step on shorting of the two electrodes is ignored. To calculate the electrical energy consumed per gram of adsorbent during the desorption step (E), total energy consumed in the regeneration step was computed by multiplying the charges (q) exchanged by the particular potential applied to the PVF-PPy//PPy(AOT) system (E_{app}) divided by the mass of polymers on both electrodes (m)

$$E = \frac{qE_{app}}{m} \tag{3.16}$$

All the parameters involved in the calculations of energetic efficiencies for thermal or solvent regeneration of AC, and electrochemical regeneration of PVF-PPy//PPy(AOT) can be found in Table 3.2.

Table 3.3 compares the energetic efficiencies of the activated carbons and the PPy-based system with their respective regeneration methods. The PVF-PPy//PPy(AOT) asymmetric system, when regenerated at 0.9 V and reactivated at 0.3 V, is more efficient than when electrochemical modulations at 1.2 V / 0 V are used, and than the thermal regeneration of activated carbons. The SE of the thermally regenerated activated carbons for organic compounds and the PVF-PPy//PPy(AOT) system are quite similar in magnitude. An additional sensitivity analysis on the relative efficiencies of thermal regeneration of activated carbons and is performed (Figure 3-7).

Capital cost and material costs are also important factors for determining the economic viability of these alternative technologies. The high temperature operations demand deployment of stainless-steel equipment, incurring high capital costs, and require large-scale centralized facilities to achieve economy of scale.[51] For the PPy-based asymmetric system, the manufacturing cost of the novel materials on a large scale are yet to be determined.

Based on this analysis, it is concluded that the PVF-PPy//PPy(AOT) cell regenerated at 0.9 V and subsequently reactivated by charging the system at 0.3 V is competitive in terms of specific energy consumption (SE) among the cases considered here. The SE values for the electrochemically regenerated PVF-PPy//PPy(AOT) are conservative, and can be enhanced if the energy in the reactivation (shorting) step can be recovered and stored for subsequent desorption processes. Moreover, the adsorption capacity of the PVF-PPy//PPy(AOT) used in the calculation is obtained from the cyclic experiment where the system was exposed to very dilute solutions containing Sudan Orange G and is only $\sim 1/5$ of the maximum value measured. These considerations warrant further investigation of the electrochemically mediated separation technology and adsorbent materials to improve their robustness and economic viability.

Table 3.2: Parameters for the calculations of energetic efficiencies.

neration mode	Parameter	Value	Unit
Thermal	Heat capacity of hot air (C_{pg})	30.3	J mol^{-1} K^{-1}
	Heat capacity of AC (C_{ps})	0.8	J g^{-1} K^{-1}
	Purge gas quantity (n)	0.028	mol hot air g^{-1} AC
	Regeneration temperature (T_R)	300[92]	°C
	Reference temperature (T_0)	20[92]	°C
	Adsorption capacity (Q_e)	192[92]	mg neutral red g^{-1} AC
	Regeneration efficiency (RE)	83[92]	%
Solvent	Solvent quantity	1[103]	L ethanol g^{-1} AC
	Adsorption capacity (Q_e)	157[103]	mg orange II g^{-1} AC
	Regeneration efficiency (RE)	48[103]	%
ctrochemical	Charges exchanged (q)	-0.11	C (at 0 V)
		-0.05	C (at 0.3 V)
		0.10	C (at 0.6 V)
		0.12	C (at 0.9 V)
		0.19	C (at 1.2 V)
	Electrical energy consumed (E)	0.06	J (at 0.6 V)
		0.11	J (at 0.9 V)
		0.23	J (at 1.2 V)
	Mass (m)	8.5	g
	Adsorption capacity (Q_e)	11	mg Sudan Orange G g^{-1} PPy (at 0.9 V/0.3 V)
		12	mg Sudan Orange G g^{-1} PPy (at 1.2 V/0 V)
	Regeneration efficiency (RE)	92	% (0.9 V/0.3 V)
		91	% (at 1.2 V/0 V)

Table 3.3: Comparison of the energy efficiencies for activated carbons regenerated by thermal desorption and PVF-PPy//PPy(AOT) regenerated electrochemically.

Metric	Activated carbons	PVF-PPy//PPy(AOT)	
	Thermal	0 V - 1.2 V	0.3 V- 0.9 V
Energy consumption J g^{-1} adsorbent	235	27	12
Specific energy consumption (SE) J g^{-1} contaminant	1474	2395	1258

3.2.6 Selective separation of organic pharmaceutical compounds

It has been previously shown the robustness of the two polypyrrole-based adsorbent materials in the separation of organic species, including pharmaceuticals such as propranolol hydrochloride (PP) and carcinogenic aromatics such as bisphenol A.[61,81] Many separation scenarios involve mixtures of organic compounds to remove impurities or recover valuable molecules.[101] For example, in the manufacture of PP, a β-adrenergic blocking agent widely used to treat hypertension and angina pectoris, many intermediate products emerge from the multi-step synthesis pathway, and hence need to be removed to be compliant with the regulatory requirement that the relative concentrations of individual impurities be below 0.2%.[36] The PVF-PPy//PPy(AOT) system is challenged to separate a mixture of propranolol hydrochloride (PP) and one of the impurities found in the synthesis mixture, unreacted 1-naphthol (1-NO), which participates in an alkylation reaction with epichlorohydrin, the first reaction in the pathway to produce PP.[28]

The individual propensities of PP and 1-NO to be adsorbed on the PVF-PPy and PPy(AOT) electrodes were first determined by measuring the equilibrium distribution coefficient

$$K_d = \frac{Q_e}{C_e} \tag{3.17}$$

where Q_e (mg g^{-1} is the mass of the adsorbed organic compound (PP or 1-NO) per gram of polymer, and C_e (mg L^{-1}) is the concentration of the respective compound in the liquid phase. As shown in Figure 3-8a, the K_d values for 1-NO are higher than those for PP at the corresponding potentials, suggesting higher selectivity for 1-NO

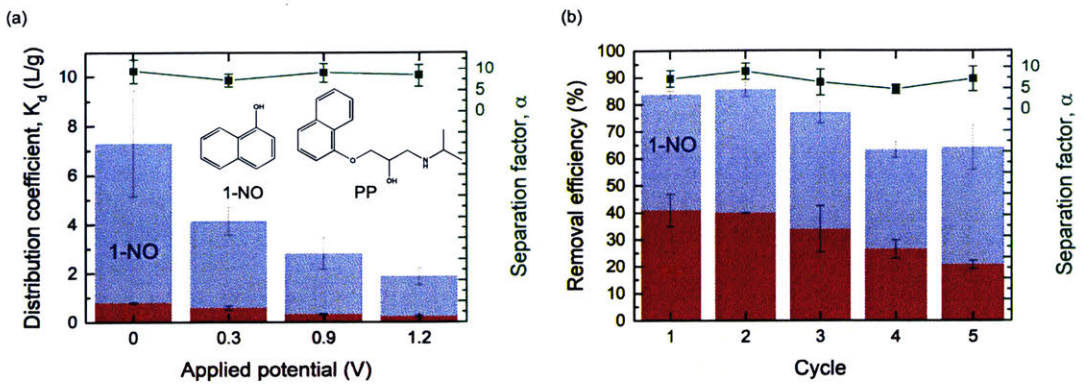

Figure 3-8: (a) Equilibrium distribution coefficients K_d for 1-NO and PP between the PVF-PPy// PPy(AOT) electrodes and the aqueous solutions containing a single component when the asymmetric system is subjected to different potentials prior to the adsorption (left y axis and bars). The resulting separation factors deduced from ratios of the measured K_d values (right y axis and squares). (b) Removal efficiencies (left y axis and bars) and separation factors (right y axis and squares) for five consecutive cycles of separations of a PP and 1-NO mixture.

impurities over PP will be afforded by the asymmetric system. The separation factor α defined as the ratio of the distribution coefficients for 1-NO and PP,

$$\alpha = \frac{K_{d,1-NO}}{K_{d,PP}} \tag{3.18}$$

is on average 8.5 for the different applied potentials (Figure 3-8a).

The selectivity and reusability of the PVF-PPy//PPy(AOT) asymmetric system was explored in five consecutive separations of a binary mixture of 30.6 mg L^{-1} PP and 3.6 mg L^{-1} 1-NO. Figure 3-8b shows that up to 85% of 1-NO can be removed while only roughly 40% of PP is taken up in the first cycle. Moreover, the removal efficiency of PP suffers a greater loss compared to that of 1-NO in subsequent cycles. The observed separation factor when the binary mixture of PP and 1-NO is challenged is on average 7.0 (Figure 3-8b), slightly lower than that deduced from the ratio of K_d values measured with a single component present in the solution (Figure 3-8a), likely due to the competitive binding of PP and 1-NO onto PVF-PPy//PPy(AOT). The interplay between different organics and their impact on the selectivity, capac-

ity, and reversibility of the electrochemically regenerable adsorbent warrant further investigation, but are beyond the scope of this paper.

3.2.7 Stability of the PPy-based polymers

Herein it has been demonstrated that the asymmetric system can maintain over 91% of the initial capacity over five consecutive adsorption/desorption cycles. Past studies have shown that the PVF-PPy and PPy(AOT) materials can sustain more than 50 cycles of electrochemical charging/discharging.[61,81] One potential source of instability is the leaching of the AOT dopants due to a decrease in electrostatic interaction when PPy(AOT) is reduced. If AOT anions leached into the desorption solution they would become new contaminants. The leaching of AOT dopants was investigated by monitoring the sulfur content in the desorption solution containing 0.1 M KCl supporting electrolyte using an inductively coupled plasma optical emission spectrometer (ICP-OES) The ICP-OES instrument allows detection of sulfur content as low as 0.1 ppm using the calibration curve in Figure 3-9.

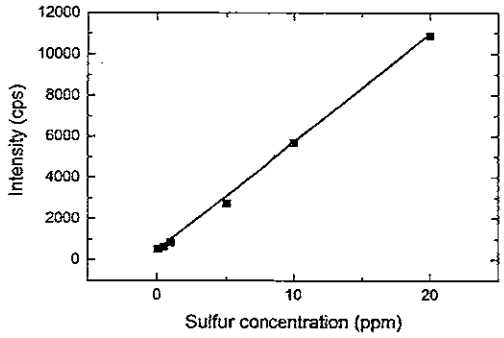

Figure 3-9: Calibration curve for the sulfur concentration in the aqueous phase using ICP-OES.

The intensities of sulfur in the solution after charging the PVF-PPy//PPy(AOT) system at 0.9 V and 1.2 V for 10 minutes were 88 cps and - 58 cps (average of 3 replicates), respectively. Compared to the standard solution containing 0.1 ppm of sulfur showing an intensity of 475 cps, the amount of sulfur in the solution after

charging the system is minimal, if not zero. It is therefore concluded that leaching of AOT anions after 15 minutes of charging is negligible.

3.3 Methods

3.3.1 Electrochemical synthesis and characterizations of polymers

The two types of polypyrrole-based electrodes were prepared through reported electropolymerization methods[61,81,104] on a PARSTAT MC 2000 potentiostat with an auxiliary electrometer (Princeton Applied Research) in a three-electrode configuration. The working, counter, and reference electrodes were carbon fiber cloth (ElectroChem Inc.), a platinum wire (BASi), and Ag/AgCl (3M NaCl), respectively. For PPy(AOT), the electropolymerization bath contained 0.3 M pyrrole (Millipore Sigma), 0.3 mg mL^{-1} bipyrrole (Toronto Research Chemicals), and 0.1 M sodium dioctyl sulfosuccinate (Millipore Sigma).[81] A constant current density of 2.5 mA cm^{-2} was applied for 5 minutes to yield a polymer loading of 2.85 $\pm$ 0.08 mg cm^{-2}.[81] For PVF-PPy, the bath contained 2 mg mL^{-1} PVF (molecular weight 50,000 g mol^{-1}, Polysciences), 0.2 M pyrrole, and 0.1 M tetrabutylammonia perchlorate (Millipore Sigma) in chloroform.[61] A constant current potential of 0.7 V was applied for 10 minutes to yield a polymer loading of 5.68 $\pm$ 0.47 mg cm^{-2}. Cyclic voltammetry (CV) measurements were done in 0.1 M potassium chloride (KCl) aqueous solution.

3.3.2 Separation of organic solutes

Adsorption studies were performed at ambient temperature in 20 mL scintillation vials continuously shaken at 150 rpm min^{-1} to increase mixing. The concentrations of the model contaminant Sudan Orange G, and pharmaceutical synthesis compounds propranolol hydrochloride (PP) and 1-naphthol (1-NO) (Millipore Sigma) in the aqueous phase (Ce) were measured by a Cary 60 Ultraviolet-visible (UV-vis) spectroscope. The mass of solute adsorbed to PPy(AOT)- and PVF-PPy-coated electrodes was de-

termined as $Q_e = \frac{(C_0 - C_e)Vol}{m}$, where Q_e (mg g^{-1} polymer) is the solute adsorbed per gram of polymer, C_0 (mg L^{-1}) and C_e (mg L^{-1}) are the initial and final solute concentrations in the solution phase, respectively, m (g) is the mass of the particular type of polymer on the carbon fiber cloth substrate, and Vol (L) is the volume of solution. The Freundlich isotherm equation was fitted to the batch adsorption data.

The two PVF-PPy//PPy(AOT) electrodes were assembled into an asymmetric system for adsorption studies and rendered both materials hydrophobic by discharging at 0 V or 0.3 V, waited until equilibrium was reached, and then regenerated the system by applying a positive potential (1.2 V or 1.5 V) for 10 minutes in 5 ml of 0.1 M KCl solution. To reuse the electrodes in subsequent cycles of adsorption, the polymer was reactivated for adsorption by applying 0 V or 0.3 V for 10 minutes in the same 0.1 M KCl desorption solution.

Concentrations of PP and 1-NO in the binary mixture were determined using high-performance liquid chromatography (HPLC) equipped with a flame-ionization detector (FID) (Agilent) and a ZORBAX Extend 80 C18 (4.6 mm × 50 mm, 5 μm) analytical column (2.1 mm × 50 mm, particle size 3.5 μm). Samples for the HPLC analysis were prepared by adding 20 μL of N-benzylmethylamine as internal standards to 1 mL of solutions. Five microliters of samples were injected and eluted using a gradient pump delivering 1 mL min^{-1} of a water and acetonitrile mobile phase, each containing 0.1 vol.% formic acid. OpenLab CDS software was used to determine the area under the peaks in the chromatograms and to carry out baseline corrections. All results reported are based on the average of three replicates.

3.3.3 pH monitoring

To assess the impact of parasitic reactions due to water electrolysis, pH was monitored in-situ during electrochemical modulations of the hydrophobicity of the materials through potential swings. A custom LabView program and the Orion ROSS Combination Semi-micro pH Electrode were used to collect the pH data. The evolution of OH^- was directly computed from pH fluctuations and subsequently converted to the charges lost to hydrogen or oxygen evolution reactions, respectively.

3.3.4 Assessment of AOT leaching

In order to assess the leaching of AOT during desorption, an inductively coupled plasma optical emission spectrometer (ICP-OES Optima 8000, PerkinElmer, USA) equipped with a GemTip Cross-flow II nebulizer and a Ryton HF-resistant Scott-type spray chamber was used to determine the sulfur content in the desorption solution. Standard solutions for creating the sulfur calibration curve were prepared by sequential dilution of a stock solution (Millipore Sigma 1000 mg L^{-1} S in H_2O). The operating conditions for the ICP-OES analyses were: wavelength 180.669 nm, radio frequency power of 1500 W, principal plasma gas flow rate of 10.0 L min^{-1}, auxiliary gas flow rate of 0.2 L min^{-1} and nebulizer gas flow-rate of 0.7 L min^{-1}.

3.4 Summary

An asymmetric system consisting of PPy(AOT) and PVF-PPy polymers is developed for electrochemically mediated separations of organics from water to exploit their complementary tunabilities in hydrophobicity. It was experimentally demonstrated the system was stable for 5 cycles of adsorption and regeneration using electrochemical means. The asymmetric system showed improvements in suppressing parasitic water splitting reactions to maintain solution pH and to reduce loss of electrical energy to side reactions. In energetic efficiency terms, the electrochemically mediated separation technology using the PVF-PPy//PPy(AOT) system is competitive in comparison with thermally regenerated activated carbons. The system also shows selectivity for certain organics present in mixtures, suggesting potential applications in pharmaceutical purifications. The ease of implementation of the PVF-PPy//PPy(AOT) system, only requiring mild electrical energy for regeneration which can potentially be derived from renewable sources, permits electrochemically mediated separations to be performed both in industrial settings and at distributed or remote locations.

THIS PAGE INTENTIONALLY LEFT BLANK

Chapter 4

Electrochemical Control of Ferrocene-Cyclodextrin Complexations

4.1 Introduction

In the pursuit of redox-responsive adsorbents with wider applicability, cyclodextrin polymers emerge as a promising candidate for the following three reasons:

- Robustness

  The unique chemical structures of cyclodextrins (CD) enable them to be "all-purpose molecular containers for organic, inorganic, organometallic, and metal-lorganic compounds that may be neutral, cationic, anionic, or even radical."[23]

- Biocompatibility

  Cyclodextrins have excellent biocompatibility[31,125] and hence are widely used in the pharmaceutical, food, agriculture, cosmetics, hygiene, medicine, and textile industries as drug delivery agents and stable additives.[93]

- Tailorability

Chemical modifications through fuctionalization or cross-linking can enhance the selectivity, capacity and adsorption kinetics of the sorbents based on CD, especially towards organic compounds.[6,23,93]

4.1.1 β-Cyclodextrin

Cyclodextrins (CD) are polysaccharides consisting of glucose units connected by α-1,4-glycosidic linkages and have truncated-cone shapes.[93] There are three types of native cyclodextrins bearing 6, 7, and 8 glucosidic units, denoted α-CD, β-CD, and γ-CD, respectively, whose structures can be found in Figure 4-1a. Because the internal cavity of a CD is hydrophobic while the external surface is hydrophilic, these macromolecules are capable of encapsulating hydrophobic organic molecules in their interior due to van der Waals forces and thermodynamic factors, and adsorbing polar species (e.g. water) on their exterior with exposed hydroxyl groups (Figure 4-1b).[93]

Among the three naturally occurring CDs, β-cyclodextrin is the most frequently used in environmental remediation due to its perfect cavity size, greater complexation ability, low solubility in water, favorable intramolecular hydrogen bond localization, and low-cost.[31,93] Therefore, a new strategy is developed to render β-CD-containing adsorbents redox-responsive and eletrically conductive.

4.1.2 Cyclodextrin-ferrocene inclusion complexes

The hydrophobic central cavity of cyclodextrins is suitable for the inclusion of various organic molecules ranging from polar compounds such as alcohols, acids, amines, and small inorganic anions to apolar compounds such as aliphatic and aromatic hydrocarbons.[27] β-cyclodextrin polymer with large surface area has been shown to sequester a variety of organic micropollutants with adsorption rate constants 15 to 200 times greater than those of activated carbons, showing a great potential for water remediation.[6,119]

Besides the high potential as an adsorbent, β-cyclodextrin also froms a 1:1 stoichiometric inclusion complex with neutral ferrocene (Fc), while oxidized ferrocenium

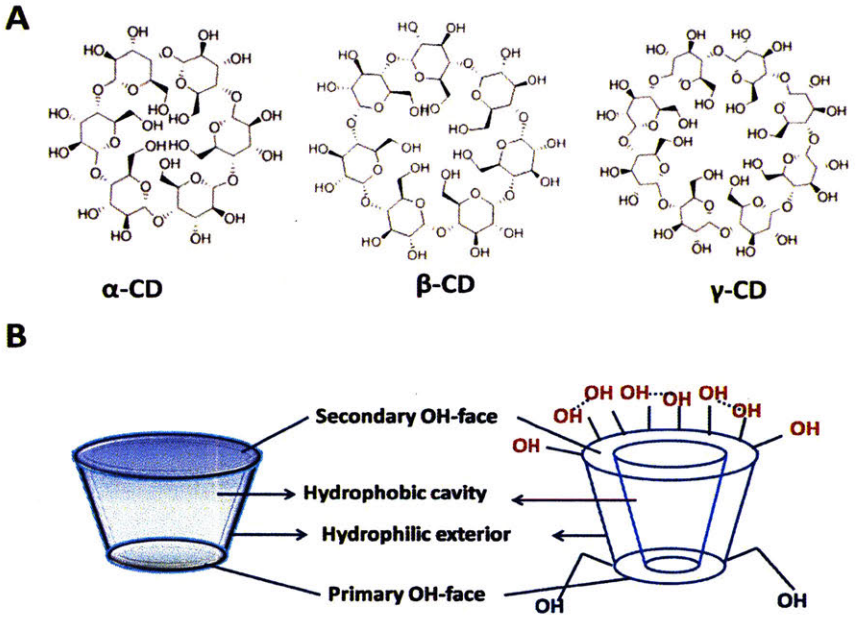

Figure 4-1: (a) Chemical structures of alpha- (α-CD), beta- (β-CD) and gamma- (γ-CD) cyclodextrins. (b) Shape and characteristics of cyclodextrins. Reprint by permission from REF.[93], Elsevier.

(Fc^+) is not significantly included in the cavity.[27] Such redox-responsive reversible complexation between ferrocene and β-CD can be exploited to control the adsorption and release of organic compounds in the hydrophobic cavity.

Figure 4-2 illustrates how the reversible complexion can serve as an underlying gating mechanism for controlling the uptake and release of competing host molecules: oxidation of the Fc moieties induces the dissociation of Fc^+ from β-CD, freeing up the cavities for binding of other organic molecules; reduction of the Fc^+ would cause the replacement of the bound organic molecule with Fc in the neutral state. Such a reversible cyclodextrin-ferrocene complexation can theoretically control the binding and rejection of molecules with a lower binding constant (K) compared to Fc ($K = 10^3 - 10^4$ M^{-1}) but higher than Fc^+ ($K \approx 50$ M^{-1}).[6,119] The wide difference between Fc and Fc^+ in terms of binding on β-CD allows many organic compounds to fall in this range, such as phenol, aniline and their derivatives ($K = 100$ M^{-1}).[15,80]

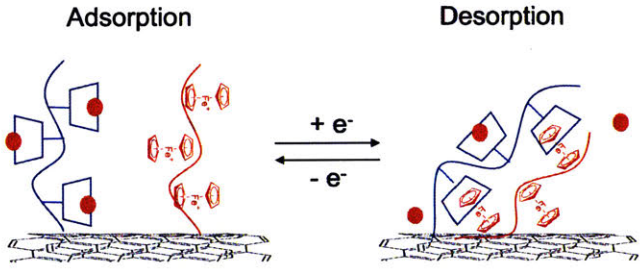

Figure 4-2: A schematic of the β-CD/Fc complexation for reversible capture and release of organic compounds in water (the orange balls represent competing organic molecules for the hydrophobic cavity).

4.2 Results and discussion

As with the polypyrrole-based adsorbent, electrical conductivity is essential for the adsorbent to be modulated by potential stimuli instead of chemical agents. Two different approaches have been developed to prepare conductive cyclodextrin-ferrocene hybrids: conjugation of β-cyclodextrin and ferrocene moieties on the surface of carbon nanotubes (CNT), and electrochemcial synthesis of a ternary hybrid containing polypyrrole (PPy), polyvinyl ferrocene (PVF), and β-cyclodextrin sulfate in one step.

4.2.1 Preparation of conductive cyclodextrin-ferrocene hybrids

4.2.1.1 Carbon nanotube-based approach

In order to prepare β-CD/Fc hybrid coatings on conductive carbon fiber substrates, carbon nanotubes (CNT) are chosen as anchors to the inclusion complex-forming hybrids onto the substrates and as electron conductors. Figure 4-3a shows the chemical structures of the individual components in a ternary β-CD/PVF/CNT hybrid. Two dispersions of β-CD/CNT (4) and Fc/CNT (5) are separately prepared. In the first dispersion, amine functionalized β-CD (1) were first covalently attached to pyrene (2), which conjugates the β-CD-containing amide (3) to CNT via $\pi - \pi$ stacking,[67] and the β-CD/CNT hybrid is subsequently dispersed in N-methyl-2-pyrrolidone (NMP). Fc/CNT is prepared by dispersing CNT with polyvinyl ferrocene (PVF) in NMP.[60] The two dispersion solutions are then mixed and the ternary β-CD/PVF/CNT hybrid is drop cast onto conductive carbon fiber substrates to form the final adsorbent.

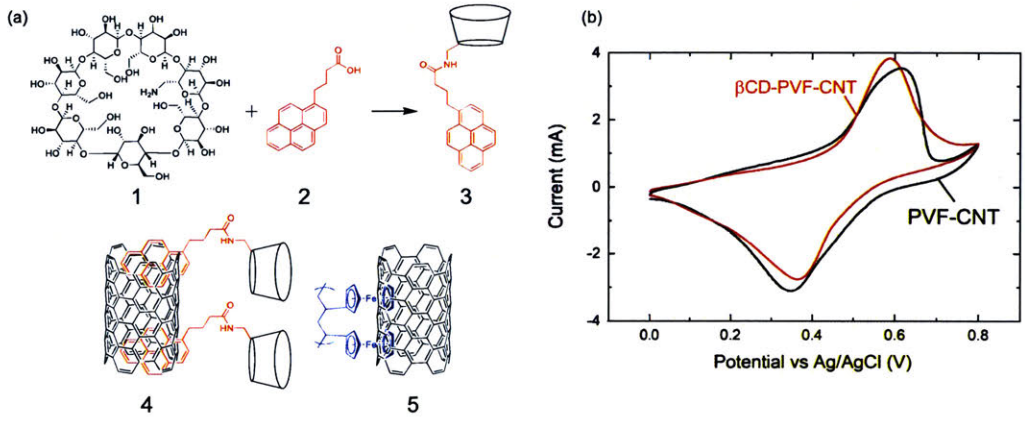

Figure 4-3: (a) Covalent modifications of β-CD to incorporate pyrene which conjugates β-CD onto carbon nanotubes. (b) Cyclic voltammograms of the β-CD/PVF/CNT ternary hybrids and PVF/CNT binary hybrids.

The cyclic voltammogram (CV) of the β-CD/PVF/CNT hybrid in Figure 4-3b shows improved redox activities over PVF/CNT as the separation between the oxidation and reduction peaks is smaller. This can be explained by enhanced hydrophilicity of the hybrid due to the incorporation of β-CD with many hydroxyl groups on the

external surface which contribute to better solvation of redox moieties in the aqueous electrolyte.

Due to the presence of carbon nanotubes, the film consisting of the ternary β-CD/CNT hybrid features nanoporous structures as shown in Figure 4-4.

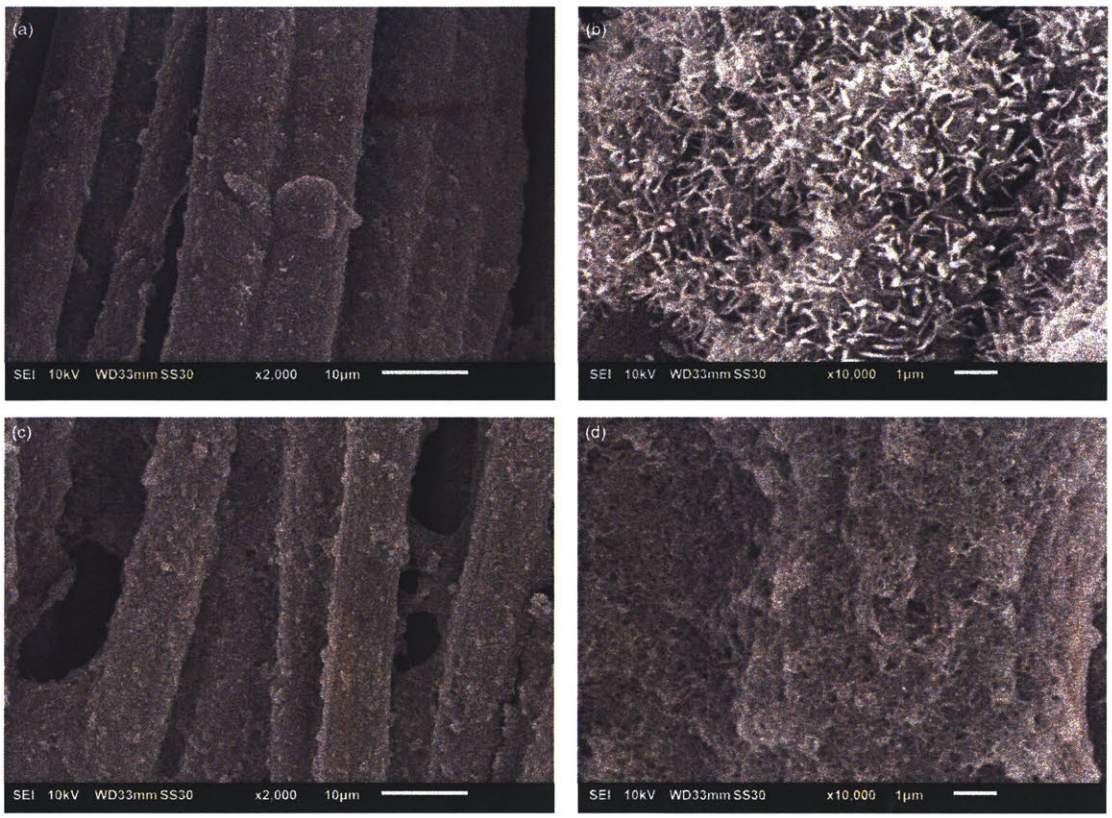

Figure 4-4: SEM images of (a)-(b) β-CD/PVF/CNT ternary hybrids and (c)-(d) PVF/CNT binary hybrids.

4.2.1.2 Conducting polymer-based approach

Alternatively, a conducting polymer such as polypyrrole can be used as a solid matrix to host both β-CD and ferrocene moieties, and provide electrical conductivity to them. Herein, the eletrochemical polymerization of pyrrole in a supporting electrolyte containing β-CD sulfate is combined with the electrodeposition of PVF. The composition and CV profile of the resulting film, refered to as PVF-PPy(β-CD), are

presented in Figure 4-5. There two pairs of redox peaks can be attributed to the insertion/repulsion of cations into the film doped with bulky anions ($E^0 \approx -0.2$ V vs. Ag/AgCl), and the reversible oxidation and reduction of the ferrocene moieties ($E^0 \approx 0.2$ V vs. Ag/AgCl).

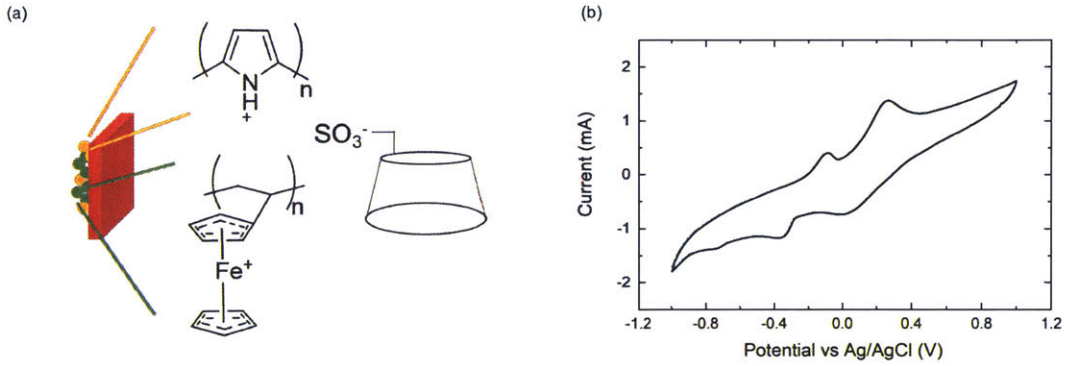

Figure 4-5: (a) Three components and (b) CV of the PVF-PPy(β-CD) film.

The resulting PVF-PPy(β-CD) forms a conformal coating on the carbon fibers and features globular structures which adds porosity to the film (Figure 4-6a-b). The incorporation of the ferrocene and β-CD sulfate salt was verified using Energy-dispersive X-ray spectroscopy (EDX). The elemental mapping of iron (Fe) and sulfur (S) confirms that the redox moieties are well distributed across the film (Figure 4-6c-d).

4.2.2 Adsorption of organics

The two different materials containing β-CD/Fc are challenged by the adsorption of propranolol hydrochloride (PP) and 1-naphthol. Both materials adsorb more organics in their respective oxidized states owing to the availability of the hydrophobic cavity (Figure 4-7 and Figure 4-8). Moreover, the reduced β-CD-PVF-CNT film can be activated by oxidizing the ferrocene moieties to recover a higher capacity observed in the initially oxidized film, suggesting the tunability in organics uptake by controlling the complexation of Fc and β-CD using electrical potential stimuli.

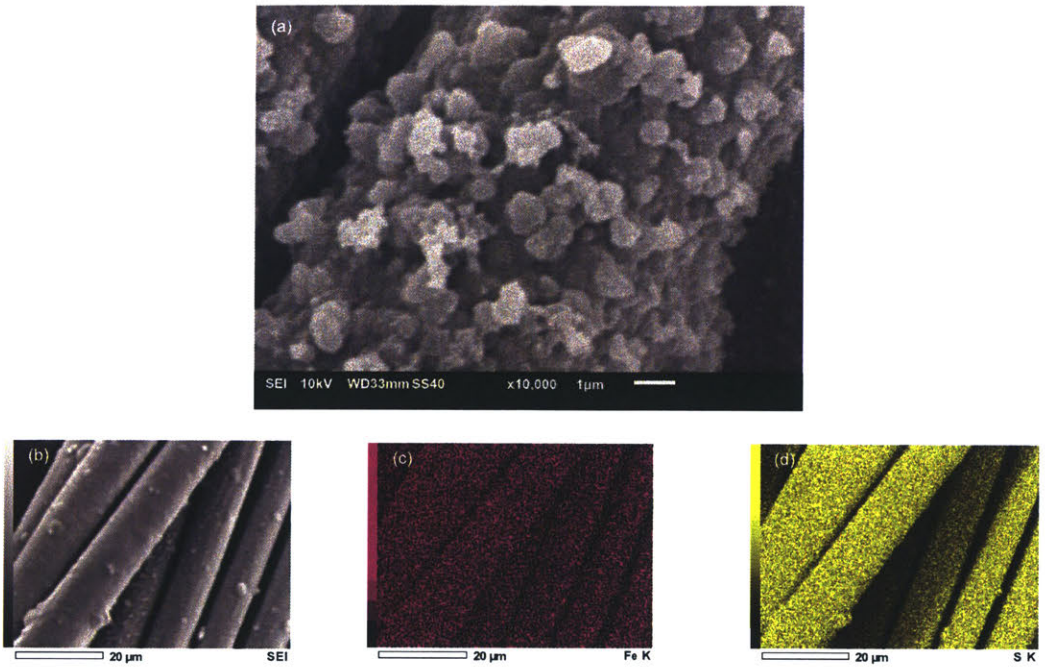

Figure 4-6: (a)-(b) An SEM image of the PVF-PPy(β-CD) film.(c)-(d) EDX mapping of iron (Fe) and sulfur (S) elements on the PVF-PPy(β-CD) film showing the presence and even distribution of Fc and β-CD moieties.

The preliminary separation experiments show the feasibility of the gating approach via redox-responsive complexation of ferrocene and β-CD. More dramatic difference in the uptake of organics by oxidized and reduced polymer films could potentially be accomplished with a precise stoichiometric ratio of ferrocene and β-CD moieties in the hybrid materials.

4.3 Materials and methods

4.3.1 Materials

Pyrrole, 6-monodeoxy-6-monoamino-β-cyclodextrin, 1-Pyrenebutyric acid, β-Cyclodextrin sulfated sodium salt (extent of labeling: 12-15 mol per mol β-CD), potassium chloride (NaCl), propranolol hydrochloride (analytical standard), 1-Naphthol ($\geq$ 99%), multi-walled carbon nanotubes (MWCNT, >98% carbon basis, O.D. $\times$ L 6-13 nm $\times$ 2.5-20 μ

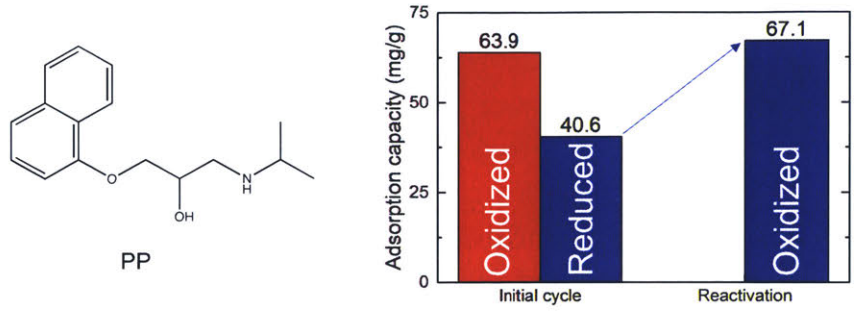

Figure 4-7: Adsorption of PP on the β-CD-PVF-CNT ternary hybrid film.

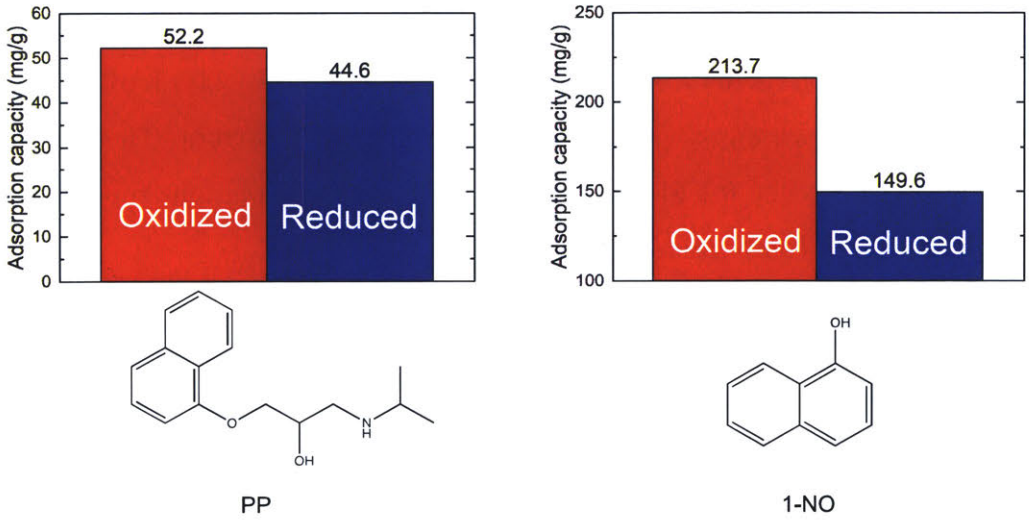

Figure 4-8: Comparison of adsorption of PP and 1-NO by PVF- PPy(β-CD) in the oxidized an reduced states.

m), ethylene glycol ($\geq$ 99%)), and N-Methyl-2-Pyrrolidone (NMP, HPLC grade) were purchased at Millipore Sigma and used as received throughout the study. Polyvinyl ferrocene (PVF, MW ~50,000) was purchased from Polysciences, Inc. Carbon fiber cloth substrates were obtained from Fuelcell.com and used without pretreatment prior to electrochemical functionalization or testing.

4.3.2 Synthesis of adsorbent

4.3.2.1 β-cyclodextrin-PVF-CNT

A condensation reaction between 6-monodeoxy-6-monoamino-β-cyclodextrin and 1-Pyrenebutyric acid was carried out following the protocol previously reported[67] to functionlize β-cyclodextrin with a pyrene moiety. The β-CD/PVF/CNT teneray mixture was prepared by drop casting a mixture of two CNT-containing dispersion solutions. Solution A contains 56 mg mL^{-1} of the pyrene functionalized β-CD and 10 mg mL^{-1} MWCNT in NMP. Solution B contains 10 mg mL^{-1} of MWCNT and PVF in NMP.[60] The two solutions are separately sonicated for 2 hours to form a smooth ink before being mixed and briefly sonicated for 10 minutes. Finally, 100 μL of the mixed dispersions was drop cast onto a piece of 2 cm^2 carbon cloth substrate. The as formed electrodes were washed by 0.1 M sodium hydroxide aqueous solutions repeatedly to remove unconjugated components.

4.3.2.2 PVF-PPy(β-CD)

The PVF-PPy(β-CD) was prepared by simultaneous electropolymerization of pyrrole and electrodeposition of PVF. The electropolymerization bath contained 0.1 M pyrrole, 3 mg mL^{-1} PVF, 1.2 g mL^{-1} β-Cyclodextrin, sulfated sodium salt dissolved in ethylene glycol (Millipore Sigma). A constant current density of 10 mA cm^{-2} was applied for 10 minutes for the electrochemical synthsis of the PVF-PPy(β-CD) film.

4.3.3 Characterizations

Scanning electron microscopy (SEM) images were taken using a JEOL-6010LA electron microscope. Cyclic voltammetry (CV) measurements were done in 0.1 M potassium chloride (KCl) aqueous solutions at a scan rate of 10 mV s^{-1}.

4.3.4 Adsorption of organic compounds

Adsorption studies were performed at ambient temperature in 20 mL scintillation vials continuously shaken at 150 rpm min^{-1} to increase mixing. Concentrations of PP and 1-NO in the binary mixture were determined using high-performance liquid chromatography (HPLC) equipped with a flame-ionization detector (FID) (Agilent) and a ZORBAX Extend 80 C18 (4.6 mm $\times$ 50 mm, 5 μm) analytical column (2.1 mm $\times$ 50 mm, particle size 3.5 μm). Samples for the HPLC analysis were prepared by adding 20 μL of N-benzylmethylamine as internal standards to 1 mL of solutions. Five microliters of samples were injected and eluted using a gradient pump delivering 1 mL min^{-1} of a water and acetonitrile mobile phase, each containing 0.1 vol.% formic acid. OpenLab CDS software was used to determine the area under the peaks in the chromatograms and to carry out baseline correction. The β-cyclodextrin-PVF-CNT electrodes were oxidized at 0.8 V and 0 V vs Ag/AgCl, respectively. The PVF-PPy(β-CD)-coated electrodes were oxidized at 0.6 V and -0.5 V vs Ag/AgCl, respectively.

4.4 Summary

β-cyclodextrin-containing polymers are a promising candidates for the separation of organic solutes from aqueous solutions. The ability to control the reversible inclusion and rejection of ferrocene moieties in the hydrophobic cavity of β-cyclodextrin via electrical potential stimuli offers a new gating mechanism for controlling the adsorption and release of organic molecules by β-cyclodextrin-containing sorbents. Further optimization of the conjugation of β-CD and ferrocene moieties onto conducting entities is required to magnify the gating effects for more dramatic change in the affinity

of the sorbent induced by electrochemcial potential stimuli.

4.5 Additional information

4.5.1 NMR spectra

4.5.1.1 NMR spectra of 6-monodeoxy-6-monoamino-β-cyclodextrin, 1 in Figure 4-3a.

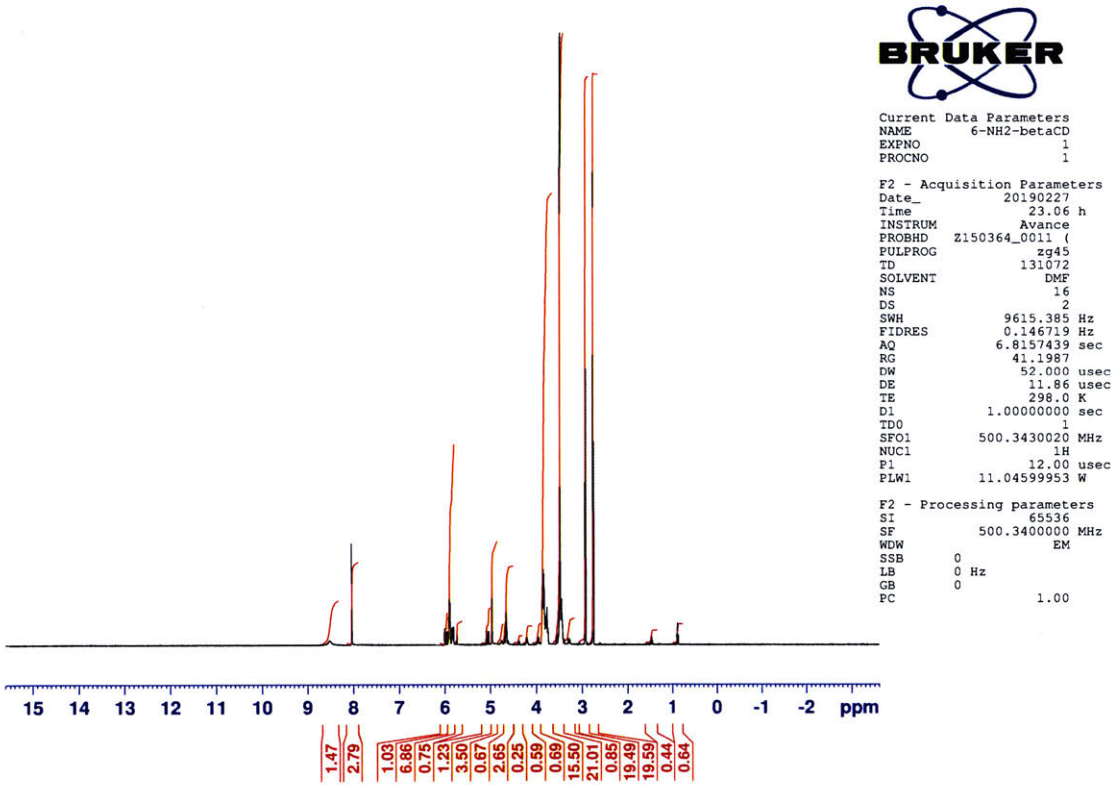

Figure 4-9: ^{1}H NMR spectrum.

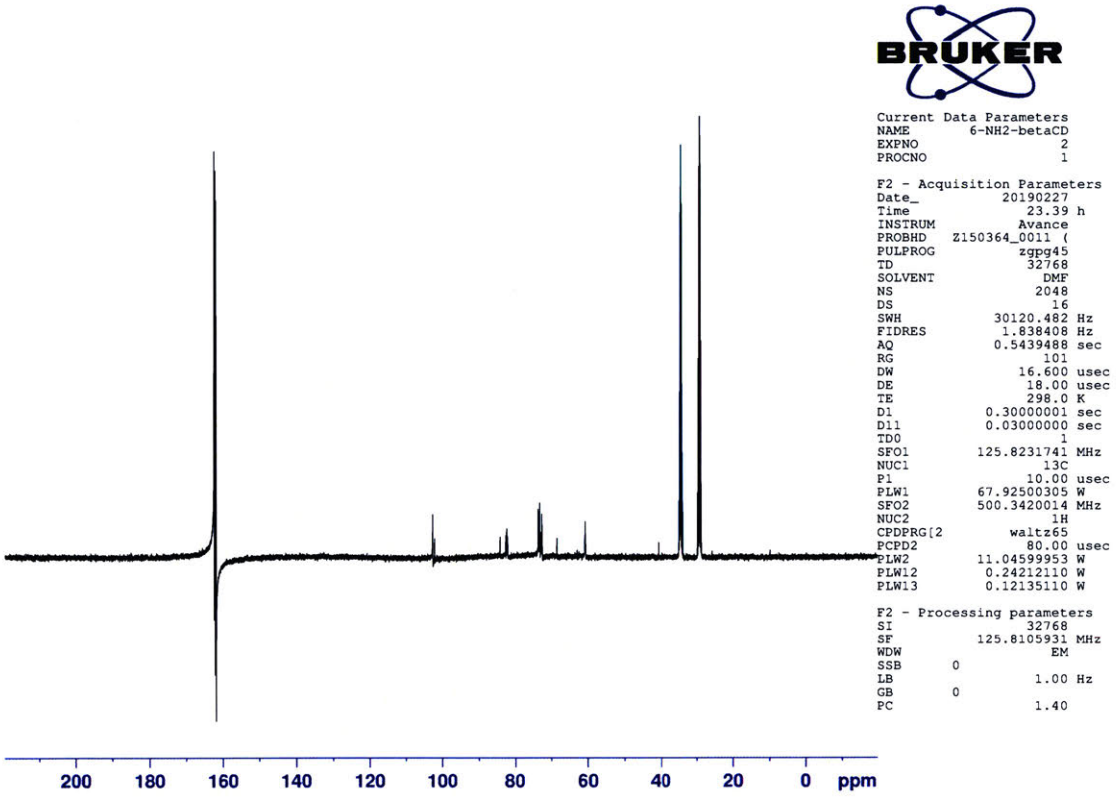

Figure 4-10: ^{13}C NMR spectrum.

4.5.1.2 NMR spectra of pyrene functionalized β-cyclodextrin, 3 in Figure 4-3a.

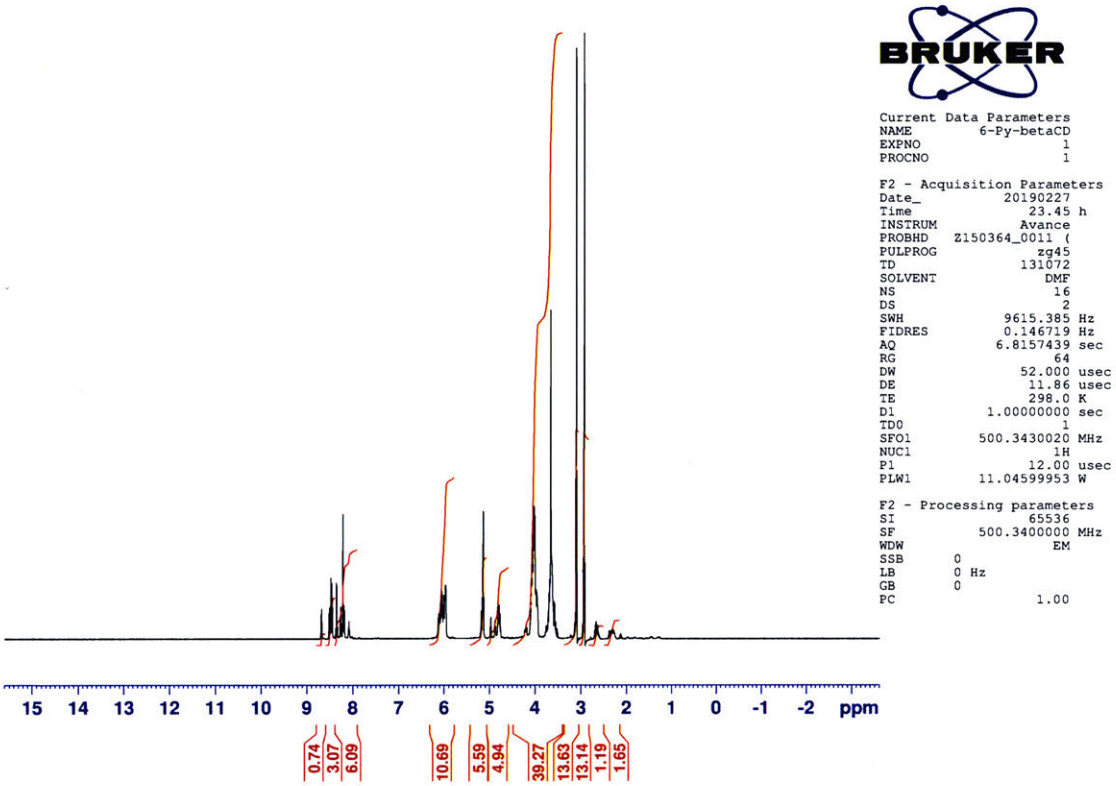

Figure 4-11: ^{1}H NMR spectrum.

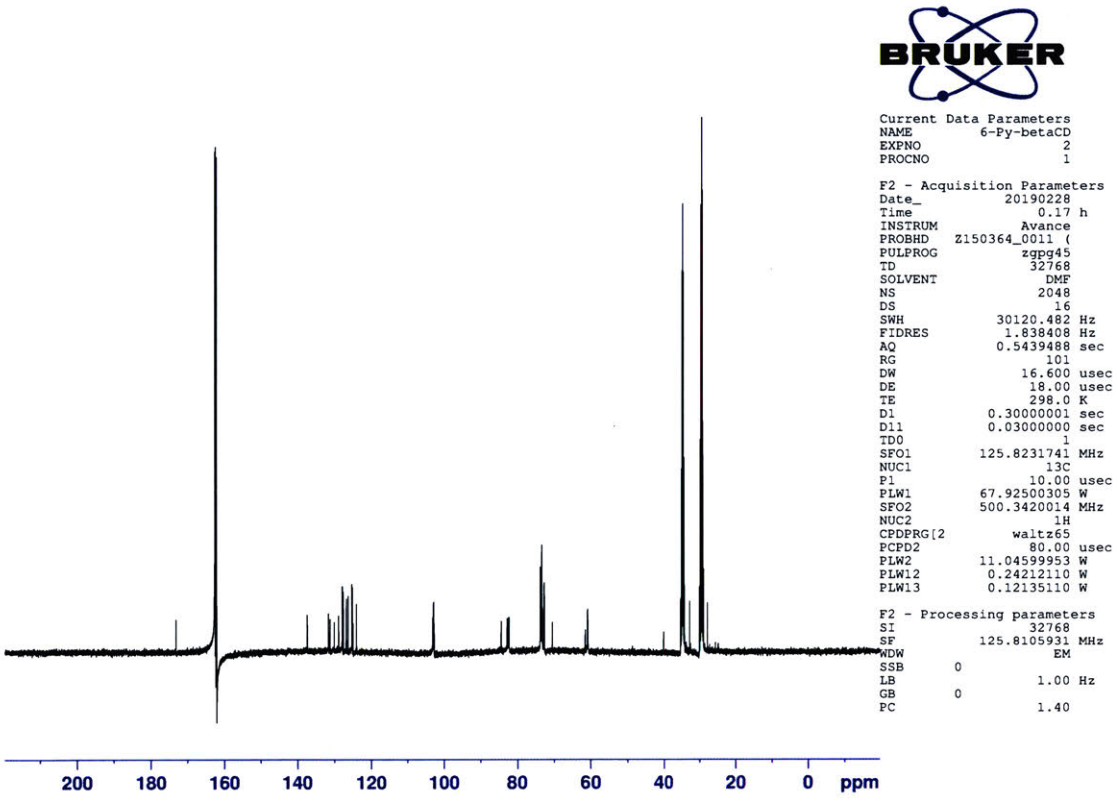

Figure 4-12: ^{13}C NMR spectrum.

THIS PAGE INTENTIONALLY LEFT BLANK

Chapter 5

Conclusion and future outlook

Selective separations of organic compounds are of great importance in many industries, such as water treatment and pharmaceutical manufacturing.[6,88,90] Conventional technologies such as distillation, evaporation, and extraction are energy intensive and costly.[19,57] Although adsorption by activated carbon (AC) has proven effective, regeneration of AC by thermal processes or solvent extraction is limited to centralized facilities to achieve economy of scale and economic viability. In many industrial processes, certain organic species are of economic value and hence need to be recovered and purified for use. For these reasons, novel technologies for electrochemcially mediated separations of organics from aqueous solutions were developed in this thesis to provide point-of-use solutions for the remediation of organic pollutants in wastewater and for the recovery of organic products.

5.1 Conclusion

The thesis began with a review of the emerging issues of water pollution throughout the world, especially those caused by organic contaminants. The common categories of organic contaminants, their sources and negative impact on human beings and aquatic life were presented. Important examples of existing technologies for remediation of organic pollution in wastewater or for separation of organic compounds from aqueous solutions were introduced along with discussions of their drawbacks.

The objective of the thesis was then introduced—to provide alternative methods for energetically efficient, molecularly selective and environmentally friendly separation of neutral organic compounds from aqueous solutions. Redox-active polymeric adsorbents with tunable hydrophobicity in response to electrical potential stimuli would enable this overarching objective to be accomplished.

In Chapter 2, a novel adsorbent based on a conducting polymer polypyrrole (PPy) doped with anionic surfactants AOT featuring a hierarchical morphology was developed for the electrochemically reversible adsorption of organics from water. The functional material was synthesized in a one-step electropolymerization reaction, leading to a homopolymer of unique structures with a high surface area for enhancing the adsorption capacity (greater than 570 mg pollutant/g polymer), and with greater exposure of the electrode surface to the electrolyte solution during the electrochemical modulations for better electroactivity. A mechanistic explanation for the improved morphology was also provided.

The surfactant-doped polypyrrole was shown to be able to function as an electrochemically regenerable adsorbent for uncharged organics. The anionic surfactant dopants within the polymer can undergo reorientation with respect to the polymer backbone to modulate the hydrophobic environment and hence affinity for organics under different applied potentials. Therefore, the adsorption and regeneration of the adsorbent can be programmed by applying mild potential swings. It was demonstrated that the material can be used repeatedly for multiple adsorption/desorption cycles.

In addition, DFT-MD simulations elucidated the physico-chemical interactions between the dopants, the polymer, and the adsorbate. Such quantitative understanding of the molecular interactions corroborated that the underlying mechanism for modulating the hydrophobicity of PPy(AOT) was due to the surfactant reorientation relative to the polymer backbone during redox reactions, as previously proposed in literature.

In Chapter 3, a system for electrochemically mediated separations of organics from water was assembled from two polypyrrole(PPy)-coated electrodes modified with dif-

ferent redox moieties: incorporation of a polyvinylferrocene (PVF) redox-responsive polymer in the PPy electrode coating, and doping of the PPy with the amphiphilic surfactant dioctyl sulfosuccinate (AOT). Since PVF-PPy is more hydrophobic when reduced, and hydrophilic when oxidized, while PPy(AOT) behaves in the opposite manner, i.e. is more hydrophilic when reduced, and more hydrophobic when oxidized, it was hypothesized that the PVF-PPy and PPy(AOT) electrodes form an attractive pair for an asymmetric system to work in tandem.

The as-assembled asymmetric system with complementary turnabilities in hydrophobicity showed three main benefits:

- Suppression of water parasitic reactions: the dual-functionalized system allowed electrons to be exchanged between the two electrodes and was successful in preventing pH fluctuations during the electroswing operation.

- Superior energetic efficiency: the complementary tunabilities in hydrophobicity in the PVF-PPy and PPy(AOT) permit the use of the two polymers in tandem for removing organic compounds from aqueous solutions. The tradeoff between energy cost and separation extent affected by the applied potentials was studied. Comparison of the asymmetric system with the widely adopted thermally regenerated activated carbons showed that the former outperforms the latter in energetic efficiency terms.

- Selectivity for target organic species: the system was able to remove organic compounds in a reversible fashion, and also showed molecular selectivity for certain organics present in mixtures, suggesting potential applications in pharmaceutical purifications.

Chapter 4 made an attempt to explore a class of robust adsorbent based on β-cyclodextrin, and achieved voltage-dependent adsorption of organic compounds due to the redox-responsive complexation between β-cyclodextrin and ferrocene.

Conventional separation processes rely on changes in temperature, pressure or solution conditions to drive capture and release of target compounds. Electrochemically

mediated separations instead use environmentally friendly and energetically efficient voltage swings to modulate material properties and attain reversibility. Electrodes functionalized with redox-active materials have been developed to remove ionic species and charged biomacromolecules from aqueous solution in a reversible manner[101]. This thesis expands the applicability of the voltage-swing approach to dissolved neutral organic species which is challenging for many conventional and modern separation technologies (e.g., ion exchange, reverse osmosis) due to the lack of electrostatic interactions or fouling.[117]

In a broader context, the ability to efficiently and selectively separate organic compounds from aqueous solutions is relevant in many scenarios such as treatment of industrial, municipal and agricultural wastewater, recovery of valuable organic products, and concentration of diluted streams for analysis or further processing. The ease of implementation of the asymmetric redox-responsive electrode system, only requiring mild electrical energy for regeneration which can potentially be derived from renewable sources, permits electrochemically mediated separations to be performed across a range of scales, both in industrial settings and at distributed or remote locations.

5.2 Future outlook

The proof-of-concept asymmetric system demonstrates the ability of potential swings to modulate material properties for electrochemically mediated separations of organic compounds in aqueous solutions. There are still engineering challenges and material design opportunities for the novel technology to become more robust.

5.2.1 Engineering challenges

The system needs to be scaled up for high-throughput separation processes, whether for wastewater treatment or for purification of organic products. One way to achieve this would require fabrication of a trilayer adsorbent and integration of the adsorbent into a flow channel for operations in a semicontinuous mode.

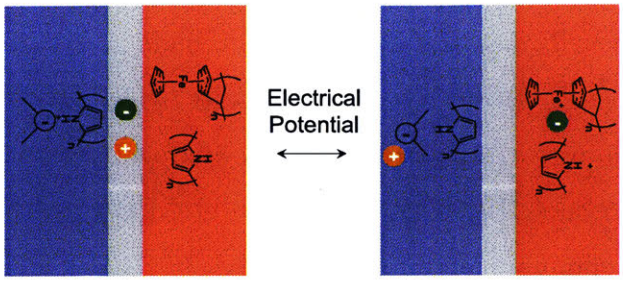

Figure 5-1: A schematic of the trilayer adsorent with conducting polymeric adsorbent on the outside (Blue and Red) and a solid-state electrolyte in the middle (Gray).

5.2.1.1 Trilayer adsorbent

Retrieving the adsorbent for regeneration in a separate desorption stream containing supporting electrolytes may add obstacles for automated separation processes. Moreover, it might be undesirable to recover the adsorbed species in a saline solution. One strategy to mitigate these complications would be fabrication of a trilayer adsorbent that combines the adsorbent and electrolyte in the solid phase. Figure 5-1 shows a schematic of the adsorbent: the two outer layers are the two complementary adsorbent materials PVF-PPy//PPy(AOT) with a solid-state matrix in the middle. The midlayer serves two purposes: first, separating the two electrodes to prevent shorting; second, hosting ionic species and facilitating their movement during charging/discharging of an electrochemical cell. When the system is discharged, i.e. PVF-PPy in the reduced state and PPy(AOT) in the oxidized state, the electrolytes will be hosted in the midlayer; when the adsorbent needs to be regenerated, the cations and anions will migrate, respectively, to the reduced PPy(AOT) negative electrode, and the oxidized PVF-PPy positive electrode.

A suitable solid-state electrolyte needs to be incorporated within the prototypical polypyrrole-based asymmetric system described in Section 3. A solid-state eletrolyte can serve as both an ionic conductor and electrode separator with added advantages of simple fabrication and liquid-leakage free.[127] Polymer-based solid electrolytes are

the most studied for applications in capacitors and can be further divided into three categories, solid polymer electrolyte (SPE), gel polymer electrolyte (GPE) and polyelectrolytes. GPE usually has the highest ionic conductivity and is composed of polymer matrix swollen by a solvent containing salts, which might be a good option for the midlayer. The polymer matrix may be a hydrogel such as polyvinyl alcohol or polymethylmethacrylate. However, integration of GPE with the two other layers requires attention to eliminate ion diffusion barriers.[127] The exact choice of the polymer matrix and salts need to be explored in conjunction with the PVF-PPy positive electrode and the AOT-doped PPy negative electrode.

5.2.1.2 Flow channel for semicontinuous operations

The trilayer adsorbent can be integrated with a flow channel for carrying out the adsorption in flow. The system will be regenerated once the adsorbent becomes exhausted. To optimize the semicontinuous process, transport processes within the flow channel and the trilayer adsorbent need to be modeled for the following purposes:

- To understand the interplay of adsorption and transport in the two regions, the flow channel and the porous polymer adsorbent.
- To guide the design of flow configurations and selection of process parameters for best separation performance (high removal efficiency and high utilization of adsorbent).
- To model the separations of a multicomponent organic mixture: by applying a potential gradient along the flow direction to render the trilayer adsorbent increasingly more hydrophobic, organics of increasing hydrophobicity will be adsorbed at further distances from the inlet. During regeneration, organics of decreasing hydrophobicity adsorbed on the adsorbent can be sequentially released to separate regeneration streams by adjusting the potential stimuli to render the adsorbent increasingly more hydrophilic.

The trilayer design and a semicontinuously operated adsorber are enablers for high-throughput water-organics separations using the proposed asymmetric system

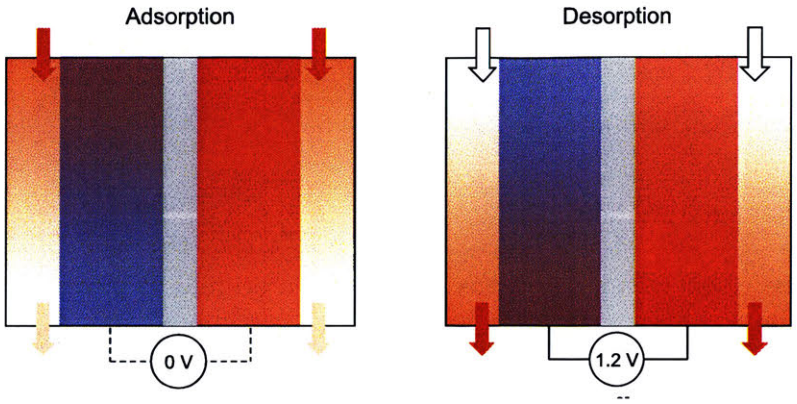

Figure 5-2: A schematic of a flow channel with the trilayer adsorbent to capture organics from aqueous streams in a semicontinuous mode.

based on two dissimilar polypyrrole polymers with complementary tunability in hydrophobicity.

5.2.2 Material design opportunities

5.2.2.1 Multicomponent separations

Multicomponent separations are challenging but required in many applications, especially for the recovery of organic products. There are two potential strategies to accomplish this formidable task with selectivity accomplished through

- Tailored material chemistry

  Similar to the Faradaic capacitive deionization (FaCDI) where the anode selectively removes anions and the cathode selectively removes cations, we can also design adsorbent materials of tailored chemistry to target different organic species present in a mixture. When the two adsorbents are immobilized on the positive and negative electrodes respectively, different organics can be adsorbed onto the surfaces of either electrode, and subsequently released into desorption streams on either side of the adsorbent (left or right) as depicted in 5-2.

  Gani et al. has developed a computational screening approach for functionalized ferrocene moieties to achieve selectivity and reversibility of organic anions

relative to perchlorate.[29] Computation can guide rational design of the chemistry for the adsorbent to selectively separate different organics into separate streams or to target an organic compound of interest through more specific adsorbent-adsorbate interactions.

- Hydrophobicity gradient

  If the adsorbent is very sensitive to potential stimuli applied, its affinities towards a target organic compound will vary depending on the magnitude of applied potential. If the target organic compound happens to be the most hydrophilic species in the mixture, the target solute can be selectively removed from the rest of the mixture by applying a potential to render the adsorbent just enough hydrphobic to take up the one species.

  One more complicated scenario of multicomponent separations involves separation of mixtures of organics of different hydrophobicity into separate streams. Potential gradients along the length of the adsorbent can induce a gradient of hydrophobicity in the material as described in the modeling of multicomponent separations in Section 5.2.1.2. The most hydrophilic organic species can be removed first followed by increasingly more hydrophoic compounds removed downstream.

5.2.2.2 Compatibility with saline solutions

Industrial wastewater generated by many industries (e.g., food, petroleum, and leather) contains salt (mainly NaCl) which strongly inhibits biological treatment.[55] Therefore, to remediate organic pollution in industrial saline wastewaters, especially those contain hypersaline, the state-of-art practice is to first implement physico-chemical processes such as coagulation-flocculation, ion exchange, reverse osmosis, electrolysis or ultrafiltration for removing the salts, and then to send the effluent for further biological treatment. In contrast, electrochemcially mediated separations can take advantage of the saline already present in the inlet and avoid the addition of supporting electrolyte during the treatment process. Moreover, because electrochemcially

mediated separations use electrical energy to control the adsorption and release of both charged ionic species via Faradaic capacitive deionization (FaCDI) and neutral organic compounds using the polypyrrole-based asymmetric system. The potential of using one technology (electrochemcially mediated separations) for remediating both charged and neutral species could avoid repeated capital investment for combination of different technologies, such as RO systems for desalination and bioreactors for biodegraation.

Although electrochemically mediated separations have the capability of removing ions and neutral organics, the compatibility of the polypyrrole-based adsorbent with salts needs to be systematically assessed. Su et al. observed that in the case of benzoate uptake by PVF-CNT hybrids, supporting electrolyte containing perchlorate anions (ClO_4^-) outperforms that of chloride ions (Cl^-),[101] while the removal of dichromate $Cr_2O_7^-$ works better in a chloride-based supporting electrolyte using the same type of sorbent.[100] Such phenomena may be explained by the interactions between the salts and the target solutes both present in the aqueous solution. Alternatively, the binding of the ionic species on the adsorbent and their chemical nature may affect the stability, capacity and selectivity of the sorbent.

Because of the infinite variety of organic compounds and salts, it is impossible to test all the combinations of organic compounds and salts and optimize material chemistry of the adsorbents and operating conditions of the separation process for each mixture. Rather, understanding of the physico-chemical interactions between salts and organics, organics and sorbent, as well as salts and sorbent will inform the general working principles of electrochemcially mediated separations of organics in saline wastewater. Such understanding will also cast light on improved material chemistry for redox-responsive adsorbents to capture the target organic compounds while being compatible with the salts present in the aqueous streams.

THIS PAGE INTENTIONALLY LEFT BLANK

Appendix A

Acknowledgements of Copyrights

1. Figure 1-1 reprinted by permission from Springer Nature Customer Service Centre GmbH: Springer Nature Springer eBook, Pervaporation: Removal of Organics from Water and Organic/Organic Separations, J. G. Wijmans, R. W. Baker, and A. L. Athayde, 1994.

2. Figure 1-2 reprinted by permission from Springer Nature Customer Service Centre GmbH: Springer Nature Nature Reviews Materials, Materials for next generation desalination and water purification membrane, Jay R. Werber, Chinedum O. Osuji, and Menachem Elimelech, 2016.

3. Chapter 2 reprinted from Superhydrophobic, Surfactant-doped, Conducting Polymers for Electrochemically Reversible Adsorption of Organic Contaminants, Yinying Ren, Zhou Lin, Xianwen Mao, Wenda Tian, Troy Van Voorhis, and T. Alan Hatton, Advanced Functional Materials, 28:1801466, 2018, with permission from John Wiley & Sons, Inc.

4. Figure 4-1 reprinted from Remediation of water pollution with native cyclodextrins and modified cyclodextrins: A comparative overview and perspectives, Md. Tajuddin Sikder, Md. Mostafizur Rahman, Md. Jakariya, Toshiyuki Hosokawa, Masaaki Kurasaki, and Takeshi Saito, Chemical Engineering Journal, 355:920-941, 2019, with permission from Elsevier.

THIS PAGE INTENTIONALLY LEFT BLANK

Appendix B

Supplementary Movies

Movie	Description	URL
1	MD trajectory of the oxidized PPy(AOT) complex	https://onlinelibrary.wiley.com/action /downloadSupplement?doi=10.1002%2Fadfm. 201801466&file=adfm201801466-sup-0001-S1.mov
2	MD trajectory of the reduced PPy(AOT) complex	https://onlinelibrary.wiley.com/action /downloadSupplement?doi=10.1002%2Fadfm. 201801466&file=adfm201801466-sup-0002-S2.mov
3	Interactions of the reduced PPy(AOT) complex with an SOG molecule	https://onlinelibrary.wiley.com/action /downloadSupplement?doi=10.1002%2Fadfm. 201801466&file=adfm201801466-sup-0003-S3.mov
4	Interactions of the oxidized PPy(AOT) complex with an SOG molecule	https://onlinelibrary.wiley.com/action /downloadSupplement?doi=10.1002%2Fadfm. 201801466&file=adfm201801466-sup-0004-S4.mov
5	Desorption of SOG by PPy(AOT)//Pt, previously adsorbed from a concentrated stream	https://onlinelibrary.wiley.com/action /downloadSupplement?doi=10.1002%2Fadfm. 201801466&file=adfm201801466-sup-0005-S5.mov
6	Desorption of SOG by PPy(AOT)//Pt, previously adsorbed from a diluted stream	https://onlinelibrary.wiley.com/action /downloadSupplement?doi=10.1002%2Fadfm. 201801466&file=adfm201801466-sup-0006-S6.mov

THIS PAGE INTENTIONALLY LEFT BLANK

Bibliography

[1] Water | United Nations.

[2] Ikuo Abe, Katsumi Hayashi, Tsuneaki Hirashima, and Mutsuo Kitagawa. Relationship between the Freundlich adsorption constants K and 1/N hydrophobic adsorption. *Journal of the American Chemical Society*, 104(23):6452–6453, 11 1982.

[3] Ikuo Abe, Katsumi Hayashi, Tsuneaki Hirashima, and Mutsuo Kitagawa. Relationship between the Freundlich adsorption constants k and 1/N for activated carbon adsorption. *Colloids and Surfaces*, 8(3):315–318, 1 1984.

[4] Demetra S. Achilleos and T. Alan Hatton. Selective Molecularly Mediated Pseudocapacitive Separation of Ionic Species in Solution. *ACS Applied Materials & Interfaces*, 8(48):32743–32753, 12 2016.

[5] Abhinav Akhoury, Lev Bromberg, and T. Alan Hatton. Redox-Responsive Gels with Tunable Hydrophobicity for Controlled Solubilization and Release of Organics. *ACS Applied Materials & Interfaces*, 3(4):1167–1174, 4 2011.

[6] Alaaeddin Alsbaiee, Brian J Smith, Leilei Xiao, Yuhan Ling, Damian E Helbling, and William R Dichtel. Rapid removal of organic micropollutants from water by a porous β-cyclodextrin polymer. *Nature*, 529(7585):190–194, 1 2016.

[7] P M Álvarez, F J Beltrán, V Gómez-Serrano, J Jaramillo, and E M RodrÄśÎĄguez. Comparison between thermal and ozone regenerations of spent activated carbon exhausted with phenol. *Water Research*, 38(8):2155–2165, 4 2004.

[8] Jin An, Jin-Feng Cui, Zhao-Qi Zhu, Wei-Dong Liang, Chun-Juan Pei, Han-Xue Sun, Bao-Ping Yang, and An Li. Conductive polymer-coated mesh films with tunable surface wettability for separation of oils and organics from water. *Journal of Applied Polymer Science*, 131(18):n/a–n/a, 9 2014.

[9] Paul S Bagus, Connie J Nelin, Dave A Hrovat, and Eugene S Ilton. Covalent bonding in heavy metal oxides. *The Journal of Chemical Physics*, 146(13):134706, 4 2017.

[10] Hua Bai and Gaoquan Shi. Gas sensors based on conducting polymers. *Sensors*, 7(3):267–307, 3 2007.

[11] Martin Bazant. 10.626 Electrochemical Energy Systems, 2014.

[12] A D Becke. Density-functional exchange-energy approximation with correct asymptotic behavior. *Physical Review A*, 38(6):3098–3100, 9 1988.

[13] Kada Boukerma, Maria Omastová, Pavol Fedorko, and Mohamed M. Chehimi. Surface properties and conductivity of bis(2-ethylhexyl) sulfosuccinate-containing polypyrrole. *Applied Surface Science*, 249(1-4):303–314, 8 2005.

[14] N W Brown, E P L Roberts, A A Garforth, and R A W Dryfe. Electrochemical regeneration of a carbon-based adsorbent loaded with crystal violet dye. *Electrochimica Acta*, 49(20):3269–3281, 8 2004.

[15] Agnes Buvári and Lajos Barcza. Complex formation of phenol, aniline, and their nitro derivatives with β-cyclodextrin. *Journal of the Chemical Society, Perkin Transactions 2*, 0(4):543–545, 1 1988.

[16] Xiaotong Cao, Jianquan Luo, John M. Woodley, and Yinhua Wan. Bioinspired Multifunctional Membrane for Aquatic Micropollutants Removal. *ACS Applied Materials & Interfaces*, 8(44):30511–30522, 11 2016.

[17] Jean H. Chang and Ian W. Hunter. A Superhydrophobic to Superhydrophilic In Situ Wettability Switch of Microstructured Polypyrrole Surfaces. *Macromolecular Rapid Communications*, 32(9-10):718–723, 5 2011.

[18] Wei Chen, Zhongli Fan, Lin Gu, Xinhe Bao, and Chunlei Wang. Enhanced capacitance of manganese oxide via confinement inside carbon nanotubes. *Chemical Communications*, 46(22):3905–3907, 6 2010.

[19] E L Cussler and Binay K Dutta. On separation efficiency. *AIChE Journal*, 58(12):3825–3831, 12 2012.

[20] C G Daughton and T A Ternes. Pharmaceuticals and personal care products in the environment: agents of subtle change? *Environmental Health Perspectives*, 107(Suppl 6):907, 12 1999.

[21] Yang Deng and Renzun Zhao. Advanced Oxidation Processes (AOPs) in Wastewater Treatment. *Current Pollution Reports*, 1(3):167–176, 9 2015.

[22] Joana M. Dias, Maria C.M. Alvim-Ferraz, Manuel F. Almeida, JosÃĺ Rivera-Utrilla, and Manuel Sánchez-Polo. Waste materials for activated carbon preparation and its use in aqueous-phase treatment: A review. *Journal of Environmental Management*, 85(4):833–846, 12 2007.

[23] Helena. Dodziuk. *Cyclodextrins and their complexes : chemistry, analytical methods, applications*. Wiley-VCH, 2006.

[24] M. M. Dubinin. The Potential Theory of Adsorption of Gases and Vapors for Adsorbents with Energetically Nonuniform Surfaces. *Chemical Reviews*, 60(2):235–241, 4 1960.

[25] Muriel Dunier and Andrzej K. Siwicki. Effects of pesticides and other organic pollutants in the aquatic environment on immunity of fish: a review. *Fish & Shellfish Immunology*, 3(6):423–438, 11 1993.

[26] Menachem Elimelech. The global challenge for adequate and safe water. *Journal of Water Supply: Research and Technology - Aqua*, 55(1):3–10, 2 2006.

[27] F. Hapiot, S. E., and E. Monflier. Cyclodextrins as Supramolecular Hosts for Organometallic Complexes. 2006.

[28] Heinz-Gerhard Franck and Jurgen W Stadelhofer. *Industrial Aromatic Chemistry: Raw Materials · Processes · Products.* Springer Science & Business Media, 12 2012.

[29] Terry Z. H. Gani, Efthymios I. Ioannidis, and Heather J. Kulik. Computational Discovery of Hydrogen Bond Design Rules for Electrochemical Ion Separation. *Chemistry of Materials*, 28(17):6207–6218, 9 2016.

[30] Dongtao Ge, Sanqing Huang, Rucai Qi, Jing Mu, Yuqing Shen, and Wei Shi. Nanowire-Based Polypyrrole Hierarchical Structures Synthesized by a Two-Step Electrochemical Method. *ChemPhysChem*, 10(11):1916–1921, 8 2009.

[31] Bina Gidwani and Amber Vyas. A Comprehensive Review on Cyclodextrin-Based Carriers for Delivery of Chemotherapeutic Cytotoxic Anticancer Drugs. *BioMed research international*, 2015:198268, 2015.

[32] Stefan Grimme. Semiempirical GGA-type density functional constructed with a long-range dispersion correction. *Journal of Computational Chemistry*, 27(15):1787–1799, 11 2006.

[33] Zenaida Guerra-Que, Hermicenda Pérez-Vidal, G. Torres-Torres, Juan Carlos Arévalo-Pérez, Adib Abiu Silahua Pavón, Adrian Cervantes-Uribe, A. Espinosa de los Monteros, and Ma. Antonia Lunagómez-Rocha. Treatment of phenol by catalytic wet air oxidation: a comparative study of copper and nickel supported on γ-alumina, ceria and γ-alumina-ceria. *RSC Advances*, 9(15):8463–8479, 3 2019.

[34] Ole Hammerich, Bernd Speiser, and Bernd Speiser. *Organic Electrochemistry, Fifth Edition.* CRC Press, 10 2015.

[35] Krista L. Hawthorne, Jesse S. Wainright, and Robert F. Savinell. Studies of Iron-Ligand Complexes for an All-Iron Flow Battery Application. *Journal of The Electrochemical Society*, 161(10):A1662–A1671, 7 2014.

[36] Per Helboe. Determination of impurities in propanol hydrochloride by high-performance liquid chromatography on dynamically modified silica. *Journal of Chromatography A*, 245(2):229–238, 8 1982.

[37] Paul R Horn and Martin Head-Gordon. Alternative definitions of the frozen energy in energy decomposition analysis of density functional theory calculations. *The Journal of Chemical Physics*, 144(8):84118, 2 2016.

[38] Paul R Horn, Yuezhi Mao, and Martin Head-Gordon. Probing non-covalent interactions with a second generation energy decomposition analysis using absolutely localized molecular orbitals. *Physical Chemistry Chemical Physics*, 18(33):23067–23079, 8 2016.

[39] Yongshun Huang, Jiaxing Li, Xiaoping Chen, and Xiangke Wang. Applications of conjugated polymer based composites in wastewater purification. *Rsc Advances*, 4(107):62160–62178, 2014.

[40] J. Isaksson, C. Tengstedt, M. Fahlman, N. Robinson, and M. Berggren. A Solid-State Organic Electronic Wettability Switch. *Advanced Materials*, 16(4):316–320, 2 2004.

[41] Rudolf Jaffé. Fate of hydrophobic organic pollutants in the aquatic environment: A review. *Environmental Pollution*, 69(2-3):237–257, 1 1991.

[42] Jyongsik Jang and Hyeonseok Yoon. Formation Mechanism of Conducting Polypyrrole Nanotubes in Reverse Micelle Systems. *Langmuir*, 21(24):11484–11489, 2005.

[43] N Jemaa, R D Noble, and C A Koval. Combined mass and energy balance analysis of an electrochemically modulated equilibrium stage process. *Chemical Engineering Science*, 47(6):1469–1479, 1992.

[44] E T Kang, K G Neoh, and K L Tan. The intrinsic redox states in polypyrrole and polyaniline: A comparative study by XPS. *Surface and Interface Analysis*, 19(1-12):33–37, 6 1992.

[45] Belgin Karabacakoğlu and Oznur Savlak. Electrochemical Regeneration of Cr(VI) Saturated Granular and Powder Activated Carbon: Comparison of Regeneration Efficiency. *Industrial & Engineering Chemistry Research*, 53(33):13171–13179, 8 2014.

[46] S. Kitanou, M. Tahri, B. Bachiri, M. Mahi, M. Hafsi, M. Taky, and A. Elmidaoui. Comparative study of membrane bioreactor (MBR) and activated sludge processes in the treatment of Moroccan domestic wastewater. *Water Science and Technology*, 78(5):1129–1136, 10 2018.

[47] Ayse Kuleyin. Removal of phenol and 4-chlorophenol by surfactant-modified natural zeolite. *Journal of Hazardous Materials*, 144(1-2):307–315, 6 2007.

[48] Ravi Kumar and Glenn R Dissinger. Nonequilibrium, nonisothermal desorption of single adsorbate by purge. *Industrial & Engineering Chemistry Process Design and Development*, 25(2):456–464, 4 1986.

[49] S. N. Kumar, G. Bouyssoux, and F. Gaillard. Electronic and structural characterization of electrochemically synthesized conducting polyaniline from XPS studies. *Surface and Interface Analysis*, 15(9):531–536, 9 1990.

[50] Hrvoje Kusic, Natalija Koprivanac, and Ana Loncaric Bozic. Minimization of organic pollutant content in aqueous solution by means of AOPs: UV- and ozone-based technologies. *Chemical Engineering Journal*, 123(3):127–137, 10 2006.

[51] George Kyzas, Jie Fu, Kostas Matis, George Z. Kyzas, Jie Fu, and Kostas A. Matis. The Change from Past to Future for Adsorbent Materials in Treatment of Dyeing Wastewaters. *Materials*, 6(11):5131–5158, 11 2013.

[52] Aurelie Lafuma and David Quéré. Superhydrophobic states. *Nature Materials*, 2(7):457–460, 7 2003.

[53] Peter L. Lallas. The Stockholm Convention on Persistent Organic Pollutants. *The American Journal of International Law*, 95(3):692, 7 2001.

[54] Chengteh Lee, Weitao Yang, and Robert G. Parr. Development of the Colle-Salvetti correlation-energy formula into a functional of the electron density. *Physical Review B*, 37(2):785–789, 1 1988.

[55] Olivier Lefebvre and RenÃľ Moletta. Treatment of organic pollution in industrial saline wastewater: A literature review. *Water Research*, 40(20):3671–3682, 12 2006.

[56] Lianhui Li, Yuanyuan Bai, Lili Li, Shuqi Wang, and Ting Zhang. A Superhydrophobic Smart Coating for Flexible and Wearable Sensing Electronics. *Advanced Materials*, 29(43):1702517, 11 2017.

[57] Ryan P Lively and David S Sholl. From water to organics in membrane separations. *Nature Materials*, 16:276–279, 2 2017.

[58] Yunlong Luo, Wenshan Guo, Huu Hao Ngo, Long Duc Nghiem, Faisal Ibney Hai, Jian Zhang, Shuang Liang, and Xiaochang C Wang. A review on the occurrence of micropollutants in the aquatic environment and their fate and removal during wastewater treatment. *Science of The Total Environment*, 473-474:619–641, 3 2014.

[59] Milton Manes and Lawrence J. E. Hofer. Application of the Polanyi adsorption potential theory to adsorption from solution on activated carbon. *The Journal of Physical Chemistry*, 73(3):584–590, 3 1969.

[60] Xianwen Mao, Fritz Simeon, Demetra S Achilleos, Gregory C Rutledge, and T Alan Hatton. Metallocene/carbon hybrids prepared by a solution process for supercapacitor applications. *Journal of Materials Chemistry A*, 1(42):13120–13127, 10 2013.

[61] Xianwen Mao, Wenda Tian, Yinying Ren, Dexin Chen, Sarah E Curtis, Marjorie T Buss, Gregory C Rutledge, and T Alan Hatton. Energetically efficient electrochemically tunable affinity separation using multicomponent polymeric nanostructures for water treatment. *Energy & Environmental Science*, 11(10):2954–2963, 10 2018.

[62] Xianwen Mao, Wenda Tian, Jie Wu, Gregory C. Rutledge, and T. Alan Hatton. Electrochemically Responsive Heterogeneous Catalysis for Controlling Reaction Kinetics. *Journal of the American Chemical Society*, 137(3):1348–1355, 1 2015.

[63] L. Martínez, R. Andrade, E. G. Birgin, and J. M. Martínez. PACKMOL: A package for building initial configurations for molecular dynamics simulations. *Journal of Computational Chemistry*, 30(13):2157–2164, 10 2009.

[64] Theresa M. McCormick, Colin R. Bridges, Elisa I. Carrera, Paul M. DiCarmine, Gregory L. Gibson, Jon Hollinger, Lisa M. Kozycz, and Dwight S. Seferos. Conjugated Polymers: Evaluating DFT Methods for More Accurate Orbital Energy Modeling. *Macromolecules*, 46(10):3879–3886, 5 2013.

[65] D. Mecerreyes, V. Alvaro, I. Cantero, M. Bengoetxea, P.A. Calvo, H. Grande, J. Rodriguez, and J.A. Pomposo. Low Surface Energy Conducting Polypyrrole Doped with a Fluorinated Counterion. *Advanced Materials*, 14(10):749, 5 2002.

[66] Amirmasoud Mohtasebi, Tanzina Chowdhury, Leo H. H. Hsu, Mark C. Biesinger, and Peter Kruse. Interfacial Charge Transfer between Phenyl-Capped Aniline Tetramer Films and Iron Oxide Surfaces. *The Journal of Physical Chemistry C*, 120(51):29248–29263, 12 2016.

[67] Tomoki Ogoshi, Yoshinori Takashima, Hiroyasu Yamaguchi, and Akira Harada. Chemically-Responsive Sol-Gel Transition of Supramolecular Single-Walled Carbon Nanotubes (SWNTs) Hydrogel Made by Hybrids of SWNTs and Cyclodextrins. *J. Am. Chem. Soc.*, 129(16):4878–4879, 2007.

[68] Serife Okur and Ulrike Salzner. Theoretical Modeling of the Doping Process in Polypyrrole by Calculating UV/Vis Absorption Spectra of Neutral and Charged Oligomers. *The Journal of Physical Chemistry A*, 113(31):9050–9050, 8 2009.

[69] Kevin E. O'Shea and Dionysios D. Dionysiou. Advanced Oxidation Processes for Water Treatment. *The Journal of Physical Chemistry Letters*, 3(15):2112–2113, 8 2012.

[70] Amrita Pal, Karina Yew-Hoong Gin, Angela Yu-Chen Lin, and Martin Reinhard. Impacts of emerging organic contaminants on freshwater resources: {Review} of recent occurrences, sources, fate and effects. *Science of The Total Environment*, 408(24):6062–6069, 11 2010.

[71] A C Partridge, C B Milestone, C O Too, and G G Wallace. Polypyrrole based cation transport membranes. *Journal of Membrane Science*, 152(1):61–70, 1 1999.

[72] Neelesh A. Patankar. Mimicking the Lotus Effect: Influence of Double Roughness Structures and Slender Pillars. *Langmuir*, 20(19):8209–8213, 2004.

[73] W. Pauli. Über den Zusammenhang des Abschlusses der Elektronengruppen im Atom mit der Komplexstruktur der Spektren. *Zeitschrift für Physik*, 31(1):765–783, 2 1925.

[74] Katherine T. Peter, John D. Vargo, Thilini P. Rupasinghe, Aribet De Jesus, Alexei V. Tivanski, Edward A. Sander, Nosang V. Myung, and David M. Cwiertny. Synthesis, Optimization, and Performance Demonstration of Electrospun Carbon Nanofiber-Carbon Nanotube Composite Sorbents for Point-of-Use Water Treatment. *ACS Applied Materials & Interfaces*, 8(18):11431–11440, 5 2016.

[75] Kavita Pilaniya, Harish K Chandrawanshi, Urmila Pilaniya, Pooja Manchandani, Pratishtha Jain, and Nitin Singh. Recent trends in the impurity profile of pharmaceuticals. *Journal of Advanced Pharmaceutical Technology & Research*, 1(3):302–310, 2010.

[76] Sander Pronk, Szilard Páll, Roland Schulz, Per Larsson, Par Bjelkmar, Rossen Apostolov, Michael R. Shirts, Jeremy C. Smith, Peter M. Kasson, David van der Spoel, Berk Hess, and Erik Lindahl. GROMACS 4.5: a high-throughput and highly parallel open source molecular simulation toolkit. *Bioinformatics*, 29(7):845, 4 2013.

[77] M K Purkait, A Maiti, S DasGupta, and S De. Removal of congo red using activated carbon and its regeneration. *Journal of Hazardous Materials*, 145(1):287–295, 6 2007.

[78] Mohan Qin, Akshay Deshmukh, Razi Epsztein, Sohum K Patel, Oluwaseye M Owoseni, W Shane Walker, and Menachem Elimelech. Comparison of energy consumption in desalination by capacitive deionization and reverse osmosis. *Desalination*, 455:100–114, 4 2019.

[79] Yong-Jian Qiu and John R Reynolds. Dopant anion controlled ion transport behavior of polypyrrole. *Polymer Engineering & Science*, 31(6):417–421, 3 1991.

[80] Mikhail V Rekharsky and Yoshihisa Inoue. Complexation Thermodynamics of Cyclodextrins. *Chemical Reviews*, 98(5):1875–1918, 1998.

[81] Yinying Ren, Zhou Lin, Xianwen Mao, Wenda Tian, Troy Van Voorhis, and T. Alan Hatton. Superhydrophobic, Surfactant-doped, Conducting Polymers for Electrochemically Reversible Adsorption of Organic Contaminants. *Advanced Functional Materials*, 28(32):1801466, 8 2018.

[82] Said Sadki, Philippe Schottland, Nancy Brodie, and Guillaume Sabouraud. The mechanisms of pyrrole electropolymerization. *Chemical Society Reviews*, 29(5):283–293, 1 2000.

[83] Francisco Salvador, Nicolas Martin-Sanchez, Ruth Sanchez-Hernandez, M. Jesus Sanchez-Montero, and Carmen Izquierdo. Regeneration of carbonaceous adsorbents. Part II: Chemical, Microbiological and Vacuum Regeneration. *Microporous and Mesoporous Materials*, 202:277–296, 1 2015.

[84] Francisco Salvador, Nicolas Martin-Sanchez, Ruth Sanchez-Hernandez, Maria Jesus Sanchez-Montero, and Carmen Izquierdo. Regeneration of carbonaceous adsorbents. Part I: Thermal Regeneration. *Microporous and Mesoporous Materials*, 202:259–276, 1 2015.

[85] U Salzner, J B Lagowski, P G Pickup, and R A Poirier. Comparison of geometries and electronic structures of polyacetylene, polyborole, polycyclopentadiene, polypyrrole, polyfuran, polysilole, polyphosphole, polythiophene, polyselenophene and polytellurophene. *Synthetic Metals*, 96(3):177–189, 8 1998.

[86] Abdelhamid Sayari, Safia Hamoudi, and Yong Yang. Applications of Pore-Expanded Mesoporous Silica. 1. Removal of Heavy Metal Cations and Organic Pollutants from Wastewater. *Chemistry of Materials*, 17(1):212–216, 2005.

[87] Joan M Schork and James R Fair. Parametric analysis of thermal regeneration of adsorption beds. *Industrial & Engineering Chemistry Research*, 27(3):457–469, 3 1988.

[88] Rene P Schwarzenbach, Beate I Escher, Kathrin Fenner, Thomas B Hofstetter, C Annette Johnson, Urs von Gunten, and Bernhard Wehrli. The challenge of micropollutants in aquatic systems. *Science*, 313(5790):1072–7, 8 2006.

[89] Itamar A. Shabtai and Yael G. Mishael. PolycyclodextrinâĂŞClay Composites: Regenerable Dual-Site Sorbents for Bisphenol A Removal from Treated Wastewater. *ACS Applied Materials & Interfaces*, 10(32):27088–27097, 8 2018.

[90] Mark A. Shannon, Paul W. Bohn, Menachem Elimelech, John G. Georgiadis, Benito J. Mariñas, and Anne M. Mayes. Science and technology for water purification in the coming decades. *Nature*, 452(7185):301–310, 3 2008.

[91] Yihan Shao, Zhengting Gan, Evgeny Epifanovsky, Andrew T.B. Gilbert, Michael Wormit, Joerg Kussmann, Adrian W. Lange, Andrew Behn, Jia Deng, Xintian Feng, Debashree Ghosh, Matthew Goldey, Paul R. Horn, Leif D. Jacobson, Ilya Kaliman, Rustam Z. Khaliullin, Tomasz Kuś, Arie Landau, Jie Liu, Emil I. Proynov, Young Min Rhee, Ryan M. Richard, Mary A. Rohrdanz, Ryan P. Steele, Eric J. Sundstrom, H. Lee Woodcock, Paul M. Zimmerman, Dmitry Zuev, Ben Albrecht, Ethan Alguire, Brian Austin, Gregory J. O. Beran, Yves A. Bernard, Eric Berquist, Kai Brandhorst, Ksenia B. Bravaya, Shawn T. Brown, David Casanova, Chun-Min Chang, Yunqing Chen, Siu Hung Chien, Kristina D. Closser, Deborah L. Crittenden, Michael Diedenhofen, Robert A. DiStasio, Hainam Do, Anthony D. Dutoi, Richard G.

Edgar, Shervin Fatehi, Laszlo Fusti-Molnar, An Ghysels, Anna Golubeva-Zadorozhnaya, Joseph Gomes, Magnus W.D. Hanson-Heine, Philipp H.P. Harbach, Andreas W. Hauser, Edward G. Hohenstein, Zachary C. Holden, Thomas-C. Jagau, Hyunjun Ji, Benjamin Kaduk, Kirill Khistyaev, Jaehoon Kim, Jihan Kim, Rollin A. King, Phil Klunzinger, Dmytro Kosenkov, Tim Kowalczyk, Caroline M. Krauter, Ka Un Lao, AdÃĺle D. Laurent, Keith V. Lawler, Sergey V. Levchenko, Ching Yeh Lin, Fenglai Liu, Ester Livshits, Rohini C. Lochan, Arne Luenser, Prashant Manohar, Samuel F. Manzer, Shan-Ping Mao, Narbe Mardirossian, Aleksandr V. Marenich, Simon A. Maurer, Nicholas J. Mayhall, Eric Neuscamman, C. Melania Oana, Roberto Olivares-Amaya, Darragh P. OâĂŹNeill, John A. Parkhill, Trilisa M. Perrine, Roberto Peverati, Alexander Prociuk, Dirk R. Rehn, Edina Rosta, Nicholas J. Russ, Shaama M. Sharada, Sandeep Sharma, David W. Small, Alexander Sodt, Tamar Stein, David Stück, Yu-Chuan Su, Alex J.W. Thom, Takashi Tsuchimochi, Vitalii Vanovschi, Leslie Vogt, Oleg Vydrov, Tao Wang, Mark A. Watson, Jan Wenzel, Alec White, Christopher F. Williams, Jun Yang, Sina Yeganeh, Shane R. Yost, Zhi-Qiang You, Igor Ying Zhang, Xing Zhang, Yan Zhao, Bernard R. Brooks, Garnet K.L. Chan, Daniel M. Chipman, Christopher J. Cramer, William A. Goddard, Mark S. Gordon, Warren J. Hehre, Andreas Klamt, Henry F. Schaefer, Michael W. Schmidt, C. David Sherrill, Donald G. Truhlar, Arieh Warshel, Xin Xu, AlÃąn Aspuru-Guzik, Roi Baer, Alexis T. Bell, Nicholas A. Besley, Jeng-Da Chai, Andreas Dreuw, Barry D. Dunietz, Thomas R. Furlani, Steven R. Gwaltney, Chao-Ping Hsu, Yousung Jung, Jing Kong, Daniel S. Lambrecht, WanZhen Liang, Christian Ochsenfeld, Vitaly A. Rassolov, Lyudmila V. Slipchenko, Joseph E. Subotnik, Troy Van Voorhis, John M. Herbert, Anna I. Krylov, Peter M.W. Gill, and Martin Head-Gordon. Advances in molecular quantum chemistry contained in the Q-Chem 4 program package. *Molecular Physics*, 113(2):184–215, 1 2015.

[92] Qianqian Shi, Jian Zhang, Chenglu Zhang, Cong Li, Bo Zhang, Weiwei Hu, Jingtao Xu, and Ran Zhao. Preparation of activated carbon from cattail and its application for dyes removal. *Journal of Environmental Sciences*, 22(1):91–97, 1 2010.

[93] Md. Tajuddin Sikder, Md. Mostafizur Rahman, Md. Jakariya, Toshiyuki Hosokawa, Masaaki Kurasaki, and Takeshi Saito. Remediation of water pollution with native cyclodextrins and modified cyclodextrins: A comparative overview and perspectives. *Chemical Engineering Journal*, 355:920–941, 1 2019.

[94] Steen Skaarup, Lasse Bay, Kamal Vidanapathirana, Susanne Thybo, Pentti Tofte, and Keld West. Simultaneous anion and cation mobility in polypyrrole. *Solid State Ionics*, 159(1):143–147, 3 2003.

[95] Thomas Steiner. The Hydrogen Bond in the Solid State. *Angewandte Chemie International Edition*, 41(1):48–76, 1 2002.

[96] Xiao Su and T Alan Hatton. Electrosorption at functional interfaces: from molecular-level interactions to electrochemical cell design. *Physical Chemistry Chemical Physics*, 2017.

[97] Xiao Su and T Alan Hatton. Redox-electrodes for selective electrochemical separations. *Advances in Colloid and Interface Science*, 244:6–20, 6 2017.

[98] Xiao Su, Jonas Hübner, Monique J. Kauke, Luiza Dalbosco, Jonathan Thomas, Christopher C. Gonzalez, Eric Zhu, Matthias Franzreb, Timothy F. Jamison, and T. Alan Hatton. Redox Interfaces for Electrochemically Controlled ProteinâĂŞSurface Interactions: Bioseparations and Heterogeneous Enzyme Catalysis. *Chemistry of Materials*, 29(13):5702–5712, 7 2017.

[99] Xiao Su, Heather J. Kulik, Timothy F. Jamison, and T. Alan Hatton. Anion-Selective Redox Electrodes: Electrochemically Mediated Separation with Heterogeneous Organometallic Interfaces. *Advanced Functional Materials*, 26(20):3394–3404, 5 2016.

[100] Xiao Su, Akihiro Kushima, Cameron Halliday, Jian Zhou, Ju Li, and T. Alan Hatton. Electrochemically-mediated selective capture of heavy metal chromium and arsenic oxyanions from water. *Nature Communications*, 9(1):4701, 12 2018.

[101] Xiao Su, Kai-Jher Tan, Johannes Elbert, Christian Rüttiger, Markus Gallei, Timothy F. Jamison, and T. Alan Hatton. Asymmetric Faradaic systems for selective electrochemical separations. *Energy & Environmental Science*, 10(5):1272–1283, 5 2017.

[102] Jana Tabačiarová, Matej Mičušík, Pavol Fedorko, and Maria Omastová. Study of polypyrrole aging by XPS, FTIR and conductivity measurements. *Polymer Degradation and Stability*, 120:392–401, 10 2015.

[103] Hajime Tamon, Takashi Saito, Masaaki Kishimura, Morio Okazaki, and Ryozo Toei. Solvent Regeneration of Spent Activated Carbon in Wastewater Treatment. *Journal of Chemical Engineering of Japan*, 23(4):426–432, 1990.

[104] Wenda Tian, Xianwen Mao, Paul Brown, Gregory C. Rutledge, and T. Alan Hatton. Electrochemically Nanostructured Polyvinylferrocene/Polypyrrole Hybrids with Synergy for Energy Storage. *Advanced Functional Materials*, 25(30):4803–4813, 8 2015.

[105] Henry D. Tran, Yue Wang, Julio M. D'Arcy, and Richard B. Kaner. Toward an Understanding of the Formation of Conducting Polymer Nanofibers. *ACS Nano*, 2(9):1841–1848, 9 2008.

[106] Yao-Tsan Tsai, Chang-Hwan Choi, Ning Gao, and Eui-Hyeok Yang. Tunable Wetting Mechanism of Polypyrrole Surfaces and Low-Voltage Droplet Manipulation via Redox. *Langmuir*, 27(7):4249–4256, 4 2011.

[107] Habib Ullah, Anwar-ul-Haq Ali Shah, Salma Bilal, and Khurshid Ayub. Doping and Dedoping Processes of Polypyrrole: DFT Study with Hybrid Functionals. *The Journal of Physical Chemistry C*, 118(31):17819–17830, 8 2014.

[108] United Nations. The Sustainable Development Goals Report 2018. Technical report, 2018.

[109] United States Environmental Protection Agency. How Wastewater Treatment Works... The Basics, 1998.

[110] Kohei Urano, Yoshinobu Koichi, and Yasushi Nakazawa. Equilibria for adsorption of organic compounds on activated carbons in aqueous solutions I. Modified Freundlich isotherm equation and adsorption potentials of organic compounds. *Journal of Colloid and Interface Science*, 81(2):477–485, 6 1981.

[111] OW US EPA. Drinking Water Health Advisories for PFOA and PFOS.

[112] Katherine L. VanâĂĚAken, Majid Beidaghi, and Yury Gogotsi. Formulation of Ionic-Liquid Electrolyte To Expand the Voltage Window of Supercapacitors. *Angewandte Chemie International Edition*, 54(16):4806–4809, 4 2015.

[113] Susana Vaquero, Jesus Palma, Marc Anderson, and Rebeca Marcilla. Improving Performance of Electric Double Layer Capacitors with a Mixture of Ionic Liquid and Acetonitrile as the Electrolyte by Using Mass-Balancing Carbon Electrodes. *Journal of The Electrochemical Society*, 160(11):A2064–A2069, 9 2013.

[114] Susana Vaquero, Jesus Palma, Marc Anderson, and Rebeca Marcilla. Mass-Balancing of Electrodes as a Strategy to Widen the Operating Voltage Window of Carbon/Carbon Supercapacitors in Neutral Aqueous Electrolytes. Technical report, 2013.

[115] K.P Vidanapathirana, M.A Careem, S Skaarup, and K West. Ion movement in polypyrrole/dodecylbenzenesulphonate films in aqueous and non-aqueous electrolytes. *Solid State Ionics*, 154-155:331–335, 12 2002.

[116] Fatima Wasim, Tariq Mahmood, and Khurshid Ayub. An accurate cost effective DFT approach to study the sensing behaviour of polypyrrole towards nitrate ions in gas and aqueous phases. *Physical Chemistry Chemical Physics*, 18(28):19236–19247, 7 2016.

[117] Jay R. Werber, Chinedum O. Osuji, and Menachem Elimelech. Materials for next-generation desalination and water purification membranes. *Nature Reviews Materials*, 1(5):16018, 5 2016.

[118] J. G. Wijmans, R. W. Baker, and A. L. Athayde. Pervaporation: Removal of Organics from Water and Organic/Organic Separations. In *Membrane Processes in Separation and Purification*, pages 283–316. Springer Netherlands, Dordrecht, 1994.

[119] Leilei Xiao, Yuhan Ling, Alaaeddin Alsbaiee, Chenjun Li, Damian E. Helbling, and William R. Dichtel. β-Cyclodextrin Polymer Network Sequesters Perfluorooctanoic Acid at Environmentally Relevant Concentrations. *Journal of the American Chemical Society*, 139(23):7689–7692, 6 2017.

[120] Lianbin Xu, Wilfred Chen, Ashok Mulchandani, and Yushan Yan. Reversible Conversion of Conducting Polymer Films from Superhydrophobic to Superhydrophilic. *Angewandte Chemie International Edition*, 44(37):6009–6012, 9 2005.

[121] Mustafa T. Yagub, Tushar Kanti Sen, Sharmeen Afroze, and H.M. Ang. Dye and its removal from aqueous solution by adsorption: A review. *Advances in Colloid and Interface Science*, 209:172–184, 7 2014.

[122] Chongyang Yang, Jiali Shen, Chunyan Wang, Haojie Fei, Hua Bao, and Gengchao Wang. All-solid-state asymmetric supercapacitor based on reduced graphene oxide/carbon nanotube and carbon fiber paper/polypyrrole electrodes. *J. Mater. Chem. A*, 2(5):1458–1464, 12 2014.

[123] Kun Yang and Baoshan Xing. Adsorption of Organic Compounds by Carbon Nanomaterials in Aqueous Phase: Polanyi Theory and Its Application. *Chemical Reviews*, 110(10):5989–6008, 10 2010.

[124] Victor Yangali-Quintanilla, Sung Kyu Maeng, Takahiro Fujioka, Maria Kennedy, and Gary Amy. Proposing nanofiltration as acceptable barrier for organic contaminants in water reuse. *Journal of Membrane Science*, 362(1):334–345, 10 2010.

[125] Jianxiang Zhang and Peter X Ma. Cyclodextrin-based supramolecular systems for drug delivery: recent progress and future perspective. *Advanced drug delivery reviews*, 65(9):1215–33, 8 2013.

[126] Chunli Zheng, Ling Zhao, Xiaobai Zhou, Zhimin Fu, and An Li. Treatment Technologies for Organic Wastewater. In *Water Treatment*. InTech, 1 2013.

[127] Cheng Zhong, Yida Deng, Wenbin Hu, Jinli Qiao, Lei Zhang, and Jiujun Zhang. A review of electrolyte materials and compositions for electrochemical supercapacitors. *Chemical Society Reviews*, 44(21):7484–7539, 10 2015.

[128] Xin Zhuang, Ying Wan, Cuimiao Feng, Ying Shen, and Dongyuan Zhao. Highly Efficient Adsorption of Bulky Dye Molecules in Wastewater on Ordered Mesoporous Carbons. *Chemistry of Materials*, 21(4):706–716, 2 2009.